The Role of *Tcrb* Subnuclear Positioning in V(D)J Recombination

by

Elizabeth Ann Wilcox Chan

Department of Immunology
Duke University

Date: _____

Approved:

_____
Michael Krangel, Supervisor

_____
Weiguo Zhang, Chair

_____
Yuan Zhuang

_____
Qi-Jing Li

_____
Arno Greenleaf

_____
Joel Meyer

Dissertation submitted in partial fulfillment of the requirements for the degree
of Doctor of Philosophy in the Department of Immunology
in the Graduate School of Duke University

2014

ABSTRACT

The Role of *Tcrb* Subnuclear Positioning in V(D)J Recombination

by

Elizabeth Ann Wilcox Chan

Department of Immunology
Duke University

Date:_____

Approved:

_____
Michael Krangel, Supervisor

_____
Weiguo Zhang, Chair

_____
Yuan Zhuang

_____
Qi-Jing Li

_____
Arno Greenleaf

_____
Joel Meyer

An abstract of a dissertation submitted in partial fulfillment of the requirements for the degree of Doctor of Philosophy in the Department of Immunology in the Graduate School of Duke University

2014

Copyright by
Elizabeth Ann Wilcox Chan
2014

Abstract

T cells and B cells each express unique antigen receptors used to identify, eliminate, and remember pathogens. These receptors are generated through a process known as V(D)J recombination, in which T cell receptor and B cell receptor gene loci undergo genomic recombination. Interestingly, recombination at certain genes is regulated so that a single in-frame rearrangement is present on only one allele per cell. This phenomenon, termed allelic exclusion, requires two steps. First, recombination can occur only on one allele at a time. In the second step, additional recombination must be prevented. Though the mechanism of the second step is well-understood, the first step remains poorly understood.

The first step of recombination necessitates that alleles rearrange one at a time. This could be achieved either through inefficient recombination or by halting further recombination in the presence of recombination. To separate these mechanisms, we analyzed recombination in nuclei unable to complete recombination. We found that rearrangement events accumulated at antigen receptor loci, suggesting that the presence of recombination does not stop additional rearrangements and asynchronous recombination likely results from inefficient recombination at both alleles.

Association with repressive subnuclear compartments has been proposed to reduce the recombination efficiency of allelically excluded antigen receptor loci. Of the

alleleically excluded loci, *Tcrb* alleles are uniquely regulated during development. Other allelically excluded alleles are positioned at the transcriptionally-repressive nuclear periphery prior to recombination, and relocate to the nuclear interior at the stage in which they recombine. However *Tcrb* alleles remain highly associated with the nuclear periphery during rearrangement. Here we provide evidence that this peripheral subnuclear positioning of *Tcrb* alleles does suppress recombination. We go on to suggest that peripheral localization mediates the first step of allelic exclusion.

In search of the mechanism by which recombination is suppressed on peripheral *Tcrb* alleles, we investigated the subnuclear localization of a recombinase protein. Two recombinase proteins are required for recombination, one of which is recruited to actively transcribing (and more centrally located) DNA. Here we demonstrate that one recombinase protein is unable to localize to peripheral *Tcrb* alleles, potentially serving as the mechanism by which recombination is suppressed on peripheral alleles.

Contents

List of Tables

List of Figures

List of Abbreviations

3′ CBE	CTCF-binding element
3D FISH	Three-dimensional fluorescence *in situ* hybridization
3′E_κ	3′ *Igk* enhancer
3′RR	3′ *Igh* regulatory region
53BP1	p53 binding protein 1
AEJ	Alternative end joining
ATM	Ataxia telangiectasia mutated
ATR	Ataxia telangiectasia related
BAC	Bacterial artificial chromosome
BCR	B cell receptor
bp	Base pairs
C	Constant
CE	Coding end
ChIP	Chromatin immunoprecipitation
CJ	Coding joint
CT	Chromosome territory
CTCF	CCCTC-binding factor
D	Diversity

Dam	DNA adenine methyltransferase
dE_κ	*Igk* downstream enhancer
DN	$CD4^-CD8^-$ double negative
DN1	$CD44^+CD25^-$ double negative
DN2	$CD44^+CD25^+$ double negative
DN3	$CD44^-CD25^+$ double negative
DN4	$CD44^-CD25^-$ double negative
DNA	Deoxyribonucleic acid
DNA-PK	DNA-dependent protein kinase
DP	$CD4^+CD8^+$ double positive
DSB	Double strand break
E_α	*Tcra* enhancer
E_β	*Tcrb* enhancer
E_δ	*Tcrd* enhancer
E_μ	*Igh* intronic enhancer
H2AX	Histone 2 variant
H3	Histone 3
H4	Histone 4
HDAC	Histone deacetylase

HR	Homologous recombination
HP1	Heterochromatin protein 1
hs	DNase I hypersensitivity site
HSC	Hematopoietic stem cell
iE_κ	*Igk* intronic enhancer
Ig	Immunoglobulin
IGCR1	Intergenic control region 1
Igh	Immunoglobulin heavy
Igk	Immunoglobulin kappa
Igl	Immunoglobulin lambda
J	Joining
kb	Kilobase pairs
LacI	Lactose repressor
lacO	Operator sequence from the lactose operon
LAT	Linker fore activation of T cells
Mb	Megabase pairs
Me	Methylation
MHC	Major histocompatibility complex
NHEJ	Non-homologous end joining

NPC	Nuclear pore complex
PAIR	Pax5-activated intergenic repeat
PCH	Pericentromeric heterochromatin
PHD	Plant homeodomain
PolII	RNA polymerase II
PD_β	D_β promoter
qPCR	Quantitative real time polymerase chain reaction
RAG	Recombination activating gene
RSS	Recombination signal sequence
SE	Signal end
Sis	Silencer in intervening sequence
SJ	Signal joint
SP	Single positive
TEA	T early a promoter
TCR	T cell receptor
Tcrb	T cell receptor beta
Tcra/Tcrd	T cell receptor alpha/T cell receptor delta
Tcrg	T cell receptor gamma
tg	transgene

V	Variable

Acknowledgements

First and foremost, thank you Mike. I appreciate the time and effort you put into training me, not only to conduct good research, but also to present it well. The suggestions and advice you gave also challenged me to develop the ability to think differently. Similarly, I would like to thank my committee for always taking the time to understand and improve the path of my project.

I have also been fortunate to be able to work alongside people I consider friends. Thank you Ryan, Chrys, Han-Yu, Shyam, Beth, Shiwei, and Zach for creating such an enjoyable lab environment.

I must also acknowledge Youngjoo, a rotation student who performed the DamID analyses, and Michael, an undergraduate student who came for a summer and looked at DSBs at *Tcrd* loci. Additionally, the DamID analyses could not have been completed without samples sent from Joseph Zullo, a previous graduate student in Harinder Singh's lab.

And last, but far from least, I have to thank my family. My amazing parents have supported me in every endeavor, and I cannot thank them enough for all they have done. And finally, to my wonderful husband Francis, who, among many other things, moved across an ocean for me. For that alone, I am forever grateful.

1. Introduction

1.1 Overview of V(D)J Recombination

The adaptive immune system is composed of highly specialized cells that eliminate or prevent pathogenic infection (Janeway 2005). These cells enable the immune system to recognize new infectious agents and remember specific pathogens encountered in the past. The main effector cells of the adaptive immune system are T- and B- lymphocytes, nearly all of which express a single unique receptor. The diverse repertoire of T cell receptors (TCR) and B cell receptors (BCR) identifies and eliminates infectious agents.

Antigen receptor locus recombination occurs in a highly-regulated lineage- and stage-specific manner. Each locus contains uniquely organized gene segments and regulatory elements (Cobb *et al.* 2006). BCR gene rearrangement takes place in the bone marrow, and occurs at immunoglobulin heavy (*Igh*), Ig kappa (*Igk*), and Ig lambda (*Igl*) loci. *Igh* loci undergo recombination first, in order to generate a functional (in-frame) IgH protein (Cobb *et al.* 2006). Then *Igk* and *Igl* loci recombine to form the Ig light chain. Heavy and light chains heterodimerization forms the BCR, which can allow for the cell to develop into a mature B-cell.

TCR gene rearrangement occurs in the thymus. TCRs are encoded by either *Tcrb* and *Tcra* or *Tcrd* and *Tcrg* loci. *Tcrb*, *Tcrd*, and *Tcrg* loci recombine first (Krangel 2009).

If productive *Tcrd* and *Tcrg* rearrangements are generated, the thymocyte will develop into a γδ T cell. If a functional TCRβ chain is generated, the cell will recombine *Tcra* loci. When a compatible TCRα chain is produced, it will pair with the TCRβ chain and the cell will proceed down the path to becoming an $\alpha\beta$ T cell.

Diverse TCRs and BCRs are generated in a molecular process of genetic rearrangement known as V(D)J recombination (Janeway 2005). B and T cell antigen receptor gene loci each contain multiple variable (V), joining (J), and sometimes diversity (D) gene segments (Cobb *et al.* 2006). During V(D)J recombination these gene segments are restructured, through the breaking and rejoining of DNA at antigen receptor loci. This process is mediated by two recombinase proteins, recombination activating gene 1 and 2 (RAG1/2) (Oettinger *et al.* 1990). Additional antigen receptor diversity is gained by the imprecise repair of the DNA breaks (Malu *et al.* 2012).

During V(D)J recombination, RAG1/2 proteins recognize and bind to recombination signal sequences (RSSs) that flank V, D, and J gene segments (Schatz and Swanson 2011) (Fig. 1). One RSS is located 3′ of each V gene segment and 5′ of each J segment, while RSSs are located both 5′ and 3′ of D gene segments. RSSs are composed of three DNA sequence components. At the 5′ end there is a conserved palindromic heptamer sequence (CACAGTG), then a nonrandom and less conserved spacer sequence

of either 12 or 23 base pair (bp), and finally a conserved AT-rich nonamer sequence (ACAAAAACC) at the 3′ end (Schatz and Swanson 2011).

Recombination occurs most efficiently between two RSSs containing different spacer lengths (i.e. one 12 bp RSS and one 23 bp RSS), a phenomenon known as the 12/23 rule (Bassing *et al.* 2000, Tillman *et al.* 2004). This rule safeguards against undesirable recombination events, such as a J segment with a 12 bp spacer rearranging with another J segment that also bears a 12 bp spacer. However the 12/23 rule is insufficient to solely regulate which RSSs recombine, as T cell receptor loci with V_β, D_β, and J_β gene segments will have potentially compatible spacers on the 3′ V_β gene segment RSS and both the 5′ D_β and 5′ J_β gene segment RSSs. V gene segments do not recombine with the compatible 5′ J_β RSS, in a restriction termed "beyond 12/23" (Tillman *et al.* 2004).

For recombination to occur, a synaptic complex consisting of a 12 bp RSS, a 23 bp RSS, and at least one RAG tetramer (two RAG1 and two RAG2 proteins) must be formed (Gellert 2002, Grundy *et al.* 2009) (Fig. 1). Synaptic complex formation is mediated by RAG1/2 (Hiom and Gellert 1998), which likely binds to (D)J gene segments (Ji *et al.* 2010) and 'captures' the distal V gene segment (Curry *et al.* 2005). Once a synaptic complex is formed, RAG1/2 complexes cleave DNA at the two sites that will later be joined, generating four double strand break (DSB) ends (Nishana and Raghavan 2012). Specifically, RAG1 nicks the 3′ hydroxyl group on one strand precisely between the RSS

and the coding gene sequences. The 3′ hydroxyl group then attacks the other strand of the DNA, forming a closed hairpin at the coding end and leaving the signal end DNA as a blunt DSB.

Both DNA pairs are ligated via the non-homologous end joining (NHEJ) pathway (Helmink and Sleckman 2012). The two coding ends form a coding joint, with previously distanced antigen receptor gene segments becoming located adjacent to each other (Lieber 2010) (Fig. 1). The two signal ends form a signal joint. If the RSSs are similarly oriented, the signal joint will be on an extrachromosomal DNA excision circle. If the RSSs are oriented in opposite directions, a DNA inversion will occur. If the V(D)J joined gene segments create an open reading frame, an antigen receptor protein chain can be expressed.

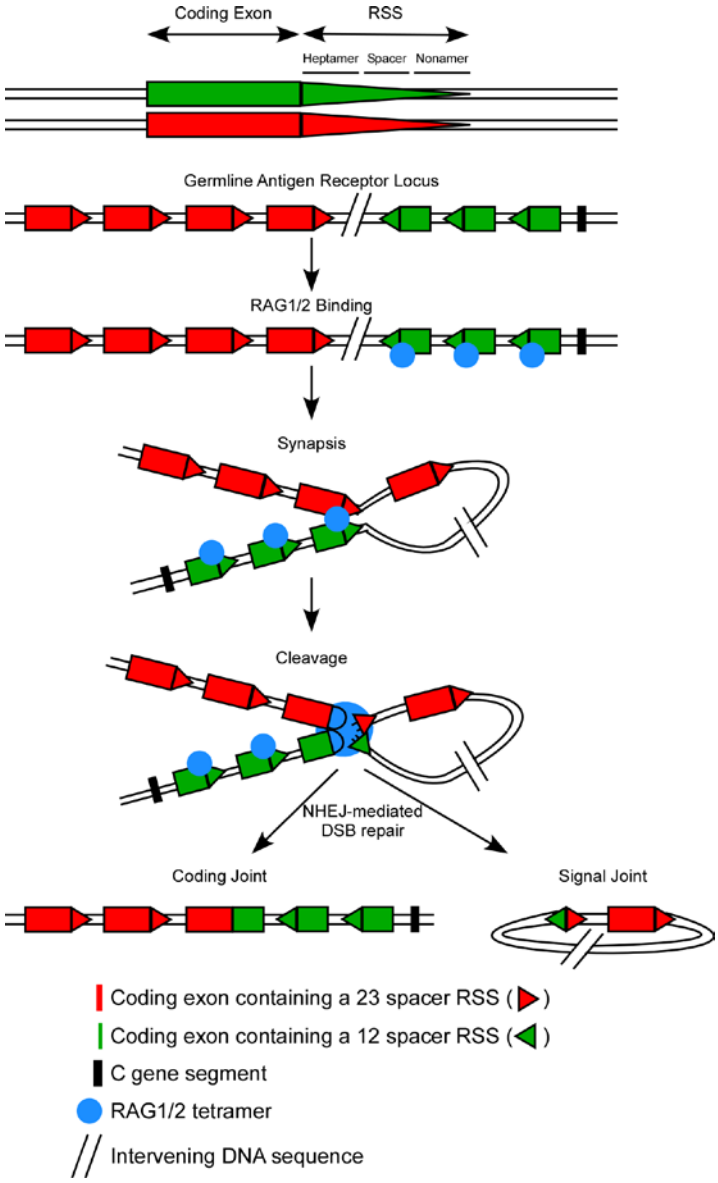

Figure 1: V(D)J recombination

Diagram of V(D)J recombination. Each V, D, and J gene segment is flanked by at least one RSS, which is composed of a heptamer, a 12 or 23 bp spacer sequence, and a nonamer. RSSs dictate the location of RAG1/2 binding. RAG1/2 then mediates synapsis formation and DNA cleavage between two gene segments and their adjacent RSSs. The two resulting DSBs recruit NHEJ repair factors in order to join the two coding exons to form a coding joint, and join the two RSSs to form a signal joint.

During NHEJ-mediated DSB repair, additional nucleotides are introduced into the antigen receptor coding sequence via two mechanisms (Schatz and Ji 2011). P nucleotides result from Artemis (Art)-dependent opening of the sealed coding end hairpins. After the single-stranded (ss) hairpins are opened, which occurs randomly, the resulting ssDNA tail is filled in with complementary nucleotides to form a blunt DNA end containing a short palindromic sequence (Janeway 2005). N nucleotides are added by a very different mechanism. N nucleotides are non-template-encoded, and up to 20 nucleotides can be added to ssDNA ends by the enzyme terminal deoxynucleotidyl transferase.

Tcrb and *Igh* loci are allelically excluded, so that only one allele per cell expresses a functional V-to-DJ rearranged protein (Fig. 2). This ensures that each lymphocyte displays only a single receptor. Allelic exclusion involves two steps: asynchronous recombination and feedback inhibition (Krangel 2009). The first step, also known as the initiation of allelic exclusion, must result from the recombination of one allele at a time. This asynchronous recombination may result either from infrequent stochastic recombination of both alleles, or the selection of one allele to recombine before the other. The second step, also known as the maintenance of allelic exclusion, prevents additional recombination once a functional rearrangement has been generated.

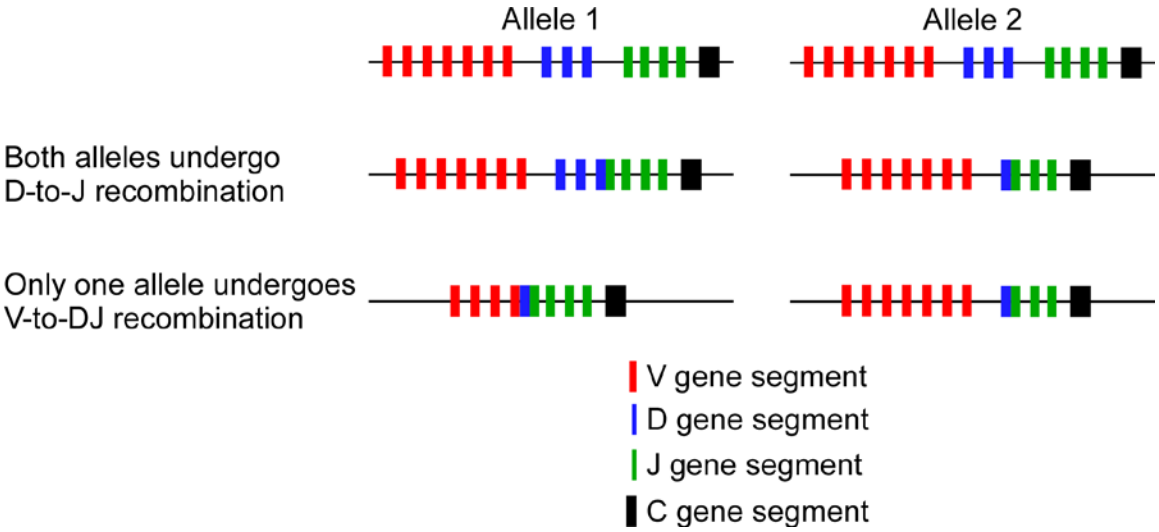

Figure 2: Allelic exclusion of *Tcrb* and *Igh* antigen receptor loci

Representation of allelic exclusion at *Tcrb* and *Igh* antigen receptor loci. Though both alleles within an individual cell undergo D-to-J recombination, only one allele generates a functional protein. *Igk* alleles are also subject to V-to-J allelic exclusion.

As antigen receptor loci are large and regions separated by many kilobases (kb) must be brought together in order to undergo V(D)J recombination, the conformations that antigen receptor loci adopt may permit or restrict V(D)J recombination (Sayegh *et al.* 2005, Skok *et al.* 2007, Shih and Krangel 2010). Loci contract, so that the regions to be recombined are situated in close proximity. Following recombination, loci ends decontract, reducing the likelihood of additional rearrangement (Roldan *et al.* 2005, Skok *et al.* 2007).

Recombination of antigen receptor loci may also be regulated by the subnuclear localization of antigen receptor alleles. Several studies have suggested that the subnuclear localization of antigen receptor genes may play an important role in regulating the frequency of recombination (Skok *et al.* 2001, Kosak *et al.* 2002, Roldan *et al.* 2005, Skok *et al.* 2007, Schlimgen *et al.* 2008), potentially serving as the mechanism of asynchronous recombination or feedback inhibition.

1.2 Lymphocyte Development

1.2.1 Hematopoiesis

Cells of the immune system, including T and B cells, develop from self-renewing hematopoietic stem cells (HSC) in the bone marrow (Ichii *et al.* 2010). HSCs have the ability to differentiate into many different cell types, and various stages of HSC differentiation have been identified using cell surface protein markers (Ichii *et al.* 2010). HSCs undergo asymmetric cell division, producing two daughter cells with differing functional fates. One daughter cell is programmed to differentiate into a more developmentally mature cell type, while the other retains HSC capabilities (Ho and Wagner 2007).

In the process of becoming T and B cells, HSCs first give rise to multipotent progenitor cells (MPP) (Weissman *et al.* 2001) which lack the ability to self-renew. MPPs can further differentiate into common lymphoid progenitors (CLP). CLPs can differentiate directly into B cells (Fig. 3) (Ramirez *et al.* 2010). T cell differentiation is a bit more complex (Bhandoola *et al.* 2007). CLPs migrate from the bone marrow to the thymus, a primary lymphoid organ, where T cell lineage specification and selection processes occur (Schlenner and Rodewald 2010). While CLPs can differentiate into T cells in the thymus, it is thought that *in vivo* lymphoid primed multipotent progenitors (LMPP) (Adolfsson *et al.* 2005) are the major source of early thymic progenitors (ETP).

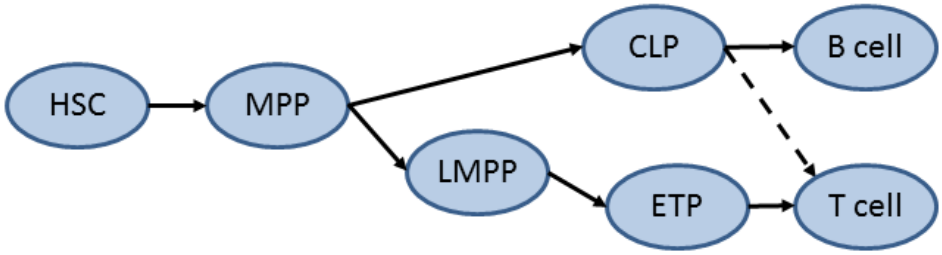

Figure 3: Overview of T and B cell differentiation

Schematic of major hematopoietic steps involved in T and B cell differentiation. HSC, hematopoietic stem cell; MPP, multipotent progenitor cell; CLP, common lymphoid progenitor; LMPP, lymphoid primed multipotent progenitor; ETP, early thymic progenitor; solid line, major pathway; dashed line, minor pathway.

1.2.2 B Cell Development

CLPs that will differentiate into B cells remain in the bone marrow and progress into the next stage of B cell development, the pre-pro B cell stage (Ramirez *et al.* 2010). In pre-pro B cells RAG1/2 proteins are expressed and ordered V(D)J recombination of immunoglobulin (Ig) gene segments (*Igh*, *Igk*, and *Igl*) begins. First, at *Igh* loci, D_H segments rearrange to J_H segments, usually on both *Igh* alleles within a cell (Fig. 4) (Cobb *et al.* 2006). In the following pro B cell stage, upstream V_H segments recombine with the DJ_H segments. Interestingly, V_H-to-DJ_H recombination is restricted so that only one allele per cell completes an in-frame rearrangement (Sonoda *et al.* 1997). If an in-frame V_H-to-DJ_H rearrangement occurs, the expressed IgH protein chain will heterodimerize with the surrogate light (L) chains and be exported to the cell surface as a pre-BCR (Vettermann *et al.* 2006). Signaling from the pre-BCR downregulates RAG1/2 expression, initiates proliferation, and promotes differentiation into the pre B cell stage.

In pre-B cells RAG1/2 proteins are again expressed, and *Ig* light chain loci undergo V-to-J recombination. There are two light chain gene loci, *Igk* and *Igl*, and *Igk* rearrangement precedes *Igl* rearrangement (Engel *et al.* 1999). If the first V-to-J rearrangement at an *Igk* locus is out-of-frame or generates a self-reactive BCR, the locus can undergo additional rearrangement events. These subsequent rearrangement events are known as secondary rearrangements. Additionally, if *Igk* primary and secondary

recombination ultimately proves unsuccessful, pre-B cells can be rescued by *Igl* recombination. If an in-frame light chain is generated, the heavy and light chains will pair to form the completed BCR.

Prior to migration into the periphery, naïve B cells must pass a tolerance checkpoint. If the BCR on the cell surface binds to antigen in the bone marrow, the cell will undergo receptor editing, apoptosis, or anergy in order to prevent B cell autoreactivity in the periphery (Monroe *et al.* 2003, Edry and Melamed 2004, Allman and Pillai 2008). Impressively, V(D)J recombination generates a B cell repertoire expressing antibodies capable of identifying more than 5×10^{13} distinct antigens (Pieper *et al.* 2013). B cells in the midst of an immune response undergo further genetic alterations in germinal centers (Muramatsu *et al.* 2000), altering both the antibody affinity and the isotype (Maul and Gearhart 2010).

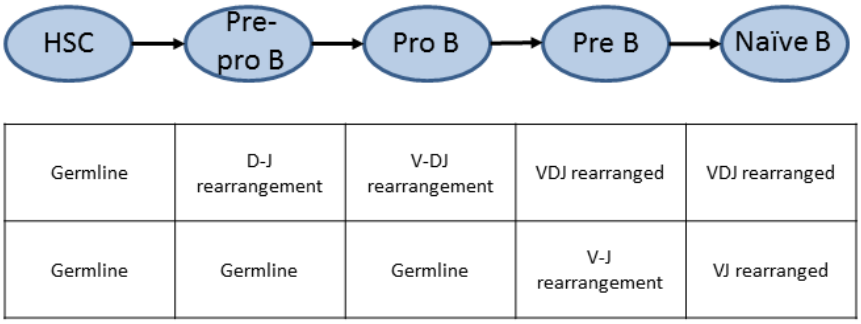

Figure 4: Diagram of B cell development

Major stages of B cell development occurring in the bone marrow, as well as the recombination events taking place at each developmental stage. HSC, hematopoietic stem cell.

1.2.3 T Cell Development

Until recently, the thymus was believed to be devoid of self-renewing cells. However in the absence of competitive precursor cells, early stage thymocytes can self-renew and sustain T cell development (Martins *et al.* 2012, Peaudecerf *et al.* 2012). CD4 and CD8 cell surface expression status varies during thymocyte development, allowing for convenient identification and separation of developmental stages based on these surface markers. Thymic immigrants initially lack expression of both CD4 and CD8, and are thus termed double negative (DN). DN thymocytes can be further divided into DN1-DN4 stages based on CD25 and CD44 expression (DN1: $CD44^{+}$ $CD25^{-}$, DN2: $CD44^{+}CD25^{+}$, DN3: $CD44^{-}CD25^{+}$, DN4: $CD44^{-}CD25^{-}$). T cell specification occurs upon progression into the DN2 stage, and cells are committed to the T lineage in the DN3

stage (Godfrey and Zlotnik 1993, Porritt *et al.* 2004). During the DN2/3 stages, *Tcrg* and *Tcrd* antigen receptor loci recombine (Fig. 5) (Livak *et al.* 1999). If a DN2/3 thymocyte successfully generates productive rearrangements at both *Tcrd* and *Tcrg* loci, a γδ TCR can be expressed, development will be diverted toward the γδ T cell lineage, and the cell may exit the thymus as a γδ T cell (Kreslavsky *et al.* 2010).

However most DN3 thymocytes go on to become αβ T cells. In order to do so, *Tcrb* alleles must undergo recombination, also initiating at the DN2/3 stages (Livak *et al.* 1999). *Tcrb* alleles, like *Igh* alleles, require two sequential steps of recombination (Krangel 2009). *Tcrb* alleles first undergo D_β-to-J_β rearrangement which begin in DN2 thymocytes, and usually occurs on both alleles (Jackson and Krangel 2006). Then individual DN3 thymocytes undergo V_β-to-DJ_β recombination. Again analogous to *Igh* alleles, *Tcrb* alleles are regulated so that only one allele carries a complete in-frame VDJ exon per cell, termed allelic exclusion (Khor and Sleckman 2002). If rearrangements at a *Tcrb* allele generate an in-frame TCRβ chain, the TCRβ chain will heterodimerize with pre-Tα to form the pre-TCR. Pre-TCR signaling satisfies the β-selection checkpoint, and cells progress into DN4 thymocytes. DN4 thymocytes proliferate and downregulate *Rag1/2* expression (Michie and Zuniga-Pflucker 2002), prior to transitioning into DP thymocytes. In DP thymocytes, *Rag1/2* genes are re-expressed and *Tcra* recombination occurs (Krangel 2009).

Once an αβ TCR is expressed on the cell surface, it must be tested for reactivity with self-antigens in the context of the major histocompatibility complexes (MHC) (Starr *et al.* 2003). Importantly, cells expressing TCRs that strongly bind self-antigen presented by MHC will be deleted to avoid self-reactivity in the periphery, termed negative selection. Additionally, cells that do not bind MHC fail to undergo positive selection and will not survive, in order to ensure that TCRs in the periphery can engage MHC (Lo and Allen 2013). DP thymocytes have only 3-4 days in which to undergo *Tcra* recombination, express a complete αβ TCR and engage with MHC-expressing thymic cortical epithelial cells (Cosgrove *et al.* 1992) to be positively selected, and avoid programmed cell death (Huesmann *et al.* 1991).

Interestingly, it is common for individual *Tcra* alleles to undergo several rounds of recombination (Krangel *et al.* 2004, Krangel 2009). This allows thymocytes that initially expressed a TCR unable to engage MHC the chance to undergo additional *Tcra* recombination that may alter binding specificity (Kisielow *et al.* 1988). In addition, *Tcra* alleles are not subject to allelic exclusion, as both alleles in individual DP thymocyte nuclei often contain in-frame V_α-to-J_α rearrangements (Borgulya *et al.* 1992). *Tcra* recombination occurs from the inside out (Krangel *et al.* 2004). In other words, primary *Tcra* recombination preferentially occurs at 3′ V_α and 5′ J_α gene segments and secondary rearrangements use more 5′ V_α and 3′ J_α gene segments. Following engagement of an

αβ TCR with MHC in the thymus, RAG1/2 and either CD4 or CD8 expression is downregulated, and cells leave the thymus as single positive (SP) T cells (Krangel *et al.* 2004).

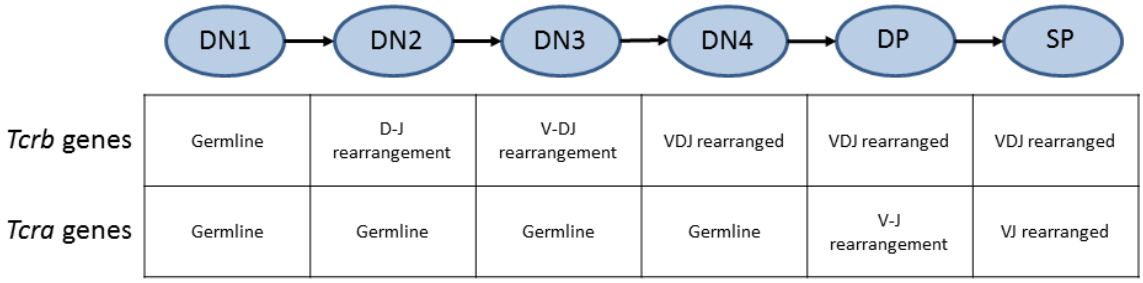

Figure 5: Diagram of T cell development

Stages of T cell development occurring in the thymus. DN, double negative, DP, double positive; SP, single positive.

1.3 Antigen Receptor Locus Organization

The seven antigen receptor proteins (IgH, Igκ, Igλ, TCRβ, TCRα, TCRδ, and TCRγ) are encoded by six genetic loci (*Igh*, *Igk*, *Igl*, *Tcrb*, *Tcra*/*Tcrd*, and *Tcrg*) (Fig. 6) in the murine genome (Cobb *et al.* 2006). Loci range in size from a couple hundred kilobasepairs (kb) to over 3 megabasepairs (Mb), and are fundamentally similar in structure. All loci contain multiple gene segments that can be joined to each other and then expressed with a constant (C) region gene. V gene segments are located at the 5′ end of each locus, J gene segments at the 3′ end, and D segments, if present, are located

between the V and J segments. Located 3′ of J segments are C region genes, which do not undergo V(D)J recombination.

Transcription regulates accessibility and recombination (Abarrategui and Krangel 2009). Transcription of antigen receptor gene loci is regulated by several elements, such as enhancers, promoters, and insulators. Each V gene segment is 3′ of a promoter, which drives transcription prior to and following recombination (if that gene segment has not been excised by rearrangement events). Transcription at downstream D and J gene segments is generally controlled by 3′ enhancer elements that activate promoters associated with D or J gene segments.

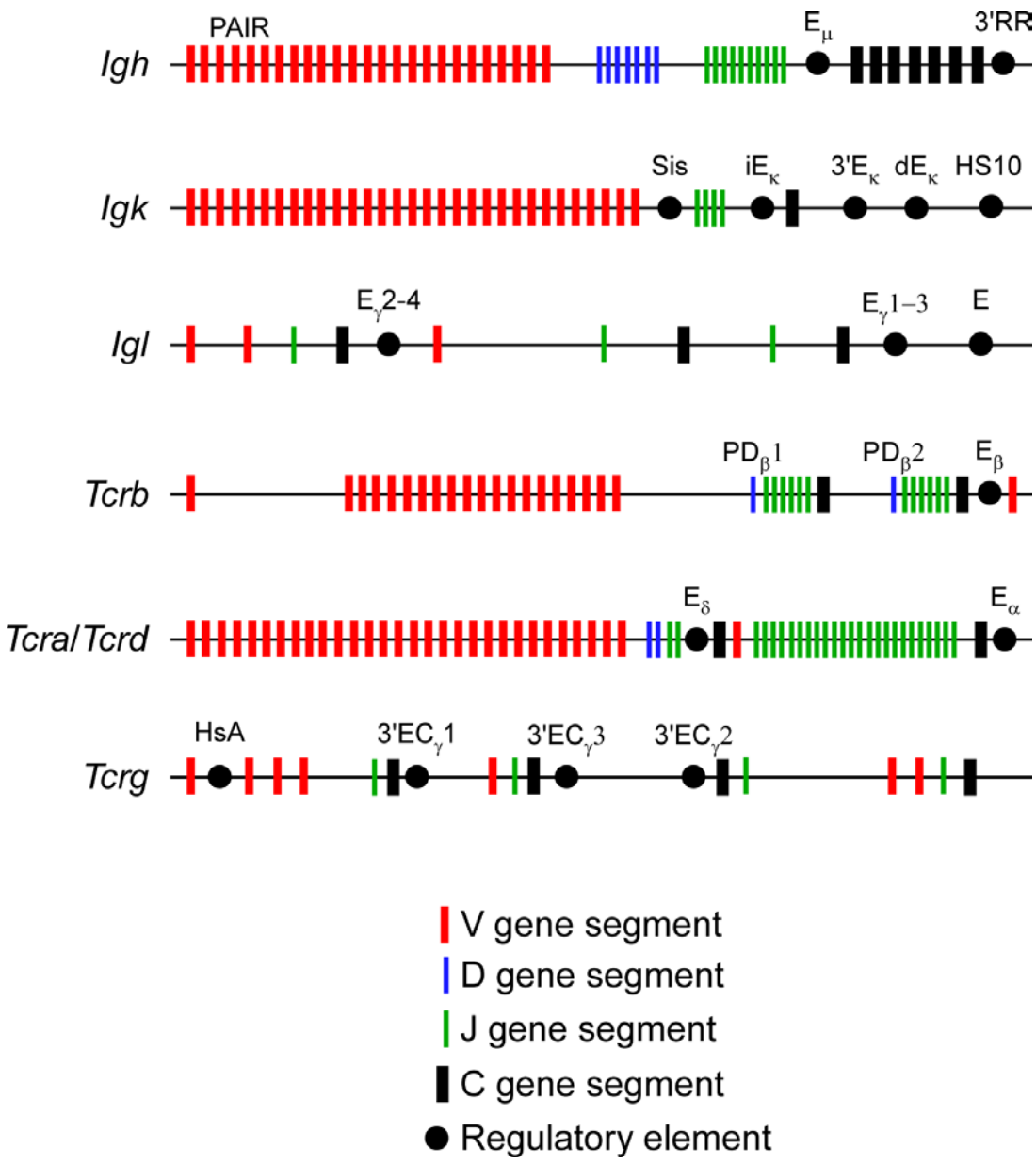

Figure 6: Germline organization of murine antigen receptor loci

Diagram of the six murine antigen receptor loci, not drawn to scale. V gene segments are represented by red rectangles, D gene segments are represented by blue rectangles, J gene segments are represented by green rectangles, constant regions are represented by black rectangles, and regulatory elements are represented by black circles.

1.3.1 B Cell Antigen Receptor Locus Organization and Regulation

The three BCR proteins are encoded by three genetic loci, each located on a different chromosome. The locus that encodes the IgH chain is located on murine chromosome 12, the locus that encodes the Igκ chain is on chromosome 6, and the locus that encodes the Igλ chain is on chromosome 16 (Honjo *et al.* 2004).

1.3.1.1 *Igh* locus

The C57BL/6 murine *Igh* locus extends 3.3 Mb and includes nearly 200 V_H gene segments spanning nearly 3 Mbps, between 10 and 15 D_H gene segments spanning roughly 120 kb, 4 J_H gene segments, and 8 C_H region gene segments spanning 190 kbps (Johnston *et al.* 2006, Jung *et al.* 2006). The multiple C_H gene segments permit class switch recombination in peripheral mature B cells, in order to generate antibody isotypes capable of distinct effector functions (Xu *et al.* 2012). All D_H segments are grouped between the V_H and J_H segments, permitting each *Igh* allele only one chance to generate an in-frame V_H-to-DJ_H rearrangement.

Transcription and chromatin structure at the *Igh* locus is controlled by several regulatory regions (Roy *et al.* 2011). The intronic enhancer, (E_μ), is positioned between the J_H and C_H clusters. E_μ is required for efficient *Igh* V(D)J recombination because it controls transcription and chromatin accessibility across the DJ_H region, and likely

because it controls the initial D_H-to-J_H recombination step (Perlot *et al.* 2005, Afshar *et al.* 2006, Chakraborty *et al.* 2009). E_μ is also required for relocation of *Igh* loci away from the repressive nuclear periphery prior to recombination (Guo *et al.* 2011).

As *Igh* loci are quite large and distant regions must be brought into close proximity for recombination to occur, the three-dimensional (3D) conformation plays an important role in regulating recombination (Bossen *et al.* 2012). Interestingly, E_μ is involved in large-scale locus contraction and the formation of a loop at the 3′ end of the *Igh* locus (Guo *et al.* 2011, Medvedovic *et al.* 2013). Two other E_μ independent loop domains have been identified at the 5′ end of the locus (Guo *et al.* 2011).

Another regulatory element, the 3′ regulatory region (RR), spans about 40 kb downstream of the most 3′ C_H gene (Pinaud *et al.* 2011). The 3′ RR contains seven DNA hypersensitivity (hs) sites. The first four hs sites serve as enhancers in late B cell development, during class switch recombination (Vincent-Fabert *et al.* 2010). The last three play a minor role in distal V_H usage, by weakly insulating transcription of nearby (~65 kb) downstream genes and contributing slightly to locus contraction (Volpi *et al.* 2012).

Conformational changes that bring together distant regions of the *Igh* locus are often achieved by forming chromatin loops, mediated by CCCTC-binding factor (CTCF) and cohesin (Merkenschlager and Odom 2013). Interestingly, there are 9 CCTF-binding

elements located downstream of the 3′ RR, which may also demarcate the 3′ edge of the *Igh* locus (Garrett *et al.* 2005) known as the 3′ CTCF binding element (CBE) (Garrett *et al.* 2005, Degner *et al.* 2011). The 3′ CBE supports germline transcription, loop formation, and class switch recombination (CSR) (Birshtein 2012).

Approximately 100 kb of intergenic sequence located between D_H and J_H gene segments is responsible for preventing V_H-to-DJ_H recombination in thymocyte nuclei (Giallourakis *et al.* 2010). Loss of that 100 kb resulted in increased sense and antisense transcription beginning at the D_H cluster, as well as increased D_H-to-J_H recombination and some V_H-to-DJ_H recombination in developing T cells. Further analysis showed that a shorter 4.1 kb stretch within that 100 kb intergenic region, termed the intergenic control region 1 (IGCR1), maintains ordered, lineage-specific, and allelically excluded *Igh* recombination (Johnston *et al.* 2006, Guo *et al.* 2011). There are two CBE sites within the IGCR1 that reduce transcription and usage of proximal (within 100 kb) V_H gene segments (Guo *et al.* 2011). Additionally, the two CBE sites in the IGCR1 are required for lineage-specific *Igh* V_H-to-DJ_H recombination.

Recently, transcription at distal V_H gene segments was found to be regulated by 14 conserved sequences, named Pax5-activated intergenic repeat (PAIR) elements (Ebert *et al.* 2011). Pax5, E2A, CTCF, and Rad21 bind the PAIR elements, and form chromatin loops that support interactions between the upstream V_H gene segments and Eμ

(Verma-Gaur *et al.* 2012), likely promoting efficient rearrangement of 5′ V_H gene segments.

1.3.1.2 *Igk* locus

The *Igk* locus and extends 3.2 Mb and contains roughly 120 V_κ gene segments, 4 J_κ gene segments, and one C_κ gene segment (Brekke and Garrard 2004). The J_κ and C_κ genes occupy only 20kb of this large locus, at the 3′ end.

There are four known *Igk* enhancers, each with various functions that often overlap with each another. The intronic enhancer (iE_κ) is located between the J_κ and C_κ gene segments (Queen and Baltimore 1983), the 3′ enhancer ($3'E_\kappa$) is downstream of C_κ, the downstream enhancer (dE_κ) enhancer is located 3′ of $3'E_\kappa$ (Schlissel 2004), and the hs site 10 (HS10) is located approximately 10 kb downstream of dE_κ (Zhou *et al.* 2012). To investigate the function of each enhancer, they were each individually deleted (Gorman *et al.* 1996, Xu *et al.* 1996, Xiang and Garrard 2008, Zhou *et al.* 2012). iE_κ and $3'E_\kappa$ regulate recombination (Gorman *et al.* 1996, Xu *et al.* 1996), whereas $3'E_\kappa$, dE_κ, and HS10 mediate *Igk* transcription (Gorman *et al.* 1996, Xiang and Garrard 2008, Zhou *et al.* 2012). Interestingly, double deletion of iE_κ and $3'E\kappa$ completely prevents *Igk* recombination (Xiang and Garrard 2008), and deletion of $3'E_\kappa$ and dE_κ abolishes transcription (Inlay *et al.* 2002).

There are ~60 CTCF-bound sites at *Igk* loci in pre B cells (Degner *et al.* 2011, Ribeiro de Almeida *et al.* 2011). It is therefore unsurprising that CTCF plays an important role in the regulation of *Igk* recombination. Pre B cells from mice lacking CTCF in B-lineage cells and containing a pre-rearranged Igμ transgene (tg) showed a strong bias toward usage of proximal V_κ gene segments (Ribeiro de Almeida *et al.* 2011). In addition, germline transcription of proximal V_κ gene segments and interactions between two *Igk* enhancers (iE_κ and $3'E_\kappa$) and proximal V_κ gene segments were increased in the absence of CTCF. It appears that CTCF functions as an insulator at *Igk* loci, limiting enhancer interaction with proximal V_κ gene segments.

A recombination silencer known as silencer in intervening sequence (Sis) was identified at the *Igk* locus (Liu *et al.* 2002). Sis is located between the V_κ and J_κ gene segments, and supports proper V_κ usage (Xiang *et al.* 2011). Sis contains CTCF binding sites, which reduce the usage of proximal V_κ gene segments, likely by functioning similarly to other CTCF sites at *Igk* loci, as a transcriptional insulator.

Sis is also involved in the monoallelic subnuclear positioning of both *Igk* and *Igh* alleles at pericentromeric heterchromatin (PCH), a known repressive subnuclear compartment (Xiang *et al.* 2011). Some have postulated that monoallelic positioning at repressive subnuclear compartments may mediate allelic exclusion (Roldan *et al.* 2005). However, both loci are still allelically excluded in Sis-deficient B cells, suggesting that

PCH-association does not play a role in either the initiation or maintenance of allelic exclusion at *Igh* and *Igk* loci.

1.3.1.3 *Igl* locus

The murine *Igl* locus spans only 240 kb, is more limited, and is structured differently than *Igh* and *Igk* loci. The locus contains two clusters of VJ gene segments. The first contains two V_λ gene segments followed by one functional J_λ segment and one C_λ segment. The second contains a single V_λ gene followed by two sets of functional J_λ and C_λ segments. There are also three known enhancers, one located downstream of the first JC_λ cluster and two located downstream of the second JC_λ cluster (Eccles *et al.* 1990, Hagman *et al.* 1990).

1.3.2 T Cell Antigen Receptor Locus Organization and Regulation

The four TCR proteins are encoded by only three gene loci. The gene that encodes the TCRβ chain is located on murine chromosome 6 (Caccia *et al.* 1984), the gene that encodes the TCRγ chain is on chromosome 13, and the gene locus that encodes both the TCRα and TCRδ chains is on chromosome 14 (Kranz *et al.* 1985).

1.3.2.1 *Tcrb* locus

The *Tcrb* locus is spans approximately 700 kb. The locus includes 25 functional V_β gene segments and two DJC_β clusters each containing one D_β segment, 6 J_β segments, and one C_β region (Sikes and Oltz 2012). Each of the two DJC_β clusters can undergo D_β-J_β recombination, and V_β can recombine with either of the two DJ_β rearrangements. This gives each *Tcrb* allele up to two chances to generate a function V(D)J rearrangement. Two of the V_β genes are separated from the main V_β gene cluster. $V_\beta2$ is located 150 kb upstream of the V_β gene cluster, and $V_\beta14$ is downstream of the $DJC_{\beta2}$ cluster. The main V_β gene cluster is separated from the two DJC_β clusters by a trypsinogen region spanning roughly 250 kb. Recombination of either DJ_β to any V_β other than $V_\beta14$ would excise the trypsinogen region, whereas recombination to $V_\beta14$ results in a DNA inversion.

There is one known enhancer (E_β), located between $C_\beta2$ and $V_\beta14$, which is essential for *Tcrb* transcription and recombination. Loss of E_β blocks thymocyte development at the DN stage, as it prevents both D_β-to-J_β and V_β-to-DJ_β recombination (Bories *et al.* 1996, Leduc *et al.* 2000). Recombination is likely halted at *Tcrb* loci lacking E_β because the enhancer directs chromatin accessibility and transcription over both DJC_β clusters (Mathieu *et al.* 2003, Oestreich *et al.* 2006). E_β is also thought to support long-range chromatin interactions and stabilize coding ends, allowing for more frequent

distal V_β usage (Mathieu *et al.* 2003). However E_β is not required for the expression of a functionally pre-rearranged TCRβ chain (Busse *et al.* 2005).

5′ of each DJC_β cluster sits a relatively strong promoter ($PD_\beta1$ and $PD_\beta2$) (Sikes *et al.* 1998, Sikes *et al.* 2002, McMillan and Sikes 2008). Each promoter locally controls the activity of the DJC_β cluster with which they are associated (Whitehurst *et al.* 1999).

1.3.2.2 *Tcra/Tcrd* locus

The *Tcra/Tcrd* locus spans 1.6 Mb, 1.5 Mb of which is composed of ~100 $V_{\alpha/\delta}$ gene segments (Shih *et al.* 2011). The 3′ 100 kb is predominantly composed of 61 J_α gene segments, with a single C_α and the *Tcra* enhancer (E_α) at the very end (Krangel 2009). The *Tcrd* locus is composed of two D_δ gene segments, two J_δ segments, and one C_δ region. The D_δ and J_δ gene segments of the *Tcrd* locus are embedded within the *Tcra* locus, between the V_α and J_α segments. Though most V gene segments can recombine with J_α gene segments, only some recombine with J_α gene segments. Interestingly, if V_α-to-J_α *Tcra* rearrangement occurs, the entire *Tcrd* locus will be excised and the thymocyte will be unable to differentiate into a γδ T cell.

Each locus contains a single enhancer, both adjacent to their respective C region exons. The delta enhancer (E_δ) is positioned between $J_\delta2$ and C_δ, and promotes *Tcrd* recombination in DN thymocytes. However, deletion of E_δ does not completely

abrogate *Tcrd* recombination (Monroe *et al.* 1999). E_δ promotes transcription and chromatin accessibility locally in adult DN thymocytes (Hao and Krangel 2011), but is not required for expression of a fully-rearranged TCRδ chain in γδ T cells (Monroe *et al.* 1999).

E_α is a robust enhancer located 3′ of the C_α segment (Sleckman *et al.* 1997). E_α is activated in DP thymocytes and is required for *Tcra*/*Tcrd* transcription (Sleckman *et al.* 1997), *Tcra* recombination (Hernandez-Munain *et al.* 1999), and *Tcra*/*Tcrd* locus conformational changes (Shih and Krangel 2013). Interestingly, E_α is required for the expression of a TCRδ chain in γδ T cells (Sleckman *et al.* 1997).

The *Tcra*/*Tcrd* locus also contains a powerful promoter positioned at the 5′ end of the J_α array, called T early α (TEA) (Villey *et al.* 1996, Hernandez-Munain *et al.* 1999). TEA is activated by E_α and promotes transcription of 5′ J_α gene segments, and is required for ordered usage of the J_α array (Villey *et al.* 1996, Hawwari and Krangel 2005, Abarrategui and Krangel 2007).

1.3.2.3 *Tcrg* locus

The *Tcrg* locus spans 205 kb and includes four clusters of one or more V_γ gene segments, one J_γ gene segment, and one C_γ gene segment (Vernooij *et al.* 1993). The most 5′ cluster contains four V_γ gene segments, whereas the other three contain only a

single V_γ gene segment. Two proximal V_γ gene segments recombine only in the early fetal thymus, and at later developmental stages a different V_γ gene segment dominates (Krangel 2009). Like the *Igl* locus, the *Tcrg* locus is relatively limited.

Two regulatory elements, HsA and 3′EC_γ1, synergistically support C_γ1 transcription, but only have a small effect on *Tcrg* rearrangement (Xiong *et al.* 2002). HsA is positioned between the two most 5′ V_γ gene segments (Baker *et al.* 1998) and 3′EC_γ1 is 3′ of the first C_γ gene segment (Spencer *et al.* 1991). Interestingly, V_γ promoter activity and locus organization play more important roles in the regulation of V_γ usage (Baker *et al.* 1998, Xiong *et al.* 2004, Xiong *et al.* 2008).

1.4 Nuclear Organization

1.4.1 Chromatin and Chromosomes

DNA within the mammalian nucleus is highly organized (Cheung and Reddy 2012). In the broadest sense, DNA can be divided into heterochromatin and euchromatin, which tend to occupy distinct subnuclear locations. Euchromatin is gene-dense and can be efficiently transcribed, whereas heterochromatin tends to be gene-poor and is less frequently expressed. Fluorescence *in situ* hybridization (FISH) and live cell imaging using fluorescently tagged protein probes has permitted visualizing of the

location of specific DNA sequences within nuclei, and ultimately provided insight into the preferred subnuclear positions of various types of chromatin.

Chromosomes reside in individual territories, which have been identified using three dimensional (3D) FISH chromosome 'painting' techniques (Carter 1994). CT positioning within nuclei is evolutionarily conserved and cell-type-specific (Misteli 2004, Cremer *et al.* 2006). CT location with respect to subnuclear compartments, such as the nuclear periphery, is also biased, with gene-dense chromosomes favoring the nuclear interior and gene-poor chromosome segments more commonly located at the nuclear periphery. Gene-dense regions of chromosomes are found more frequently at the border of their chromosome territory (CT), and highly transcribed genes may 'loop out' of their territory to allow more efficient transcription (Kalhor *et al.* 2012). However positioning of genes outside of their chromosome territory may not be sufficient to activate or increase transcriptional activity (Morey *et al.* 2009). In addition, multiple distinct regions of highly transcribed genes along linear DNA cluster together (Palstra *et al.* 2008). Interestingly, maintenance of these long-range interactions does not require continued transcription.

Recombination at antigen receptor loci may be influenced by the positioning of the gene locus relative to the CT. One *Tcra* allele per cell was shown to 'loop out' of its CT in DP thymocytes (Chaumeil *et al.* 2013). Intriguingly, the looped out allele was

more often transcribed, free of repressive subnuclear compartments, and undergoing recombination than the non-looped allele. It is currently unknown whether *Tcrb* alleles loop out of their CT, or whether looping regulates *Tcrb* recombination.

1.4.2 Transcription Factories

Transcription is an important regulator of recombination at antigen receptor loci (Abarrategui and Krangel 2009). Most protein-coding genes are transcribed by RNA polymerase II (PolII) in a complex process involving many factors (Kornberg 2007). Transcription is initiated by phosphorylation of PolII at serine (Ser) 5 and Ser7 residues on the C-terminal domain (CTD), whereas elongating PolII gains phosphorylation of Ser2 and loses Ser5 phosphorylation.

PolII forms concentrated regions within nuclei, termed a 'factories' (Iborra *et al.* 1996, Cook 2010). These clusters of concentrated PolII have been visualized, the locations of which coincide with many actively transcribing genes in both fixed (Osborne *et al.* 2004, Ragoczy *et al.* 2006, Osborne *et al.* 2007, Mitchell and Fraser 2008, Sutherland and Bickmore 2009, Ferrai *et al.* 2010, Schoenfelder *et al.* 2010) and live cells (Ghamari *et al.* 2013). Intriguingly, certain genes may be recruited to transcription factories (Osborne *et al.* 2004, Ragoczy *et al.* 2006, Osborne *et al.* 2007, Schoenfelder *et al.* 2010).

Transcription factories can be specialized, and contain splicing, polyadenylation, and DNA repair factors (Cheung and Reddy 2012). RNA splicing is required to remove introns from pre-mRNA transcripts, converting pre-mRNA into functional transcripts that are then exported to the cytoplasm (Will and Luhrmann 2011). Nuclear speckles are also enriched in splicing factors, and there are typically 15-40 nuclear speckles in each nucleus. Nuclear speckles are often found in close proximity to the survival of motor neuron protein (SMN) complex (Gubitz *et al.* 2004). The SMN complex is required for spliceosome assembly and is composed of SMN, small nuclear ribonucleic particles (snRNP), and Gem-associated proteins (Will and Luhrmann 2011). Together, the subnuclear location of transcription and transcript processing likely play an important role in the regulation of transcription.

1.4.3 Pericentromeric Heterochromatin

Antigen receptor alleles have been reported to frequently associate with PCH (Skok *et al.* 2001, Schlimgen *et al.* 2008). Nearly 100 years ago, regions that remained condensed throughout the cell cycle were identified and termed heterochromatin, as they happened to be present on both homologous chromosomes (Probst and Almouzni 2008). Since then various constitutive and facultative forms of heterochromatin have been identified, one of which is located adjacent to the chromosome centromeres,

termed pericentromeric heterochromatin (PCH) (Towbin *et al.* 2013). Centromeres are involved in the regulation of chromosome organization and segregation during mitosis (Westhorpe and Straight 2013). PCH DNA was found to be highly repetitive, gene poor, and highly methylated at CpG sites (Lewis *et al.* 1992). PCH regions cluster together, forming subnuclear domains that can be visualized by staining with 6-diamidino-2-phenylindole (DAPI) as bright foci (Guenatri *et al.* 2004). These clusters function in subnuclear organization, serving as sites where transcription is reduced or silent (Sadaie *et al.* 2008).

There is a strong correlation between PCH-gene association and transcriptional repression. For example, in B cells only the expressed *Cd19* gene is free of PCH, whereas the unexpressed *Cd2*, *Cd4*, and *Cd8a* genes are brought to a PCH cluster (Brown *et al.* 1997). Conversely, *Cd8a* is free of PCH when it is expressed in DP thymocyte nuclei (Merkenschlager *et al.* 2004). Positioning at PCH may be mediated in *trans* by the transcription factor Ikaros, as Ikaros colocalizes with genes that associate with and are repressed at PCH in a developmentally regulated manner (Brown *et al.* 1997, Brown *et al.* 1999).

PCH DNA is transcriptionally silenced via two known mechanisms. The first is through PCH association with heterochromatin protein 1 (HP1). HP1 can induce and maintain heterochromatization via a chromodomain that binds H3K9me (Lomberk *et al.*

2006). In yeast, silencing of PCH is mediated by repeats located in the centromeric DNA that encode small interfering RNAs (siRNAs) (Reinhart and Bartel 2002, Volpe *et al.* 2002). The siRNA accumulates at nearby transcription sites, and mediates H3K9me-dependent heterochromatin formation and gene repression (Grewal and Moazed 2003, Buhler *et al.* 2007).

1.4.4 The Nuclear Periphery

Nearly all antigen receptor loci are positioned at the nuclear periphery in non-lymphoid cells or in early lymphoid progenitors, but relocate away from the periphery prior to recombination (Kosak *et al.* 2002, Schlimgen *et al.* 2008). This suggests that association with the nuclear periphery may regulate recombination at antigen receptor loci. The nuclear envelope is composed of a double lipid bilayer (the inner and outer nuclear membranes), nuclear pore complexes, and the nuclear lamina (Gerace and Huber 2012). The nuclear envelope separates the nucleoplasm from the cytoplasm within a cell, and also organizes chromatin and regulates gene function (Fig. 7) (Cheung and Reddy 2012, Raices and D'Angelo 2012). The outer nuclear membrane is contiguous with the endoplasmic reticulum, whereas the inner nuclear membrane connects to the outer nuclear membrane via nuclear pore complexes and encloses the nucleoplasm. The

nuclear lamina covers the nucleoplasmic side of the inner nuclear membrane, and serves as a structuring element for the nucleus and as a chromatin scaffold (Cortelli *et al.* 2012).

The nuclear periphery is thought to exemplify a repressive subnuclear compartment. Certain genes are regulated so that transcriptional activity correlates with gene positioning at or away from the nuclear periphery (Hewitt *et al.* 2004, Zink *et al.* 2004, Williams *et al.* 2006, Peric-Hupkes and van Steensel 2010). Furthermore, when certain active genes are forcibly relocated to the nuclear periphery, their transcription was reduced (Finlan *et al.* 2008, Kumaran and Spector 2008, Reddy *et al.* 2008, Zullo *et al.* 2012).

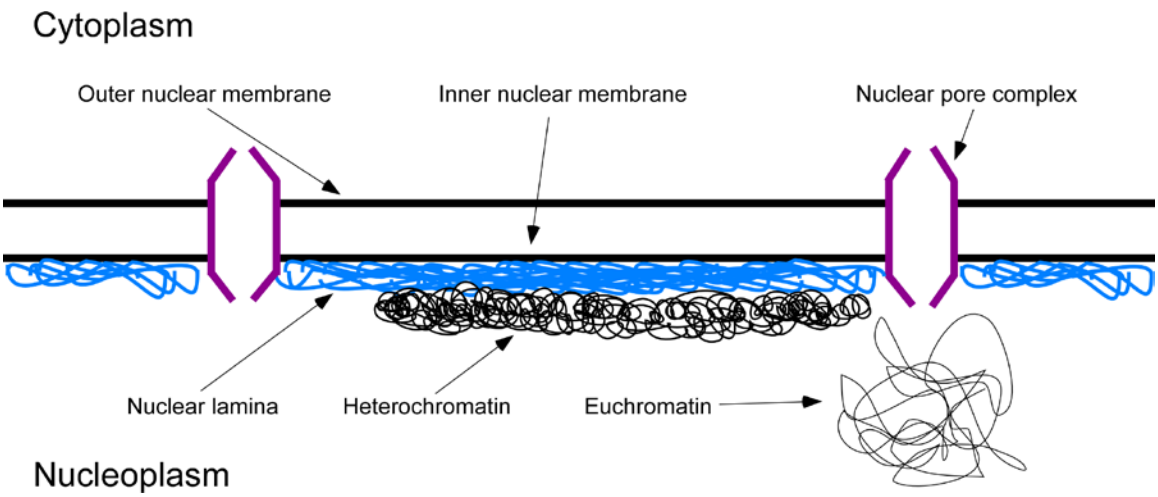

Figure 7: The nuclear periphery

Overview of the nuclear envelope, including the inner and outer nuclear membrane, nuclear pore complexes, and the nuclear lamina. Specifically, the nuclear lamina and nuclear pore complexes organize the subnuclear localization of heterochromatin and euchromatin, respectively.

1.4.4.1 The Nuclear Lamina

The nuclear lamina is a thin but dense network of intermediate filaments and membrane associated proteins (Cortelli *et al.* 2012). Lamins are type V intermediate filaments. A single gene codes for lamin A and lamin C, which are splice variants of a single gene transcript. A- and B-type lamins contain a nuclear localization signal (NLS) at the C-terminus, and a phosphorylation site that regulates conformational changes and lamina disassembly prior to mitosis. A-type (A/C) and B-type (B1/B2) lamins differ in sequence, biochemical properties, and localization during the cell cycle. A-type lamins are located both at the nuclear periphery and in the nucleoplasm, whereas B-type lamins

are only found at the inner nuclear membrane (Rusinol and Sinensky 2006, Vlcek and Foisner 2007). Lamin monomers associate head-to-tail to form antiparallel protofilaments. Protofilaments again aggregate to form intermediate-like filaments, which can support nuclear structure, anchor nuclear pore complexes, organize chromatin, and regulate DNA replication (Bridger *et al.* 2007).

Lamins, emerin, nesprins, lamin-associated polypeptides (LAP) 2, and lamin B receptor (LBR) proteins form the macromoleular complex that links the nucleoskeleton to the cytoskeleton (Meinke *et al.* 2011). There are several known ways in which this macromolecule complex can interact with the genome. For example, lamins contain a chromatin binding site in the tail domain that can directly interact with core histones (Taniura *et al.* 1995). Lamins can also interact with matrix attachment regions (MARs) through their α-helical domains. (Goldman *et al.* 2002). MARs are 300-1000 bp sequences which attach to the nuclear matrix, a network of fibers throughout the nucleus.

Other components of the complex are also involved in nuclear structure, chromatin binding, and chromatin organization. Emerin is a serine-rich nuclear membrane protein that interacts with lamin A and mediates the anchoring of the nuclear membrane to the cytoskeleton (Clements *et al.* 2000, Sakaki *et al.* 2001). Nesprins are predominantly located in the outer nuclear membrane and provide additional structural

support (Lombardi *et al.* 2011). LAP2α interacts with lamin A and LAP2β interacts with lamin B (Gant *et al.* 1999). Both LAP2 proteins mediate lamina assembly and chromatin attachment to the inner nuclear membrane. The transmembrane protein LBR2β interacts indirectly with lamin B and methylated residues of histone 3 (Wilson and Foisner 2010).

LBR and LAP2β have been implicated in mediating a repressive environment at the nuclear periphery. The LBR interacts with HP1, and induces heterochromatization (Lomberk *et al.* 2006). LAP2β can interact with histone deacetylase (HDAC) 3 (Somech *et al.* 2005). Deacetylation allows histones to more tightly wrap DNA, potentially reducing transcriptional activity (Gallinari *et al.* 2007).

Several studies have fused the bacterial DNA adenine methyltransferase (Dam) to a protein of the nuclear periphery, and identified genomic regions which were preferentially positioned at the nuclear periphery (Greil *et al.* 2006). The adenine (A) nucleotide of GATC sequences in genomic regions near the periphery becomes methylated. Methylated sequences can then be enriched with a methylation-specific enzyme digest, and identified using PCR-amplification and DNA tiling arrays.

This technique, known as DamID, has been used in *Drosophila* to demonstrate that genes nearby laminB1 are typically transcriptionally silent, late replicating, and lack active histone marks (Pickersgill *et al.* 2006). DNA regions frequently in close proximity to the lamina were termed lamina-associated domains (LAD). LADs extend between

0.1-10 Mb, and human cell lines were found to have more than 1300 distinct LADs. Human LAD borders are demarcated by CTCF and CpG islands (Guelen *et al.* 2008), suggesting that LADs loop away from active chromatin. LADs were gene-poor, enriched for the H3K27me3 mark, and depleted in the H3K4me2 mark. Also, promoters tended to be oriented away from LADs, so that transcription more commonly occurs in regions between LADs.

Some LADs appear to be constitutive, whereas other LADs are cell-type specific. Constitutive LADs (cLADs) may regulate steady-state chromatin organization, whereas facultative LADs (fLADs) are developmentally regulated. LADs are facultative at hundreds of sites during both lineage commitment and terminal differentiation (Peric-Hupkes and van Steensel 2010). fLADs include both individual transcriptional units and mutigene regions. Losing LAD-status can result in either concomitant activation, or priming for activation in a later differentiation step. Interestingly, cLADs can be distinguished from fLADs purely on the basis of A/thymine (T) content, with most cLADs having higher A/T content, and most constitutive inter-LADs (ciLADs or non-LADs) having lower A/T content (Meuleman *et al.* 2013).

Interactions with the nuclear lamina have also been evaluated in individual living cells (Kind *et al.* 2013). Lamin interactions are dynamic, with only approximately 30% of LADs located at the outer periphery of the nucleus in any one cell. LAD

positioning is randomly rearranged following each cell division, suggesting that the repressive effects of peripheral positioning do not require constitutive molecular interaction with the lamina.

Regions of chromatin have been artificially tethered to the nuclear periphery, via emerin, laminB1, and LAP2β. Regions tethered by either emerin or LAP2β reduced transcription levels (Finlan *et al.* 2008, Reddy *et al.* 2008). Conversely, a stably integrated plasmid that was recruited through laminB1 showed no change in activity level (Kumaran and Spector 2008). Transcription can likely be regulated by both the subnuclear location and the strength of local promoters and distant enhancers. If transcriptional repression depends on both the subnuclear localization of the gene locus and the strength of nearby promoters, it makes sense why some, but not all, genes relocated to the nuclear periphery become transcriptionally repressed.

1.4.4.2 The Nuclear Pore Complex

Nuclear pore complexes (NPC) connect the inner and outer nuclear membranes and allow for transport between the nucleoplasm and cytoplasm (Raices and D'Angelo 2012). Proper NPC function is required for cell survival and homeostasis, as NPCs support the passive diffusion of small molecules, and the active transport of macromolecules (Mosammaparast and Pemberton 2004).

NPC structure is highly conserved between *Xenopis laevis* and human fibroblasts, but NPCs can differ in size (Raices and D'Angelo 2012). NPCs are large multiprotein channels, composed of multiple copies of at least thirty different nucleoporin (NUP) proteins. NPCs are stable, immobile structures in the nuclear envelope, and contribute to genome architecture. Whereas the majority of DNA at the nuclear envelope is heterochromatinized, NPCs are surrounded by decondensed chromatin, suggesting that NPCs are sites of active transcription (Casolari *et al.* 2004). A microarray performed in yeast showed that many active genes associate with NPC components. These genes are recruited to the NPC through *cis*-acting DNA 'zip codes' located in the gene promoters (Brickner *et al.* 2012). Once genes are relocated to the NPCs, the NPCs act as a scaffolding platform to allow the recruitment and/or assembly of transcriptional machinery.

NPCs also influence transcription by mediating DNA looping (Hampsey *et al.* 2011). Loops containing inducible genes are thought to promote transcriptional memory, in which reactivation can occur more quickly. For example, the *GAL1* and *HXK1* genes are developmentally turned on, off, and then back on again. These genes become repositioned at NPCs following their initial activation, then myosin-like protein1 (Mlp1) mediates the gene interaction with the NPC. Mlp1 forms and maintains

a ‘memory gene loop’ that contains *GAL1* and *HXK1* which likely allows for efficient gene re-activation.

1.5 V(D)J Recombination

1.5.1 RAG1/2

1.5.1.1 RAG1/2 Proteins

V(D)J recombination is catalyzed by the RAG1/2 proteins (Schatz and Ji 2011) at antigen receptor loci within the nuclei of developing lymphocytes. Deficiency in either RAG1 or RAG2 completely abrogates V(D)J recombination, blocking lymphocyte development (Mombaerts *et al.* 1992, Shinkai *et al.* 1992). RAG1 and RAG2 proteins interact with each other in order to recombine antigen receptor loci.

RAG1 controls DNA binding to RSSs, and is responsible for cleaving DNA between the RSSs and gene segments (Schatz and Ji 2011). Full length RAG1 is 1,040 amino acids long and contains several functional domains (Fig. 8). Beginning at the N-terminus, there are elements involved in mediating protein stability and interaction with other proteins, zinc binding sites, and elements that enhance recombinatorial activity. The central region contains a nonamer binding domain (NBD), elements capable of nicking ssDNA, a heptamer binding site, a really interesting new gene (RING) domain that functions as an E3 ligase, and an element that facilitates RAG2 interaction. Though

containing NBD and heptamer binding sites, RAG1 alone can bind DNA nonspecifically. DNA nicking is mediated by three acidic residues at amino acid 600, 708, and 962 (Landree *et al.* 1999). The C-terminal domain (CTD) includes double stranded DNA (dsDNA) binding elements and two zinc binding sites.

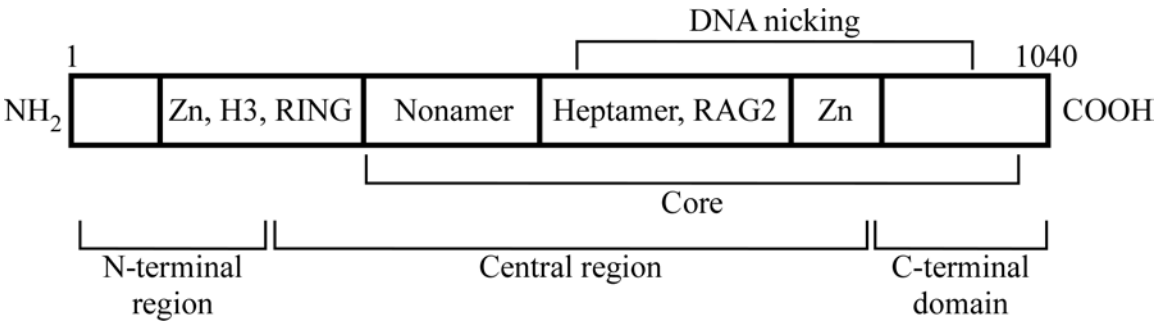

Figure 8: RAG1 protein

Diagram of the RAG1 protein. The locations of various binding sites are demarcated by their name. The core region and the three regions (N-terminal, central, and C-terminal) are also shown. Not drawn to scale. Modified from Schatz and Ji, 2011. Zn, zinc; H3, histone 3; RING, really interesting new gene.

RAG2 enhances RAG1 binding and is required for RAG1-mediated DNA cleavage (Schatz and Ji 2011). Full length RAG2 is composed of 527 amino acids and can also be divided into three distinct regions (Fig. 9). The N-terminal region RAG2 includes six Kelch-like motifs, the last of which is thought to interact with RAG1. The central region is acidic and serves as a hinge for the protein. The C-terminal region contains a

noncanonical plant homeodomain (PHD) that recruits RAG2 to H3 trimethylated at lysine 4 (H3K4me3) (Liang *et al.* 2002, Matthews *et al.* 2007), stabilizes the RAG1/2 tetramer, and enhances RAG1 nicking activity (Schatz and Ji 2011). As a result of the PHD, RAG2 binding reflects H3K4me3 genome-wide (Ji *et al.* 2010). The C-terminus also has a conserved threonine at residue 490 which facilitates the cell-cycle regulated degradation of RAG2. RAG2 is only present during G_0/G_1, preventing the formation of RAG-mediated DSBs in cycling cells (Lin and Desiderio 1993).

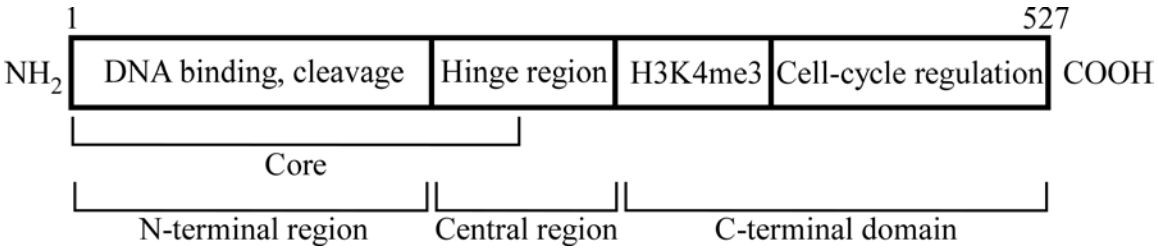

Figure 9: RAG2 protein

Diagram of the RAG2 protein. The locations of various functional and binding sites are depicted. Not drawn to scale. Modified from Schatz and Ji, 2011.

Full-length RAG1 and RAG2 are insoluble when overexpressed, and consequently difficult to purify (McBlane *et al.* 1995). Therefore, biochemical functions of RAG1 and RAG2 have been characterized *in vitro* using core (c) regions of both genes, which are capable of mediating V(D)J recombination. Amino acids 384-1,008 comprise

cRAG1, whereas cRAG2 is composed of amino acids 1-383 (Fig. 8 and 9). Though cRAG1/2 can catalyze recombination *in vitro*, mice with *cRag1* (Dudley *et al.* 2003) or *cRag2* (Liang *et al.* 2002) knocked-into the endogenous locus display defective V-to-DJ recombination. On the other hand, D-J recombination is unaffected. In solution, cRAG1 and cRAG2 form a 1:1 mixed tetramer complex (Swanson *et al.* 2009).

1.5.1.2 RAG1/2 Expression

All jawed vertebrates express RAG1/2 proteins in developing lymphocytes (Nishana and Raghavan 2012). *Rag1/2* gene sequences are evolutionarily conserved, and the two genes are located adjacent to each other on mouse chromosome 2. Due to their proximity to each other, *Rag1/2* genes can be co-regulated and convergently transcribed (Schatz and Swanson 2011). As indiscriminate DSBs could lead to oncogenic translocations or cell death (Jones and Gellert 2004, Helmink and Sleckman 2012), V(D)J recombination is tightly regulated by largely restricting *Rag1/2* expression to developing lymphocytes (Kuo and Schlissel 2009).

1.5.1.3 RAG1/2 Chromatin Accessibility

RAG1/2 binding is also regulated. RAG1/2 binding correlates with transcription, endonuclease sensitivity, histone acetylation, and DNA hypo-methylation (Cobb *et al.*

2006). RAG1 and RAG2 bind antigen receptor loci, in a lineage- and stage-specific manner (Ji *et al.* 2010). Additionally, RAG1 and RAG2 can both be independently recruited to specific genomic sites *in vivo*.

Transcription factors can regulate RAG1/2 binding. For example, c-Fos directs RAG1/2 recruitment in thymocytes so that D_β-to-J_β recombination precedes V_β-to-DJ_β recombination (Wang *et al.* 2008). c-Fos is a component of the activator protein-1 (AP-1) transcription factor complex (Chinenov and Kerppola 2001) and can interact with the RAG1/2 complex *in vitro (Wang et al. 2008)*. c-Fos binds an AP-1 site at the 3′ $D_\beta1$ RSS, bringing RAG1/2 to that site. *In vivo*, c-Fos deficiency resulted in reduced recombination efficiency and V_β-to-D_β recombination prior to D_β-to-J_β recombination. Together, these data suggest that c-Fos may mediate ordered V(D)J recombination by bringing RAG1/2 to the 3′RSS and potentially sterically hindering RAG1/2 binding to the 5′ RSS.

At antigen receptor loci both RAG proteins preferentially bind to D and J gene segments (Ji *et al.* 2010). RAG1/2 binding is restricted to J gene segments in *Tcra* and *Igk* loci, and 3′ DJ gene segments in *Tcrb* and *Igh* loci. Also, both RAG1 and RAG2 proteins independently localize to antigen receptor loci. RAG2 bind to thousands of actively transcribing sites in the genome, likely due to PHD-mediated interactions with H3K4me3. RAG1 occupancy is high only at RSSs flanking D and J gene segments.

Together, (D)J gene segments seem to serve as 'recombination centers' that capture distant V gene segments in order to undergo recombination.

RAG1/2 preferentially binds to 'accessible' RSSs (Sleckman *et al.* 1996). The accessibility hypothesis proposes that chromatin structure dictates the accessibility of RAG1/2 proteins to RSSs (Yancopoulos and Alt 1985). It arose from the observation that germline transcription of V_H gene segments coincided with *Igh* recombination. A great deal of additional evidence has supported this model, demonstrating that the accessibility required for transcription also permits access of recombination factors to antigen receptor loci (Hesslein and Schatz 2001, Schlissel 2003, Goldmit and Bergman 2004, Cobb *et al.* 2006, Jung *et al.* 2006, Krangel 2007).

Accessibility of antigen receptor loci is developmentally regulated (Stanhope-Baker *et al.* 1996), and like transcription, is controlled by enhancers and nearby promoters (Cobb *et al.* 2006). In general, enhancers impact accessibility at distant sites, whereas the effect of promoters is more local. Accessibility may be regulated by transcription-mediated changes in chromatin structure and nucleosome positioning. Nucleosomes consist of eight histone proteins cores, around which 147 DNA bp are wrapped, and serve as the basic unit of DNA packaging in eukaryotic nuclei (Richmond and Davey 2003). Transcription drives the mobilization or partial disassembly of

nucleosomes at antigen receptor loci, in support of RSS accessibility (Felsenfeld *et al.* 2000, Kondilis-Mangum *et al.* 2010).

Transcription correlates with active chromatin marks such as H3K4me3, which recruits RAG2 proteins (Liang *et al.* 2002, Matthews *et al.* 2007). To separate the effects mediated by TEA transcription at the *Tcra* locus from any effects potentially mediated by other structural or functional properties of the promoter region, a transcription terminator was inserted into the locus 3' of the TEA promoter (Abarrategui and Krangel 2006, Abarrategui and Krangel 2007). This disrupted noncoding transcription from TEA, but left the TEA promoter intact. Interestingly, histone acetylation, histone methylation, and chromatin accessibility were reduced in the J_α array, showing that transcription, and not promoter activity, is required for *Tcra* recombination.

However accessibility alone is insufficient for rearrangement to occur. Though *Tcrb* alleles containing E_α remained accessible at the DP stage, that accessibility did not induce recombination (Jackson *et al.* 2005). Therefore although V(D)J recombination likely requires RAG1/2 accessibility to RSSs, additional layers of regulation (such as locus contraction and relocalization away from repressive subnuclear compartments) may also exist. Once these factors have been overcome, RAG1/2 generates two DSBs between two RSSs and two gene segments (Kondilis-Mangum *et al.* 2011).

1.5.2 Double-Strand Break Repair

The presence of a DSB at any point in the cell-cycle activates checkpoints that halt cell-cycling (Hoeijmakers 2001). Cell cycle arrest likely offers the cell additional time in which to repair the DSB. Arrest is mediated by the activation of phosphatidylinositol 3-kinase (PI3K) -like kinases ataxia telangiectasia mutated (ATM) and ataxia telangiectasia related (ATR). ATM and ATR phosphorylate and activate the cell-cycle regulators p53, Chk1, and Chk2 (Khanna and Jackson 2001). Eukaryotic cells can repair DSBs through two major pathways, which are evolutionarily conserved from yeast through vertebrates (Sonoda *et al.* 1997). The two pathways differ in the type of repair performed and when in the cell cycle each can be executed.

1.5.2.1 Non-Homologous End Joining

RAG-mediated DSBs are repaired via the non-homologous end-joining (NHEJ) repair pathway. NHEJ repairs DSBs imprecisely, but can function at any point in the cell cycle (Sonoda *et al.* 1997). NHEJ is a complicated process, but can be broken down into three general phases: (1) DNA-end capture, (2) formation of a molecular bridge between the two DNA ends, (3) DNA ligation (Weterings and Chen 2008). Many portions of the process of NHEJ remain incompletely understood.

NHEJ begins with the binding of Ku70/80 heterodimers to broken DNA ends (Lees-Miller and Meek 2003). Ku heterodimers are thought to provide a scaffold for the assembly of other early repair proteins. DNA-bound Ku70/80 recruits DNA-dependent protein kinase catalytic subunit (DNA-PKcs), which brings the two DNA ends into synaptic complex (Weterings and Chen 2008). DNA ends are then processed by various nucleases and polymerases to generate a blunt DNA end. DNA end ligation requires DNA ligase IV and X-ray repair cross-complementing protein 4 (XRCC4), and XRCC4-like factor (XLF)/Cernunnos.

ATM is an integral component of the DNA damage response (DDR) pathway, leading to DSB repair (Shiloh and Ziv 2013). ATM is involved in the phosphorylation and activation of many DSB repair proteins, such as DNA-PKcs, P53-binding protein 1 (53BP1), the histone variant H2AX, and ATM itself (Chen *et al.* 2007, van Gent and van der Burg 2007).

Following RAG-mediated DSB generation, ATM functions to keep all four DNA ends located in repair complexes and promote correct V(D)J recombination (Bredemeyer *et al.* 2006). Hairpin coding ends are opened by the Art nuclease, in a complex with DNA-PKcs. Art cleaves the coding end hairpin to generate an overhang of 0-10 bp, and will sometimes use its exonuclease capabilities to remove the overhang. Once the

hairpins have been opened, classical NHEJ, requiring ligase IV and XRCC4, proceeds and V, D, and J gene segments are ligated.

Many DSB repair factors form foci visible via microscopy, allowing for the visualization and localization of recent DSBs within the nucleus. Phosphorylated H2AX (γH2AX) is one of the most rapid markers of DNA damage, and persists for a number of hours following DSB formation. ATM is required for the phosphorylation of γH2AX (Rogakou *et al.* 1998). Most active repair factors, including ATM and 53BP1, are quickly recruited to sites of DNA damage and remain there for several hours (Anderson *et al.* 2001, Asaithamby and Chen 2009). 53BP1 is activated by phosphorylation at several serine residues, and is recruited to γH2AX (Mochan *et al.* 2004).

1.5.2.2 Homologous Recombination

DSBs can also be repaired via the homologous recombination (HR) repair pathway, at certain points in the cell cycle. HR utilizes the sister chromatid as a template to accurately restoring the broken DNA to its original sequence (Li and Heyer 2008). The unbroken sister chromatid is present only during the synthesis (S) and growth 2 (G2) phases of the cell cycle (Fig. 10). HR is well-suited to repair DNA replication-associated DSBs, as the broken ends are in close proximity to the unbroken

sister chromatid (Sonoda *et al.* 1997). HR cannot occur during the G1 or G0 (resting) stage of the cell cycle.

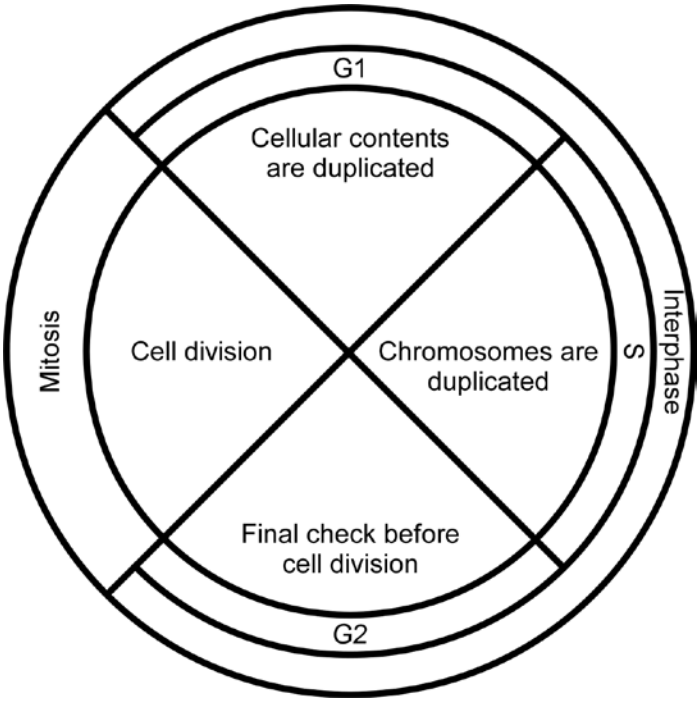

Figure 10: Cell-cycle phases

Cycling cells are either preparing for or undergoing cell division. Interphase, the preparation for cell division, can be separated into three distinct stages. In the first stage, G1, environmental signals induce cell growth. In S phase, a second copy of genomic DNA is synthesized. Growth and preparation for cell division continues in the G2 phase, and then cells exit interphase and enter mitosis, in which cells divide. Size of stage does not represent length of time the cell remains at that stage. G, growth; S, synthesis.

Though HR is a complex process that involves many factors, it can be divided into four stages: (1) DNA-end resection, (2) synaptic complex formation, (3) displacement (D) loop formation and, (4) DSB resolution (Daley *et al.* 2013). After the DSB has been identified by the cell, DNA-ends are resected by nucleolytic degradation, leaving a 3′ overhang. The resulting ssDNA overhand is initially bound by replication protein A (RPA), and later replaced by the Rad51 recombinase, forming the presynaptic filament. Synaptic complex formation occurs when the presynaptic filament interacts with homologous double-stranded (ds) DNA. The homologous pair invades the DNA template, forming a D-loop, and the invading DNA-end is extended via template-dependent DNA synthesis. DSB repair is then completed and the DNA structure is dissolved.

1.5.2.3 Repair Pathway Choice

The point in the cell cycle (Fig. 10) is the most important factor when determining which DSB repair pathway will be used (Takata *et al.* 1998, Weterings and van Gent 2004). HR is restricted to the S and G2 cell cycle stages as it requires a DNA template, whereas NHEJ does not require homology and can be accomplished at any point in the cell cycle. However when both pathways are available, they are thought to compete. For example, DNA-end binding by either Ku70/80 (mediating NHEJ) or Rad52

(mediating HR) may determine the repair pathway used (Van Dyck *et al.* 1999). Ku80/80 binds to all DNA ends, whereas Rad52 preferentially binds to DNA ends with ssDNA overhangs (Ristic *et al.* 2003). This suggests that repair pathway choice may depend on the type of DNA at the break. There is also evidence that repair pathway choice may be flexible. When NHEJ is prevented, forms of repair requiring homology are increased (Pierce *et al.* 2001).

The repair pathway choice is relatively simple for RAG-dependent DSBs. As RAG-dependent DSBs are generated in the G1/G0 stages of the cell cycle, no homologous template is available for HR. Therefore RAG-dependent DSBs will preferentially be repaired via the NHEJ pathway. However if NHEJ is blocked, RAG-dependent DSBs can be inefficiently repaired by a third repair pathway, alternative NHEJ (aNHEJ), which uses microhomology (homology of <25 bp) more often than classical NHEJ (cNHEJ) (Corneo *et al.* 2007). Interestingly, the C terminus of the RAG2 protein is required to prevent efficient aNHEJ repair at antigen receptor loci DSBs. In addition, the repair of non-RAG-mediated DSBs can be forced to proceed down the NHEJ pathway if RAG1/2 complexes are present at the site of the DSB (Cui and Meek 2007). Upon closer inspection of RAG2, the acidic hinge region was found to stabilize the post cleavage complex (RAG1/2 bound to the RSSs of the four broken DNA ends) and skew repair pathway choice toward cNHEJ (Coussens *et al.* 2013).

Several other repair factors direct repair pathway choice toward HR. For example, CtIP promotes DNA resection, which generate the ssDNA overhang required for HR (Yun and Hiom 2009). This function depends on CtIP phosphorylation upon entering S phase of the cell cycle. If CtIP cannot become phosphorylated, HR is abrogated (Yun and Hiom 2009). Additionally, without the histone variant H2AX, CtIP can bind to and resect the ends of RAG-dependent DSBs, leading to repair via HR (Helmink *et al.* 2011). Therefore CtIP plays an important role in regulating DSB repair pathway choice toward HR.

The MRN complex (MRE11-RAD50-NBS1) is one of the first responders to DSBs, and directs repair to proceed toward either NHEJ or HR via the 3'-5- exonuclease activity and ssDNA hairpin endonuclease activity of MRE11 (Stracker and Petrini 2011). Recently, the function of MRE11 in repair pathway choice was investigated by inhibition of the various nuclease activities of MRE11 (Shibata *et al.* 2014). Endonuclease activity directed repair toward HR, while exonuclease activity is required for efficient repair by either pathway. Hence the MRN complex is also important for directing DSB repair pathway choice.

1.5.3 Locus Contraction and Decontraction

Antigen receptor loci extend over kb-Mb spans of linear DNA, but gene segments undergoing V(D)J recombination must be physically close to each other for synapsis to occur. 3D FISH techniques have been used to ascertain the conformation of antigen receptor loci throughout B and T cell development. In FISH analyses of locus conformations, BAC clones have been used to identify the subnuclear position of various 100-200 kb regions of DNA. Confocal microscopy can be used to localize those regions, which form foci, within 3D nuclear space. Using BACs, the two ends of each antigen receptor locus were shown to contract prior to recombination and decontract following recombination at *Igh*, *Igk*, *Tcrb* and *Tcra* loci (Kosak *et al.* 2002, Roldan *et al.* 2005, Fitzsimmons *et al.* 2007, Skok *et al.* 2007). As loci are undergoing transcription during contraction (Abarrategui and Krangel 2009), the reduction in 3D distance is probably not heterochromatinization of loci. Contraction is thought to result from the formation of chromatin loops, which bring the 5′ V regions and 3′ DJ gene segments into close proximity, allowing for long-range V(D)J recombination events (Sayegh *et al.* 2005, Fitzsimmons *et al.* 2007, Skok *et al.* 2007). In support of this theory, pro-B cells lacking the B-lineage transcription factor Pax5 (Medvedovic *et al.* 2011) fail to contract, and also fail to recombine distal V_H gene segments (Fuxa *et al.* 2004). Expression of Pax5 in these cells overcomes both phenotypes.

The 5′ and 3′ ends of the *Igh* locus were initially found to be closer in *Rag2*$^{-/-}$ pro-B cells (during *Igh* recombination) than cultured wild-type (WT) B cells or CD8^{+} T cells (after recombination had been completed) (Kosak *et al.* 2002, Sayegh *et al.* 2005). Additionally, in *Rag2*$^{-/-}$ pre-pro-B cells and pre-B cells the V_H gene segments were farther from the DJ_H gene segments than in pro-B cells, when the *Igh* locus is prepared to undergo V_H-to-DJ_H recombination. This is in line with what would be expected if the V_H gene segments were distanced from the DJ_H gene segments prior to recombination, and are then brought into close proximity in preparation for recombination. Addition of a third internal BAC probe was used to gain a better understanding of overall locus conformation. Interestingly, the 3′ probe switched places with the central probe in ~25% of alleles, suggesting that the internal sequence can loop away while the 5′ and 3′ regions remain in close proximity to each other (Sayegh *et al.* 2005). This allows distal V_H gene segments to interact with downstream DJ_H gene segments.

Igh locus conformation has been characterized throughout B cell development at a relatively high resolution (<50 nanometers (nm)) (Jhunjhunwala *et al.* 2008). The locus structure was mapped using 12 markers each ~10 kb in length, and the average topography at each stage was calculated. Prior to *Igh* recombination, the locus is separated into distinct compartments, in which the distal V_H gene segments are distanced from the DJ_H segments. However during *Igh* recombination, the entire locus

contracts into a single compartment. This contraction is thought to allow all V_H gene segments similar opportunities to interact and recombine to DJ_H gene segments. Remarkably, contracted *Igh* loci display more conformational flexibility than decontracted loci (Jhunjhunwala *et al.* 2008), likely promoting the interactions of all V_H genes with DJ_H segments.

Tcra/*Tcrd* loci also contract prior to, and decontract following, V(D)J recombination (Skok *et al.* 2007). However as the *Tcrd* locus recombines in the DN stage and the *Tcra* locus recombines in the DP stage, contraction at *Tcra*/*Tcrd* loci is more complex than at other antigen receptor loci. Initially in the DN stage both the 3′ and 5′ regions of the *Tcra*/*Tcrd* locus were contracted, presumably so that 5′ V_δ gene segments have the chance to undergo *Tcrd* recombination (Shih and Krangel 2010). In the following DP stage, only the 3′ region of the *Tcra*/*Tcrd* locus is contracted, probably to support inside-out *Tcra* recombination (Krangel *et al.* 2004). Interestingly, these large-scale *Tcra*/*Tcrd* conformational changes observed by 3D FISH do not require the presence of E_α or E_δ regulatory elements (Shih *et al.* 2012).

Investigations into the molecular mechanisms behind BCR locus contraction have generated interesting findings. Contraction is independent of RAG1/2 expression (Fuxa *et al.* 2004, Roldan *et al.* 2005, Skok *et al.* 2007, Jhunjhunwala *et al.* 2008), but *Igh* contraction requires interleukin (IL) -7 signaling (Nodland *et al.* 2011) and the

transcription factors Pax5, yin-yang 1, and Ikaros (Fuxa *et al.* 2004, Liu *et al.* 2007, Reynaud *et al.* 2008). *Igh* and *Igk* contraction are dependent upon E_{μ} and $3'E_{\kappa}$, respectively (Hewitt *et al.* 2008, Guo *et al.* 2011). Additional work is needed to understand the mechanism of *Tcr* locus contraction, as local enhancers likely do not play a role (Shih and Krangel 2010).

1.5.4 Subnuclear Localization

As both *Tcrb* alleles are contracted (Skok *et al.* 2007) and actively transcribing (Jia *et al.* 2007) in DN thymocyte nuclei, another mechanism must be responsible for asynchronous recombination. Subnuclear localization has arisen as a potential regulator of recombination (Kosak *et al.* 2002). Transcriptionally repressive subnuclear compartments, such as the nuclear periphery and pericentromeric heterochromatin, may repress V(D)J recombination.

1.5.4.1 The Nuclear Periphery

The developmental regulation of subnuclear localization of antigen receptor has been well documented (Skok *et al.* 2001, Kosak *et al.* 2002, Skok *et al.* 2007, Schlimgen *et al.* 2008). *Ig* loci tend to be located at the nuclear periphery in non-lymphoid or T-lineage cells, but away from the periphery during the stage at which each locus

recombines (Kosak *et al.* 2002). *Tcra*/*Tcrd* loci are also located at the periphery in non-T lineage cells, and repositioned away from the periphery prior to recombination (Schlimgen *et al.* 2008). However *Tcrb* alleles are different, and associate frequently (~50-70%) and stochastically with the nuclear periphery throughout T cell development (Schlimgen *et al.* 2008). Therefore the nuclear periphery seems to function as a compartment that represses V(D)J recombination, though direct evidence for this is currently lacking.

Roughly 50% of *Igh* alleles, which are inactive in progenitor cells and thymocytes, were found to be located in the outer 20% of the nucleus by 2D FISH in ES cells and MPP (Kosak *et al.* 2002). In DN thymocytes, the frequency was slightly lower, at approximately 30%. *Igh* subnuclear relocalization in pro-B cells requires IL -7 signaling, and is thought to create a more permissive and accessible nuclear environment. In pro-B cells almost no alleles were located at the nuclear periphery. Similarly, about half of *Igk* alleles were located at the periphery in ES cells, MPPs, and DN thymocytes, but less than 10% are at the periphery in pro-B cells. In contrast, 10% of *Igl* loci were located at the nuclear periphery in all cell types analyzed. The differences in subnuclear positioning correlates with the size of the loci, and *Igh* and *Igk* loci span ~3 Mb, whereas the *Igl* locus only expends ~200 kb. It is possible that larger loci require an additional level of regulation to prevent recombination earlier stages of development.

Though 65% of *Tcra*/*Tcrd* loci colocalize with the nuclear periphery in pro-B cells, only 19% and 28% of alleles colocalize with the periphery in DN and DP thymocytes, respectively (Schlimgen *et al.* 2008). The *Tcra*/*Tcrd* locus is also large, spanning nearly 2 Mb. *Tcra*/*Tcrd* locus seem to be regulated similarly to *Igh* alleles, as they are peripherally-positioned prior to recombination, and then relocalize to the nuclear interior to undergo V(D)J recombination.

Tcrb allele colocalization with the nuclear periphery is regulated differently during thymocyte development than *Igh* or *Tcra* alleles during B cell and thymocyte development, respectively. 55% of *Tcrb* alleles colocalized with the nuclear periphery in pro-B cells, 67% colocalize in DN thymocytes, and 47% colocalize in DP thymocytes (Schlimgen *et al.* 2008).

Using a BAC probe that targets the trypsinogen region located between the V_β region and the DJC_β region, alleles that had undergone V_β-to-DJ_β rearrangement and their location relative to the nuclear periphery could be identified and localized. A bias was found for V_β-to-DJ_β unrearranged *Tcrb* alleles to be positioned at the nuclear periphery (Schlimgen *et al.* 2008). This result could suggest that positioning of *Tcrb* alleles at the nuclear periphery may suppress recombination. However the reduction of rearranged *Tcrb* alleles at the periphery could also be explained if recombination occurred freely at the nuclear periphery, but in-frame V_β-to-DJ_β rearranged *Tcrb* alleles

relocate away from the nuclear periphery following recombination. In order to determine whether *Tcrb* positioning at the nuclear periphery during thymocyte development reduces the efficiency of recombination, the location of V(D)J recombination would need to be visualized in thymocyte nuclei.

1.5.4.2 Pericentromeric Heterochromatin

3D FISH has been used to evaluate the localization of antigen receptor alleles to PCH during B and T cell development. Both *Igh* and *Igk* loci appear to associate with PCH monoallelically in pre B cells (Goldmit and Bergman 2004, Roldan *et al.* 2005, Fitzsimmons *et al.* 2007). It was suggested that the associated allele is unrearranged, which would imply that the monoallelic association may function to prevent recombination. Monoallelic *Igk* association may occur following recombination, and be dependent upon RAG1 and ATM (Hewitt *et al.* 2009). However this finding conflicts with previous reports suggesting that monoallelic *Igk* association occurs prior to *Igk* recombination, and is a result of replication timing differences between the two alleles (Mostoslavsky *et al.* 2001). Indeed, the late replicating allele also tends to be the unrearranged allele (Mostoslavsky *et al.* 2001, Goldmit and Bergman 2004).

Tcr loci also associate with PCH. *Tcra/Tcrd* loci are located at PCH in non-T lineage cells, and repositioned away from PCH prior to recombination (Skok *et al.* 2007,

Schlimgen *et al.* 2008). *Tcrb* allele association with PCH is a bit controversial. The first report regarding *Tcrb* association with PCH suggested that it occurred monoallelically during *Tcrb* recombination, potentially serving as the mechanism by which only one *Tcrb* allele rearranged per thymocyte (Skok *et al.* 2007). Shortly thereafter, it was reported that *Tcrb* alleles remain highly (~50%) associated with PCH throughout T cell development (Schlimgen *et al.* 2008). Moreover, this association occurred stochastically, with at least 30% of cells containing neither allele at PCH and 10% of cells containing both alleles at PCH. Nevertheless, both reports propose that antigen receptor locus association with PCH likely represses V(D)J recombination.

1.6 Allelic Exclusion

Most B and T cells express monospecific BCRs and TCRs, respectively (Brady *et al.* 2010). Antigen receptor monospecificity is the result of allelic exclusion, the mechanism by which the product of only one allele per genetic loci is expressed on the cell surface. The product of both *Tcrb* and *Igh* alleles are expressed on the cell surface of only ~2% of T cells and 0.01% of B cells, respectively (Brady *et al.* 2010). T and B cells expressing multiple receptors each capable of binding different antigens (aka allelically included) may escape self-tolerance mechanisms and cause autoimmunity (Iliev *et al.* 1994, Zal *et al.* 1996, Sarukhan *et al.* 1998, Morris and Allen 2009).

Allelic exclusion can be enforced at various levels. For example, TCRα chain allelic exclusion is enforced post-translationally (Gascoigne and Alam 1999). This was first described when T cell clones expressing two TCRα chains in the cytoplasm expressed only one at the cell surface (Malissen *et al.* 1988, Couez *et al.* 1991, Kuida *et al.* 1991). This post-translational allelic exclusion of TCRα chains may be regulated by competition for TCRβ chain binding, in a developmentally regulated manner (Malissen *et al.* 1988, Couez *et al.* 1991, Malissen *et al.* 1992). TCRα chain allelic exclusion is more effective in mature T cells, (Alam *et al.* 1995). In mature T cells TCRα protein abundance is lower, which allows only the highest affinity chain to heterodimerize with the less-abundant TCRβ chain. Indeed, though ~30% of αβ T cells contain in-frame *Tcra* gene rearrangements on both alleles, <10% of αβ T cells express two TCRα chains on the cell surface (Casanova *et al.* 1991, Padovan *et al.* 1993).

Unlike *Tcra* loci, allelic exclusion of *Tcrb* and *Igh* loci predominantly occurs at the level of V(D)J recombination (Fig. 2) (Uematsu *et al.* 1988, Sonoda *et al.* 1997, Brady *et al.* 2010). Regulation at the level of genomic rearrangement was demonstrated by inserting pre-rearranged *Ig* or *Tcr* tg (Mostoslavsky *et al.* 2004). The tg inhibited further V-to-DJ recombination at the respective endogenous antigen receptor loci, showing that feedback mechanisms exist. Feedback inhibition is especially important to support allelic exclusion at *Tcrb* and *Igh* loci, because they must prevent recombination when

RAG1/2 proteins are re-expressed at a later developmental stage. Similar to *Tcrb* and *Igh* loci, *Ig* light chain loci are isotypically excluded in mature B cells, so that only one of the four *Igk* and *Igl* alleles has undergone in-frame recombination (Neuberger *et al.* 1989). For allelic exclusion to effectively limit V-to-DJ recombination to one *Tcrb* and *Igh* allele per cell, alleles must recombine one-at-a-time. Then, following the successful recombination of one allele, additional recombination at both alleles must be prevented.

1.6.1 Initiation of V-to-DJ Allelic Exclusion at *Tcrb* and *Igh* loci

If expression of a functional pre-TCR or pre-BCR on the cell surface signals to inhibit additional recombination at *Tcrb* and *Igh* loci, rearrangement must be temporally restricted so that only one rearrangement event occurs in the time required for feedback signals to impart their effect. Therefore *Tcrb* and *Igh* alleles must rearrange one-at-a-time, or asynchronously, to initiate allelic exclusion. However the mechanism by which recombination is initiated at only one allele at-a-time remains enigmatic.

Asynchronous recombination could occur in either a determined or stochastic manner (Murre 2008). If asynchronous rearrangement was predetermined, one allele would rearrange more efficiently than the other, making it likely that the more efficient allele attempts recombination first. Only if the first allele fails to successfully recombine would the second have sufficient time to undergo recombination. If asynchronous

recombination were to instead occur via a stochastic manner, both alleles would recombine inefficiently, so that the chance of both recombining simultaneously was quite low.

Theories that transcription and locus contraction mediate asynchronous recombination, in either a determined or stochastic manner, have proved unsuccessful. Regarding transcription, a genetic marker inserted into the *Tcrb* locus downstream of Vβ8.2 was used to analyze germline transcription at the single-cell level (Jia *et al.* 2007). Biallelic transcription was observed at *Tcrb* alleles in all DN thymocytes. Additionally, *Igk* loci are transcribed biallelically in pre B cells, (Singh *et al.* 2003, Amin *et al.* 2009) though the two alleles may be transcribed at different levels (Amin *et al.* 2009). Therefore it is unlikely that monoallelic transcription is the mechanism by which one allele is selected to rearrange. Additionally, *Igh* and *Tcrb* alleles are both contracted during the stage at which they recombine (Jhunjhunwala *et al.* 2008, Schlimgen *et al.* 2008), suggesting that monoallelic contraction does not mediate asynchronous recombination.

Though both *Igk* loci are transcriptionally active (Singh *et al.* 2003, Amin *et al.* 2009), the initiation of allelic exclusion at *Igk* loci in developing B cells is more likely linked to the asynchronous replication of alleles. Replication timing can influence chromatin repackaging following DNA synthesis (Lande-Diner *et al.* 2009). Early

replicating alleles are repackaged with nucleosomes containing acetylated histones, which promote transcription and chromatin accessibility. The *Igk* allele that replicates first is chosen randomly at a very early stage in early B cell development (Farago *et al.* 2012), and allele choice in inherited and maintained by daughter cells (Mostoslavsky *et al.* 2001). Additionally, one *Igk* allele is preferentially free of PCH and packaged into histones bearing active markers, whereas the other allele is positioned at PCH (Goldmit *et al.* 2005). Recently, early replication, histone acetylation, and recombination were shown to all occur on the same allele (Farago *et al.* 2012). To accomplish this, pre B cell clones containing *Igk* alleles that were distinguishable based on species-specific sequence differences were generated. Clones were induced to undergo *Igk* recombination with IL-7, and allele usage was assessed. Together, it seems that the initiation of *Igk* allelic exclusion results from numerous epigenetic changes that predetermine one allele to undergo recombination. Though *Igh* and *Tcrb* alleles also undergo asynchronous replication (Mostoslavsky *et al.* 2001, Skok *et al.* 2001), there has been no evidence that replication timing plays a role in allelic exclusion at these loci.

Initiation of allelic exclusion at *Tcrb* loci may be quite distinct from initiation of allelic exclusion at *Igk* loci, as there is no evidence that the two *Tcrb* alleles are non-equivalent substrates for recombination. If true, reduced recombination efficiency on both alleles could lead to the initiation of allelic exclusion. Recombination efficiency

could be reduced through various mechanisms. For example, V_β (and V_H) RSSs may be inherently inefficient, and contribute to allelic exclusion (Schlissel 2002). Indeed, when the V_β14 23 RSS was switched with the D_β1 23 RSS, recombination to V_β14 increased 9-fold (Wu *et al.* 2003). Additionally, mice expressing cRAG1/2 proteins are defective in V-to-DJ, but not D-to-J recombination. This could be interpreted to suggest that V gene segment RSSs are less efficient substrates for recombination than DJ RSSs (Liang *et al.* 2002).

Homologous 'pairing' has been suggested to regulate the initiation of recombination at *Igh* and *Igk* loci. Both *Igh* and *Igk* alleles were found to come into close proximity of their homologous partner (~1-2 μm) in ~20% of cells during the stage at which they undergo recombination (Hewitt *et al.* 2009). This pairing was partially mediated by RAG1, though the catalytic activity of RAG1 was not required for pairing. After initiating recombination, RAG1was suggested to 'mark' the unrearranged allele by positioning it at PCH, likely to prevent rearrangement on that allele while the first rearrangement product is tested at the cell surface. However, how this might function at a molecular level is unclear. In pro B cells containing one rearranged *Igh* allele and one unrearranged allele, the unrearranged allele was positioned at PCH in ~80% of cells with paired *Igh* alleles

ATM signaling enforces *Igk* allelic exclusion (Steinel *et al.* 2013). Allelically included B cells are 2.5-fold more frequent in ATM-deficient mice than in WT pre B cells. In addition, ATM-deficient pre B cells contained more RAG-dependent DSBs than ATM-sufficient cells. Repair timing did not confound these results, because cells unable to repair RAG-dependent DSBs were used. The mechanism behind ATM-mediated enforcement of *Igk* asynchronous recombination was suggested to be the downregulation of RAG1/2 expression after a DSB. The presence of a DSB was found to lead to a 6-fold decrease in RAG2 protein level and 4-fold decrease in RAG1 protein level.

Although thus far only correlations have been made, association with repressive subnuclear compartments may also reduce recombination efficiency. If correct, antigen receptor allele association with repressive compartments could suppress transcription or reduce RAG1/2 accessibility. Two well-characterized repressive subnuclear compartments with which antigen receptor loci interact are PCH and the nuclear periphery (Lin and Murre 2013). The idea that the nuclear periphery represses recombination is supported by the repositioning of all antigen receptor loci, excluding *Tcrb* alleles, away from periphery prior to recombination (Schlimgen *et al.* 2008).

Association with repressive subnuclear compartments may occur in a predetermined or stochastic manner, which, in theory, could be easily determined by

using DNA immunoFISH to visualize the loci and the repressive compartment. If one allele per cell associates with the repressive compartment, it could be inferred that associations occur in a predetermined manner. If alleles associate at a high frequency, but not strictly monoallelically, a stochastic mechanism could be assumed. Interestingly, whether *Tcrb* association with PCH prior during recombination occurs in a deterministic or stochastic manner remains controversial (Roldan *et al.* 2005, Skok *et al.* 2007, Schlimgen *et al.* 2008).

Though PCH associations seem to play a role in the maintenance of allelic exclusion, the nuclear periphery may be important for the initiation of allelic exclusion. This may be especially true for *Tcrb* alleles, which remain highly associated with the nuclear periphery in DN thymocytes that undergo V(D)J recombination (Schlimgen *et al.* 2008). Association with the periphery occurs stochastically. ~45% of nuclei contained both *Tcrb* alleles at the periphery, ~45% contained one allele at the periphery, and just ~10% contained both alleles free of the periphery. Moreover, of the nuclei containing one central and one peripheral *Tcrb* allele, the central allele was more likely to have undergone V_β-to-DJ_β recombination. These data suggest that allelic exclusion is initiated at *Tcrb* alleles by stochastic association with the nuclear periphery. However, these results could also be interpreted to mean that following in-frame V_β-to-DJ_β recombination on one allele, rearranged alleles move away from the periphery. It

remains to be seen whether positioning at the nuclear periphery directly suppresses V(D)J recombination at *Tcrb* alleles in DN thymocytes.

1.6.2 Feedback Inhibition

If feedback inhibition mechanisms were not active at *Tcrb* and *Igh* loci, 20% of peripheral T cells would contain in-frame VDJ rearrangements on both alleles. This number comes from knowing that 1/3 of rearrangements are in-frame (as there are three nucleotides per codon). Therefore 1/9 would rearrange both alleles in-frame, 2/9 of cells would rearrange the first allele out-of-frame and the second allele in frame, 2/9 would rearrange the first allele in-frame and the second out-of-frame, and 4/9 of cells would rearrange both alleles out-of-frame. The 4/9 cells containing out-of-frame rearrangements on both alleles would be eliminated by apoptosis, leaving 1/5 cells with biallelic in-frame VDJ rearrangements. However single cell analyses find only ~3% of mature T cells and B cells contain in-frame VDJ genes on both alleles (Balomenos *et al.* 1995, ten Boekel *et al.* 1998).

This feedback inhibition of allelic exclusion was established when recombination did not occur following the insertion of pre-rearranged *Igh* or *Tcrb* tg (von Boehmer *et al.* 1988). Feedback inhibition prevents recombination of *Igh* and *Tcrb* loci after a functional rearrangement occurs on one allele, and is mediated by pre-TCR and pre-BCR signaling

(Muljo and Schlissel 2000, Michie and Zuniga-Pflucker 2002). Feedback inhibition signals induce inhibitory mechanisms to prevent additional V-to-DJ recombination. For example, In DP thymocytes the V_β gene segments lose active histone modifications, decrease transcription, increase DNA methylation, and are less sensitive to endonucleases (Tripathi *et al.* 2002). Therefore loss of accessibility was proposed as a mechanism of preventing additional V-to-DJ recombination.

Allelic exclusion at *Igh* loci is maintained by changes in chromatin accessibility at V_H gene segments that reduce the efficiency of V_H-to-DJ_H recombination (Chowdhury and Sen 2003). After exposure to IL-7, a hematopoetic growth factor that stimulates cell differentiation into lymphocytes (Gonzalez-Garcia *et al.* 2012) *in vitro*, chromatin accessibility of distal V_H gene segments was induced in cultured RAG2-deficient bone marrow cells. Additionally, in the absence of IL-7, the distal V_H gene segments became less accessible, but could be reactivated upon IL-7 exposure. The transition from pro B to pre B cell is accompanied by the loss of IL-7 receptor signaling, which may provide a mechanism by which IL-7 signals alter V_H chromatin structure.

However chromatin changes cannot fully explain feedback inhibition. V_β14, which lies just downstream of the DJC_β cluster, remains highly transcribed in DP thymocytes, but does not undergo recombination (Chattopadhyay *et al.* 1998). Other V_β gene segments also transcribe when positioned near E_β, but are allelically excluded in

DP thymocytes (Senoo *et al.* 2003). In addition, the insertion of E_α into the *Tcrb* locus increased transcription, histone acetylation, and restriction enzyme sensitivity of alleles in DP thymocytes, but did not lead to allelic inclusion (Jackson *et al.* 2005). These data indicate that accessibility plays a role, but is not the sole mechanism behind the maintenance of allelic exclusion at *Tcrb* loci.

Large-scale locus contraction is likely required to bring distant coding genes together to undergo V(D)J recombination. Therefore locus decontraction could serve as a useful means of preventing recombination after a functional rearrangement. Indeed *Tcrb*, *Igk* and *Igh* locus decontraction has been observed following V(D)J recombination (Skok *et al.* 2007).

The transcription factors Ets1 and E2A regulate various developmental processes in response to extracellular signals and are integral for normal lymphocyte development (Oikawa and Yamada 2003, Murre 2005). There is evidence that Ets1 and E2A regulate feedback signals from pre-TCR and pre-BCR signaling to inhibit recombination. Ets1-deficient thymocytes containing a pre-rearranged *Tcrb* tg continued to undergo recombination at endogenous *Tcrb* loci (Eyquem *et al.* 2004). As Ets1 binds to and represses E_β (Prosser *et al.* 1992), Ets1 could reduce RAG1/2 accessibility specifically on the unexpressed allele following feedback signals. In contrast, the E2A splicing variant E47 increases V_β gene accessibility in a dose-dependent manner (Agata *et al.* 2007).

Haploinsufficiency of E47 resulted in the reduction of active histone marks and gene transcription of V_β gene segments. Additionally, following pre-TCR signaling the downregulation of E2A expression is required to enforce allelic exclusion at *Tcrb* loci.

Subnuclear positioning of antigen receptor loci at repressive compartments may also support the maintenance of allelic exclusion (Roldan *et al.* 2005, Schlimgen *et al.* 2008). For example, *Igk* allelic exclusion is likely supported by monoallelic association of the unexpressed allele with a repressive subnuclear compartment. In early B cell development, most cells contain *Igk* alleles which are both free of both the nuclear periphery and PCH (Goldmit *et al.* 2005). In mature B cells, most cells contained only one *Igk* allele associating with PCH. In line with these findings, the unexpressed *Igk* allele is often associated with PCH while the expressed allele is not associated with PCH in active B cells (Brown *et al.* 1999).

Association with repressive compartments may also be important for the maintenance of allelic exclusion at *Igh* loci. Association with PCH was suggested to support the maintenance of allelic exclusion at *Igh* loci, since in activated splenic B cells the unexpressed *Igh* allele is positioned at PCH while the active allele is free of PCH (Skok *et al.* 2001). In the stage following *Igh* recombination, 70% of cells contained a single *Igh* allele associating with PCH (Roldan *et al.* 2005). In these cells, the PCH-associated alleles were decontracted, implying that they had not undergone V_H-to-DJ_H

recombination and suggesting that relocalization of the unexpressed allele occurs quickly.

ATM may be partially required for positioning of the unexpressed allele at PCH, as the frequency of pro B and pre B cells containing biallelic *Igh* rearrangement increased slightly in the absence of ATM (pro B: 0.1% to 0.8%, pre B: 1.2% to 4.2%). However the number of events observed was quite low. Also, theses data could be alternatively interpreted to indicate that without ATM, DSB repair simply requires more time to complete (Lukas *et al.* 2011).

A recent study evaluated the requirements of locus contraction, subnuclear positioning, and chromatin accessibility in the maintenance phase of allelic exclusion (Kondilis-Mangum *et al.* 2011). Locus accessibility and decontraction, but not positioning at the nuclear periphery, were confirmed to be required to prevent *Tcrb* recombination in DP thymocyte nuclei. Despite these conclusions, certain types of recombination at *Tcrb* loci (such as V_β14-DJ_β recombination and secondary recombination to V_β gene segments immediately upstream of the rearranged V_β segment) involve V_β gene segments that remain accessible and proximal in DP thymocytes (Jackson *et al.* 2005, Yang-Iott *et al.* 2010). Therefore additional layers of regulation are likely required to suppress V(D)J recombination in DP thymocytes.

2. Thesis Prospectus

2.1 Thesis Proposal

Gene-poor and transcriptionally repressed chromatin is commonly located at the nuclear periphery, and the subnuclear localization of certain genes has proven to be an important determinant of transcriptional activity. In addition, the nuclear periphery can actively repress DNA in nearby proximity. Interestingly, positioning of antigen receptor loci at the nuclear periphery has been implicated in the regulation of V(D)J recombination (Schneider and Grosschedl 2007). However a detailed understanding of how positioning at the nuclear lamina affects recombination is lacking.

This work stems from research evaluating the 3D subnuclear localization of several *Tcr* loci during thymocyte development (Schlimgen *et al.* 2008). Subnuclear positioning was found to be developmentally regulated at both *Tcra*/*Tcrd* and *Tcrb* loci. Interestingly, though *Tcra*/*Tcrd* loci were 'freed' from the nuclear periphery prior to recombination, which is similar to the positional changes observed in *Igh* and *Igk* loci, *Tcrb* alleles behaved differently. *Tcrb* alleles remain positioned at the nuclear periphery in DN thymocyte nuclei, the stage at which they undergo rearrangement. Additionally, *Tcrb* alleles at the nuclear periphery in later developmental stages were more likely not to have undergone recombination. Together, these results suggest that positioning at

the nuclear periphery may suppress rearrangement, potentially contributing to the initiation phase of allelic exclusion.

2.2 Specific Aim 1: Characterize Tcr *recombination events in thymocyte nuclei*

This project began with the goal of visualizing the location of *Tcrb* recombination in DN thymocyte nuclei. We first analyzed the distribution of nuclei containing monoallelic and biallelic D_β-to-J_β and V_β-to-DJ_β rearrangement events, using mice containing genetically modified *Tcrb* alleles. We confirmed that V_β-to-DJ_β recombination occurred asynchronously, and discovered that D_β-to-J_β recombination also occurred monoallelically in DN thymocyte nuclei. We were also interested in determine whether the presence of a RAG-dependent DSB signaled to prevent the generation of additional RAG-dependent DSBs within a cell. We utilized genetically modified mouse models unable to repair RAG-dependent DSBs, and asked whether RAG-mediated DSBs accumulated at antigen receptor loci. We found that RAG-dependent DSBs accumulated in a stochastic, and not strictly monoallelic, manner at antigen receptor loci. We concluded that the presence of a DSB resulting from V(D)J recombination does not signal to prevent additional rearrangement events. Additionally, we inferred that the asynchronous recombination of allelically excluded *Tcrb* alleles results from inefficient recombination of both alleles.

2.3 Specific Aim 2: Determine if peripheral subnuclear positioning represses Tcrb *recombination*

Previous studies did not directly determine whether V(D)J recombination was suppressed on antigen receptor alleles positioned at the nuclear periphery, or whether unrearranged alleles were relocated to the nuclear periphery following recombination. We attempted to address these questions using 3D immunoFISH in DN thymocytes by analyzing the frequency and subnuclear location of rearranging *Tcrb* alleles. Rearranging alleles were identified by the presence of a proximal DSB. Using a subset of nuclei in which repression of recombination by the periphery would be more easily observed, we directly compared the frequency of rearranging peripheral alleles to rearranging central alleles. We found that positioning at the nuclear periphery did suppress the frequency of V(D)J recombination. We also characterized the conformations of rearranging and non-rearranging peripheral *Tcrb* loci. The orientation of the rare peripheral *Tcrb* alleles undergoing recombination suggested that when portions of loci move away from the periphery, the suppressive effects of the periphery are alleviated. We concluded that positioning of *Tcrb* alleles at the nuclear periphery reduced the frequency of V(D)J recombination, potentially contributing to the initiation of allelic exclusion.

2.4 Specific Aim 3: Determine if the subnuclear distribution of RAG2 can explain reduced recombination at the nuclear periphery

We next sought to determine the mechanism by which the nuclear periphery suppresses *Tcrb* recombination. Recombination could be repressed either by transcriptional silencing or by the restricting access to recombination factors. It is unlikely that peripheral *Tcrb* alleles are transcriptionally repressed, as at least one V_β gene segment is biallelically transcribed in all DN thymocytes (Jia *et al.* 2007). Additionally, we co-visualized *Tcrb* alleles and PolII and found that nearly all *Tcrb* alleles colocalize with PolII in DN thymocyte nuclei. This suggests that nearly all *Tcrb* alleles are capable of transcription during the stage at which they undergo recombination. We then investigated whether peripheral positioning separates *Tcrb* alleles from the recombination factor RAG2 by visualizing both in DN thymocyte nuclei. We found that RAG2 levels are reduced at the nuclear periphery, and that peripheral *Tcrb* alleles are segregated from RAG2. We concluded that segregation from RAG2 was likely the mechanism by which recombination was suppressed on peripheral *Tcrb* alleles.

3. Materials and Methods

3.1 Mice

Mice were housed in accordance with the protocols approved by the Duke University Animal Care and Use Committee. 129 and C57Bl/6 wild-type mouse strains were purchased from Jackson Labs. *Rag2*$^{-/-}$ (Shinkai *et al.* 1992), *Rag2*$^{-/-}$ containing a rearranged *Tcrb* tg (Shinkai *et al.* 1993), *Lat*$^{-/-}$ (Zhang *et al.* 1998), ω (Bassing *et al.* 2000), M4 (Bassing *et al.* 2000), DJβ (Carpenter *et al.* 2009), *Art*$^{-/-}$ (Rooney *et al.* 2002), *Atm*$^{-/-}$ (Barlow *et al.* 1996), *Rag2*$^{\Delta/\Delta}$ (Liang *et al.* 2002), μMT (Kitamura *et al.* 1991), and *Ctcf*$^{fl/}$ (Heath *et al.* 2008) were all previously described. To induce CTCF deletion in early DN thymocytes, *Ctcf*$^{fl/fl}$ mice were bred with *Lck*-Cre mice provided by Dr. Jeffrey Rathmell.

3.2 Cell collection and cultures

Murine thymuses were removed and mashed beneath mesh in 10 mls of RPMI containing 10% fetal bovine serum (FBS). Thymocytes in suspension were passed through a mesh filter, and the thymocytes were pelleted and resuspended in Hank's buffered saline solution. DN thymocytes were obtained directly from 2-3 week old mice on *Rag2*$^{-/-}$, *Lat*$^{-/-}$, and *Art*$^{-/-}$ backgrounds. Total thymocytes predominantly at the DP stage of development were obtained directly from 1-3 month old WT mice, *Rag2*$^{-/-}$ x *Tcrb*

tg mice, and *Rag2*$^{-/-}$ mice ten days after injection with 300 μg of anti-CD3 antibodies (145-2C11) as previously described (Schlimgen *et al.* 2008, Shih and Krangel 2013). DP and CD4^{+}CD8^{-} thymocytes were sorted from 2-3 week old C57BL/6 or 129 mice using FITC-conjugated anti-CD4 (GK1.5) and Pacific Blue-conjugated anti-CD8α (53-6.7). Mature splenic B cells were obtained by sorting using Fc-block, anti-CD19 BIO (6D5) plus FITC-conjugated streptavidin, and Pacific Blue-conjugated anti-B220 (RA3-6B2). Pro-B cells were sorted from 4-6 week old μMT mice using FITC-conjugated anti-CD43 (S11) and Pacific Blue-conjugated anti-B220 (RA3-6B2). CTCF-deleted DP thymocytes were sorted from *Ctcf*$^{f/f}$ *Lck*-Cre mice seven days after a single intraperitoneal injection of 75 μg anti-CD3 antibody (145-2C11) using PE-conjugated anti-CD71, PE/Cy7-conjugated anti-CD4 and APC-Cy7-conjugated anti-CD8. As CTCF deletion induces LacZ expression, cells were treated with the LacZ substrate from a FluoReporter® *lacZ* flow cytometry kit (Invitrogen) in order to identify LacZ^{+} cells by flow cytometry. LacZ^{+} cells predominantly carry two *Ctcf*-deleted alleles (Shih *et al.* 2012). Sorting purity was greater than 90% for all analyses. CTCF-sufficient DP thymocytes were sorted from control *Ctcf*$^{f/f}$ *Lck*-Cre^{-} littermates. All antibodies were obtained from BioLegend.

NIH3T3 cells were cultured in high-glucose Dulbecco's Modification of Eagle's Medium with 2% glutamine, 10% bovine calf serum, and 1X penicillin/streptomycin. P5424 cells were cultured in RPMI and 10% bovine calf serum.

3.3 FISH probes and antibodies

Bacterial artificial chromosome (BAC) clones RP23-75P5 (V_β-probe, which targets a region 5′ of the *Tcrb* locus), RP23-203H5 (trypsinogen probe, which targets a region 3′ of the V_β array and 5′ of the DJC_β cluster), RP23-457D7 (C_β-probe, which targets a region 3′ of the *Tcrb* locus), RP23-304L21 (V_α-probe, which targets a 5′ region of the $V_{\alpha/\delta}$ array), RP23-10K20 (V_α-probe, which targets a 3′ region of the $V_{\alpha/\delta}$ array), RP23-97O1 (*Actb*-probe, which targets the full *Actb* locus) were used as DNA probes. The BAC clones were grown overnight with shaking at 30°C in terrific broth (TB) media with 12.5 μg/ml chloramphenicol. Typically, 100 mls of TB media was inoculated with 100 μl of a 3 ml TB culture grown overnight from a single bacterial colony. Bacteria were pelleted, and BACs were resuspended in 7 mls of 10 mM Tris, 50 mM EDTA. Cells were lysed in 7 mls of 200mM NaOH and 1% SDS (w/v) for 5 min. The reaction was stopped and genomic DNA was precipitated by adding 10 mls of 3M potassium acetate and glacial acetic acid (pH=5.5) and incubated at 4°C for at least 15 min. The supernatant was extracted with an equal volume of phenol:chloroform (1:1) and then an equal volume of chloroform. DNA was precipitated by adding 2 volumes of ethanol (EtOH), and incubated at -80°C for 20 min. After centrifugation for 30 min at 4,000 rpm, the pellet was washed with 70% EtOH and resuspended in 10mM Tris.

BAC clones were labeled using either a digoxigenin (DIG) or biotin (BIO) nick-translation kit (Roche). Foci were visualized with either FITC-conjugated anti-biotin (200-092-211, Jackson Immunoresearch Laboratories) or Cy3-conjugated anti-DIG (200-162-156, Jackson Immunoresearch Laboratories). The nuclear lamina was visualized using a polyclonal goat anti-laminB1 (sc-6217, Santa Cruz Biotech) antibody and Cy5-conjugated anti-goat antibodies (705-605-003, Jackson Immunoresearch Laboratories) or FITC-conjugated anti-goat antibodies (705-095-003, Jackson Immunoresearch Laboratories). 53BP1 was visualized using a polyclonal rabbit anti-53BP1 (NB 100-304, Novus Biologicals) antibody and FITC-conjugated donkey anti-rabbit IgG (sc-2090, Santa Cruz Biotech). Ki67 was visualized using a polyclonal mouse anti-Ki67 antibody (556003, BD Pharmingen) and FITC-conjugated donkey anti-mouse IgG (715-095-150, Jackson Immunoresearch Laboratories). RAG2 was visualized using monoclonal rabbit anti-RAG2 antibody #39 (Coster et al., 2012) and Cy3-conjugated goat anti-rabbit IgG F(ab')2 antibody (111-166-047, Jackson Immunoresearch Laboratories). PolII was visualized using a monoclonal mouse anti-PolII antibody (NB200-598, Novus Biologicals) and FITC-conjugated donkey anti-mouse IgG (715-545-151, Jackson Immunoresearch Laboratories). H3K4me3 was visualized using a polyclonal rabbit anti-H3K4me3 antibody (ab8580, Abcam) and either Cy3-conjugated donkey anti-rabbit IgG (711-165-152, Jackson Immunoresearch Laboratories) or FITC-conjugated donkey anti-

rabbit IgG (711-095-152, Jackson Immunoresearch Laboratories). CTCF was visualized using anti-CTCF rabbit antiserum (07-729, Millipore) and FITC-conjugated donkey anti-rabbit IgG (sc-2090, Santa Cruz Biotech). CTs were identified using BIO- or DIG-conjugated chromosome paints (Chromosome 14-1187-6MB-02, Cambio, Chromosome 6-1187-14MB-0, Cambio). CTs were hybridized similarly to BAC DNA probes, and were visualized using monoclonal mouse anti-biotin antibodies (200-092-211, Jackson Immunoresearch Laboratories).

3.4 Three-dimensional DNA immunoFISH and confocal imaging

Methods for cell fixation, immunoFISH and confocal imaging were as described (Schlimgen *et al.* 2008) except that slides were denatured at 77.8°C prior to hybridization, then washed in 50% (v/v) formamide at 40°C twice and in 0.2xSSC at 60°C three times. Each slide received 0.5-1 μg of primary antibody and 3-5 μg of conjugated secondary antibody in 0.4 ml of 4% (w/v) bovine serum albumin and 2x SSC. The specificity of PolII and H3K4me3 staining was demonstrated by incubation of primary antibody with 8 ug of PolII (ab18488, Abcam) or H3K4me3 (ab1342, Abcam) peptide-immunogen, respectively, per slide for 30 minutes at 23°C prior to staining of nuclei. Slides were imaged on a Leica SP5 confocal microscope. Optical sections separated by 0.12 μm were collected, and only cells with intact laminB1 signals were analyzed. Nucleoplasmic

proteins were extracted from cells by incubation of slides as previously described (Li and de Lange 2003), except that cells were treated with 0.5% (v/v) Triton X-100, 20 mM HEPES (pH7.9), 3 mM $MgCl_2$, 300 mM sucrose containing 0 to 100 mM NaCl for only 1 minute. Slides were then processed for 3D immunofluorescence as described above.

3.5 Colocalization analysis

All colocalization experiments were performed using ImageJ software. Images were initially passed through a Kalman stack filter and were then thresholded so that (1) the laminB1 signal formed a contiguous ring around most nuclei, (2) two BAC probe signals were present within most nuclei, and (3) low level 53BP1, RAG2, Pol II, H3K4me3 and DAPI signals were eliminated. Background RAG2 staining (as judged by the signal in *Rag2*$^{-/-}$ nuclei) was higher in immunoFISH as compared to simple immunofluorescence experiments. Foci were considered colocalized with laminB1, RAG2 or PolII if at least two adjacent pixels overlapped in the combined, thresholded image.

The 3D distance between the centers of mass of two foci (ex: a 53BP1 focus and a *Tcrb* focus) was measured using the Sync Measure 3D ImageJ plugin. 53BP1 foci were considered to be located at *Tcrb* alleles if they were within 1 μm, and at *Tcrd* alleles if they were within 1.5 μm.

3.6 Conformation analysis

To determine the orientation of *Tcrb* alleles located at the nuclear periphery, images were deconvolved using Huygens Essential software with specifications appropriate for a Leica SP5 confocal microscope with a 100x objective and 2x zoom. *Tcrb* alleles were assessed for colocalization with the nuclear lamina using ImageJ software, and colocalizing alleles were selectively analyzed. The nuclear lamina was rendered into a surface and thresholded so that the lamina was roughly 2 μm thick in the middle of the nucleus. Distance from the nuclear lamina was determined by measuring from the center of mass of each focus to the nearest point on the inner edge of the nuclear lamina. Foci whose volume was >50% colocalized with the nuclear lamina were considered to have a center of mass internal to the lamina, and were assigned a positive distance value. Foci whose volume was <50% colocalized with the lamina were considered to have a center of mass external to the lamina and were assigned a negative distance value. To determine the peripheral location of the experimental focus in relation to the colocalized focus, the distance of the experimental focus was subtracted from the distance of the colocalized focus.

3.7 Fluorescence intensity traces

Fluorescence intensity plots were obtained using the Twin Slicer application of Huygens Essential deconvolution software. One z-slice within the middle 1/3rd of each nucleus was selected for analysis and fluorescence intensity was traced along a single diameter within this z-slice. Gene location relative to the nuclear periphery was determined by selecting a z-slice in the middle 1/3rd of the nucleus in which the allele focus was brightest. Lines were then traced through the brightest portion of the focus to the nearest point on the nuclear lamina.

3.8 Correlation analysis

Correlation analysis was conducted on raw image stacks, which had not undergone Kalman stack filtering. The Pearson correlation coefficient, *r*, was calculated as a measure of the average colocalization between two markers within individual cells. *r* was calculated for selected individual cells containing all markers of interest and lamin staining indicating intact nuclear structure. To this end, individual nuclei in the field of view were segmented from three dimensional image stacks using laminB1 to outline nuclear boundaries and identify individual cells. All nuclear boundaries in the field of view were identified using a fixed threshold of laminB1 signal. The resulting binary image separated pixels on the inside of each nucleus from pixels outside nuclei. The

binary image was segmented into individual nuclei using a connected components identification algorithm (Haralick and Shapiro 1992) combined with morphological closing (Soille 2003). Correlation was calculated within the interior of each identified nucleus. Image processing was performed in MATLAB.

PolII and H3K4me3 correlation was compared to PolII vs. RAG2 correlations by fitting to the model: $r_{ij} = \mu^{H} + \mu_i^{R-H} + f_i + \varepsilon_{ij}$. In this model r_{ij} is the Pearson's correlation (whole cell colocalization) for the *j*-th cell in the *i*-th field of view ($i = 1, \ldots, 10$). The baseline mean (for PolII vs. H3K4me3) is denoted by μ^{H}. For fields of view *i* in the PolII vs.RAG2 experiments, the term μ_i^{R-H} denotes the difference of the mean colocalization between PolII vs.RAG2 when compared to the colocalization between mPolII vs. H3K4me3. The term f_i is an effect which captures the variability due to the *i*-th field of view. It is assumed to be random and have a Gaussian distribution with 0 mean and constant standard deviation σ. Finally ε_{ij} denotes measurement error. Model was fitted using restricted maximum likelihood (REML) using the nlme package in the R computing platform.

3.9 DamID

The DamID technique has been described (Greil *et al.* 2006). Briefly, a fusion protein consisting of *Escherichia coli* dam methylase and laminB1 was expressed in

NIH3T3 cells *in vivo* at relatively low levels. To control for non-specific methylation resulting from differences in chromatin accessibility, unfused dam methylase was expressed separately. Dam methylates the As of nearby GATC sequences, a modification that is unique to most eukaryotes. Methylated sequences were selectively amplified with a methylation-specific PCR protocol. First, methylated GATCs were cut using the methylation-specific enzyme *Dpn*I. This generates blunt-ended DNA fragments 5′ TC and 3′ GA^{me} sequences. A double-stranded adaptor oligonucleotide with a 32 bp 5′ overhang (to force directional ligation) was ligated to the blunt ends. Then the DNA was digested with DpnII, an enzyme that specifically cuts unmethylated GATC sequences, to exclude internal fragments containing unmethylated As from amplification. Adaptor-ligated sequences were then amplified using a primer specific for 15 nucleotides of the adaptor sequence and the GA remaining following DpnI digestion. The presence of *Tcrb*-specific sequences in the amplified gDNA was determined by quantitative PCR and two-color hybridization onto a microarray.

Microarray analysis was performed by hybridizing amplified gDNA to a custom tiled array specific for 1.2 Mb of sequence along chromosome 6, containing the entire *Tcrb* locus. Probes ranged between 50-75 bp with a 10 bp interval between the start of each probe. Experimental and test samples were co-hybridized to the array. The $\log_2$-ratio of the input signals was computed and scaled to center the data around zero.

Scaling was performed by subtracting the biweight mean for the $\log_2$-ratio values for all features on the array from each $\log_2$-ratio value, in order to reduce the influence of outliers on the average value.

3.10 Statistical analysis

Statistical differences were determined using either unpaired Student's t-tests or Fisher's exact two-tailed contingency table.

4. Analysis of *Tcr* recombination events in thymocyte nuclei

Some of the work presented and discussed in this and the following chapters has been modified from the following publication:

Chan, E. A.W., G. Teng, E. Corbett, K.R. Choudhury, C.H. Bassing, D.G. Schatz, and M.S. Krangel. 2013. Peripheral subnuclear positioning suppresses *Tcrb* recombination and segregates *Tcrb* alleles from RAG2. *Proc. Natl. Acad. Sci. USA* 110:E4628-4637.

4.1 Introduction

Cellular activities that involve the formation and repair of DSBs are tightly controlled, as unrepaired or incorrectly repaired DNA DSBs can be hazardous to the genome (Goodarzi and Jeggo 2013). Unrepaired DSBs activate cell cycle checkpoints, halting the cell cycle. If the DSB remains unrepaired, the cell can enter a permanent state of dormancy, undergo programmed cell death, or begin uncontrolled cell division. Incorrectly repaired DNA is also undesirable, as mutations can arise. Mutations in the genome could adversely affect cell function and survival or cause oncogenesis.

V(D)J recombination presents an interesting situation in which to study the regulation of DSB formation. Two DSBs are generated during V(D)J recombination of a

single allele. The two DSBs activate the DNA DDR, are repaired via the NHEJ pathway, and these repair factors can be visualized by microscopy (Chen *et al.* 2000). Though only *Tcra* loci undergo recombination in DP thymocytes, three of the four *Tcr* loci (*Tcrb*, *Tcrd*, and *Tcrg*) concurrently rearrange in DN thymocyte nuclei (Livak *et al.* 1999). Multiple DSBs occurring at several different genomic loci could result in inter-locus rearrangement and gross chromosomal abnormalities. At the onset of these studies it was not known how the formation of DSBs at the three active *Tcr* loci was regulated in DN thymocyte nuclei.

Among *Tcr* loci, only *Tcrb* is allelically excluded (Krangel 2009). *Tcrb* recombination occurs in $CD4^-$ $CD8^-$ double negative (DN) thymocytes and is ordered, beginning with D_β-to-J_β rearrangement, which can occur on both alleles. Allelic exclusion is then initiated by V_β-to-DJ_β recombination, which is thought to occur asynchronously, or on one allele at a time. This allows thymocytes time to test each allele for the creation of an open reading frame. TCRβ proteins are sensed by their assembly with pre-Tα and CD3 chains to create a pre-TCR signaling complex; pre-TCR signals then suppress further *Tcrb* recombination and promote thymocyte proliferation and differentiation to the $CD4^+CD8^+$ double positive (DP) stage (Michie and Zuniga-Pflucker 2002).

Allelic exclusion is maintained in DP thymocytes in part by chromatin alterations, such as reduced V_β germline transcription and histone acetylation, that reduce access of RAG1/2 proteins to V_β gene segments (Tripathi *et al.* 2002). In addition, *Tcrb* alleles adopt a more extended, or decontracted, conformation in DP thymocytes, physically separating V_β and DJ_β segments (Skok *et al.* 2007). Loss of accessibility and locus decontraction both contribute to the maintenance of allelic exclusion, since V_β and DJ_β segments engineered to be accessible and proximal are capable of recombination in DP thymocytes (Jackson *et al.* 2005, Kondilis-Mangum *et al.* 2011). However, since both *Tcrb* alleles appear to be accessible (Jia *et al.* 2007, Ranganath *et al.* 2008) and contracted (Skok *et al.* 2007) prior to rearrangement in DN thymocytes, the mechanism by which the locus is biased to undergo asynchronous V_β-to-DJ_β recombination in DN thymocytes is unknown.

The above questions may be linked by the regulation (or lack thereof) following a DSB. It is currently unknown whether the presence of a RAG-dependent DSB actively prevents the formation of additional RAG-dependent DSBs (Hewitt *et al.* 2009, Steinel *et al.* 2013) or if V(D)J recombination occurs infrequently, with no additional layers of regulation preventing the simultaneous rearrangement of both *Tcrb* alleles in DN thymocyte nuclei. Single-cell analyses of DSBs in thymocyte nuclei both capable and unable to repair V(D)J DSBs could answer these questions.

4.2 Results

4.2.1 53BP1 foci occur infrequently in DN thymocyte nuclei

We evaluated the frequency of recent RAG-dependent DSBs by tracking DNA-repair foci using an antibody specific for the DSB repair protein 53BP1 (Fig. 11A). In order to evaluate the frequency of 53BP1 foci in DN thymocyte nuclei, we isolated thymocytes from *Lat*$^{-/-}$ mice. These thymocytes are unable to signal through pre-TCR complexes and therefore cannot progress beyond the CD44^{-}CD25^{+} DN3 stage of development (Zhang *et al*. 1998). As a control, we also isolated DN thymocytes from *Rag*2$^{-/-}$ mice, because those thymocytes are similarly blocked at the DN3 stage of development, and should accumulate only RAG-independent DSBs. We excluded from this and all following analyses those nuclei considered to be in the process of apoptosis. DN thymocyte nuclei in this category (<10% of all nuclei) contained intense and broadly distributed 53BP1 staining, or more than six 53BP1 foci per nucleus. We chose six foci as the cutoff because it is the maximum number of *Tcrb*, *Tcrg*, and *Tcrd* alleles that could potentially undergo recombination in DN thymocyte nuclei.

Among 500 *Lat*$^{-/-}$ nuclei analyzed, 23% contained a single 53BP1 focus, 5% contained two 53BP1 foci, less than 1% contained three or four foci, and none contained five or six foci (Fig. 11B). Similar examination of 500 *Rag*2$^{-/-}$ nuclei identified 12% containing one 53BP1 focus, 0.2% containing two foci, and none containing three to six

foci (Fig. 11B). Based on this we conclude that the majority of 53BP1 foci detected in *Lat*$^{-/-}$ nuclei reflect DSBs due to V(D)J recombination. Given the overall frequency of DSBs and the rarity of nuclei with more than one DSB, we conclude that V(D)J recombination occurs infrequently at *Tcr* loci in DN thymocyte nuclei. Nuclei containing two 53BP1 foci could indicate: (1) two different *Tcr* loci undergoing recombination, (2) both alleles undergoing recombination at one *Tcr* locus, and (3) recombination at one *Tcr* allele and one background DSB.

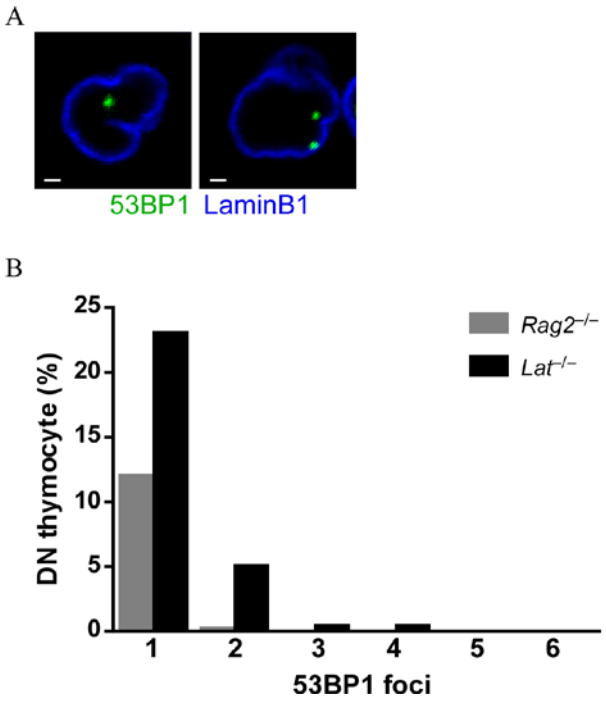

Figure 11: 53BP1 foci occur infrequently in DN thymocyte nuclei

A) Confocal immunofluorescence microscopy showing single z-slices of *Lat*$^{-/-}$ DN thymocyte nuclei containing one or two 53BP1 foci. Scale bars = 1 μm. B) Distributions of *Rag2*$^{-/-}$ and *Lat*$^{-/-}$ DN thymocyte nuclei containing one to six 53BP1 foci from 500 nuclei of each. Data were compiled from two independent experiments each.

4.2.2 53BP1 foci accumulate in DN thymocyte nuclei unable to form coding joints

We then evaluated the frequency of RAG-dependent DSBs in Art-deficient ($Art^{-/-}$) thymocyte nuclei. These thymocytes are impaired in coding joint formation, and therefore cannot repair RAG-dependent DSBs. Thymocyte development is predominantly blocked at the DN stage of development, similar to $Lat^{-/-}$ thymocyte nuclei, as most $Art^{-/-}$ thymocyte nuclei are unable to recombine *Tcrb* alleles and satisfy the β-selection checkpoint. This phenotype allows us to answer questions regarding the accumulation of DSBs, such as whether the presence of a RAG-dependent DSB has any effect on the generation of additional rearrangement events. The criteria for $Art^{-/-}$ nuclei considered to be in the process of apoptosis was identical to that of $Lat^{-/-}$ nuclei described previously.

Among the 152 $Art^{-/-}$ nuclei analyzed, 34.2% contained a single 53BP1 focus, 22.4% contained two 53BP1 foci, 4.6% contained three foci, 1.3% contained 4 foci, and none contained five or six foci (Fig. 12). These frequencies are substantially higher than those found in $Rag2^{-/-}$ or $Lat^{-/-}$ nuclei. Therefore we conclude that 53BP1 foci accumulate in $Art^{-/-}$ DN thymocyte nuclei, and that the presence of a RAG-dependent DSB may not prevent the generation of additional RAG-dependent DSBs.

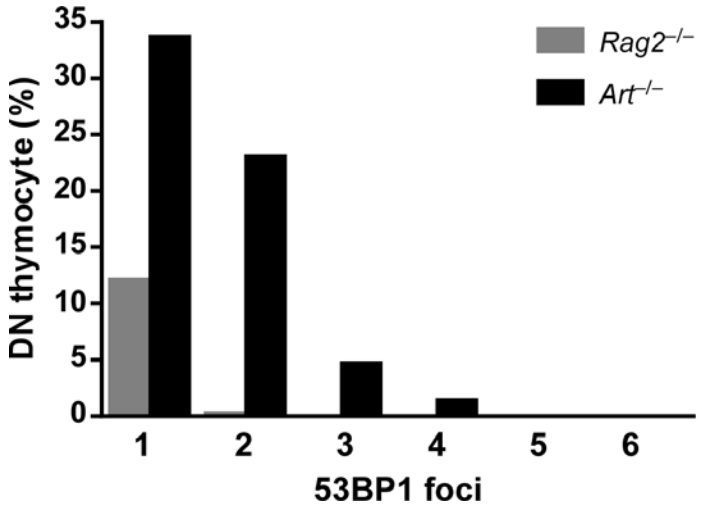

Figure 12: 53BP1 foci accumulate in DN thymocyte nuclei impaired in coding joint formation

Distributions of DN thymocyte nuclei containing one to six 53BP1 foci from 500 *Rag*2$^{-/-}$ thymocyte nuclei (data same as in Fig. 11) and 152 *Art*$^{-/-}$ thymocyte nuclei. Data were compiled from 1-2 independent experiments each.

4.2.3 53BP1 foci occur infrequently in DP thymocyte nuclei

In order to evaluate the frequency of 53BP1 foci in DP thymocyte nuclei, we sorted CD4^{+}CD8^{+} DP cells from total thymocytes of WT mice. As a control, we also isolated total thymocytes from *Rag*2$^{-/-}$ x *Tcrb* tg mice, to obtain cells that were predominantly at the DP stage but did not contain any RAG-dependent DSBs. Cells were placed on slides, fixed, and 53BP1 foci were analyzed by immunofluorescence microscopy. DP nuclei considered to be in the process of apoptosis, and therefore excluded from analysis, displayed intense and broadly distributed 53BP1 signal. Though only the two *Tcra* alleles can undergo recombination in WT DP thymocytes, we

analyzed all nuclei containing up to six total 53BP1 foci to avoid excluding cells with both RAG-dependent and -independent DSBs.

Among the 119 DP thymocytes analyzed, 21% contained a single 53BP1 focus, 6.7% contained two 53BP1 foci, none contained three foci, 0.8% contained four foci, and none contained five or six foci (Fig. 13). Similar examination of 150 *Rag*2$^{-/-}$ x *Tcrb* tg nuclei identified 6% containing one 53BP1 focus and none containing two to six foci. Based on this we conclude that the majority of 53BP1 foci detected in DP thymocyte nuclei, like those found in DN thymocyte nuclei, reflect DSBs due to V(D)J recombination. Given the low frequency of total DSBs in the *Rag*2$^{-/-}$ x *Tcrb* tg nuclei and the frequency of WT DP nuclei containing two DSB foci, we conclude that V(D)J recombination occurs infrequently at *Tcra* loci in DP thymocyte nuclei. However, we expect that the majority of nuclei containing two DSBs likely reflect biallelic *Tcra* recombination.

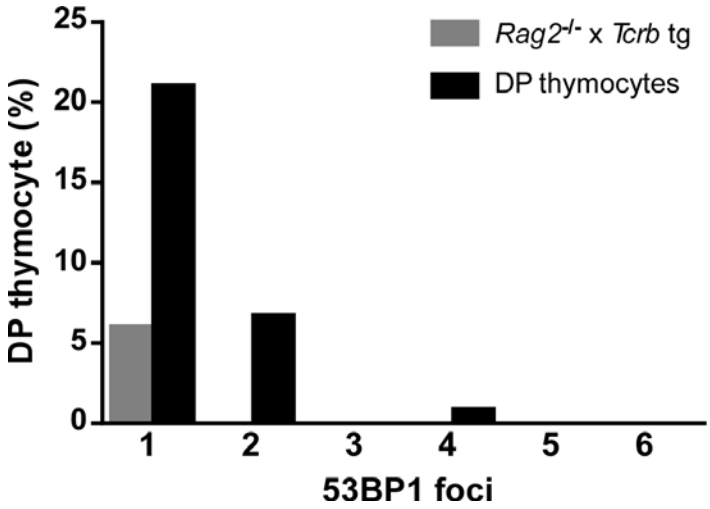

Figure 13: 53BP1 foci occur infrequently in DP thymocyte nuclei

Distributions of DP thymocyte nuclei containing one to six 53BP1 foci from 150 *Rag*2$^{-/-}$ x *Tcrb* tg thymocyte nuclei and 119 WT sorted DP thymocyte nuclei. Data were from one experiment each.

4.2.4 Identifying 53BP1^{+} *Tcr* alleles

To identify RAG-dependent DSBs at *Tcr* alleles, we used DNA immunoFISH to visualize 53BP1 and *Tcr* alleles simultaneously (Fig. 14A). As we were most interested in recombination at *Tcrb* alleles, we measured the distance between the center of each 53BP1 focus and the center of the nearest *Tcrb* focus in 500 *Lat*$^{-/-}$ and 500 *Rag*2$^{-/-}$ DN thymocyte nuclei. *Tcrb* alleles were identified using the V$_{\beta}$-end probe (Fig. 14B). We detected a discrete population of DSBs within 1 μm of a *Tcrb* focus in *Lat*$^{-/-}$ nuclei, but did not detect a similar population in *Rag*2$^{-/-}$ nuclei (Fig. 14C). Based on this we concluded that 53BP1 foci within 1 μm of a *Tcrb* allele identify *Tcrb* alleles that have

recently undergone V(D)J recombination. From this point on these will be referred to as 53BP1^{+} *Tcrb* alleles. We note that 53BP1 foci greater than 1 μm from a *Tcrb* focus were twice as frequent in *Lat*$^{-/-}$ as compared to *Rag2*$^{-/-}$ nuclei (118 vs. 61 foci). We presume that this increase reflects recent RAG-mediated DSBs at *Tcrg* and *Tcrd* loci in *Lat*$^{-/-}$ nuclei.

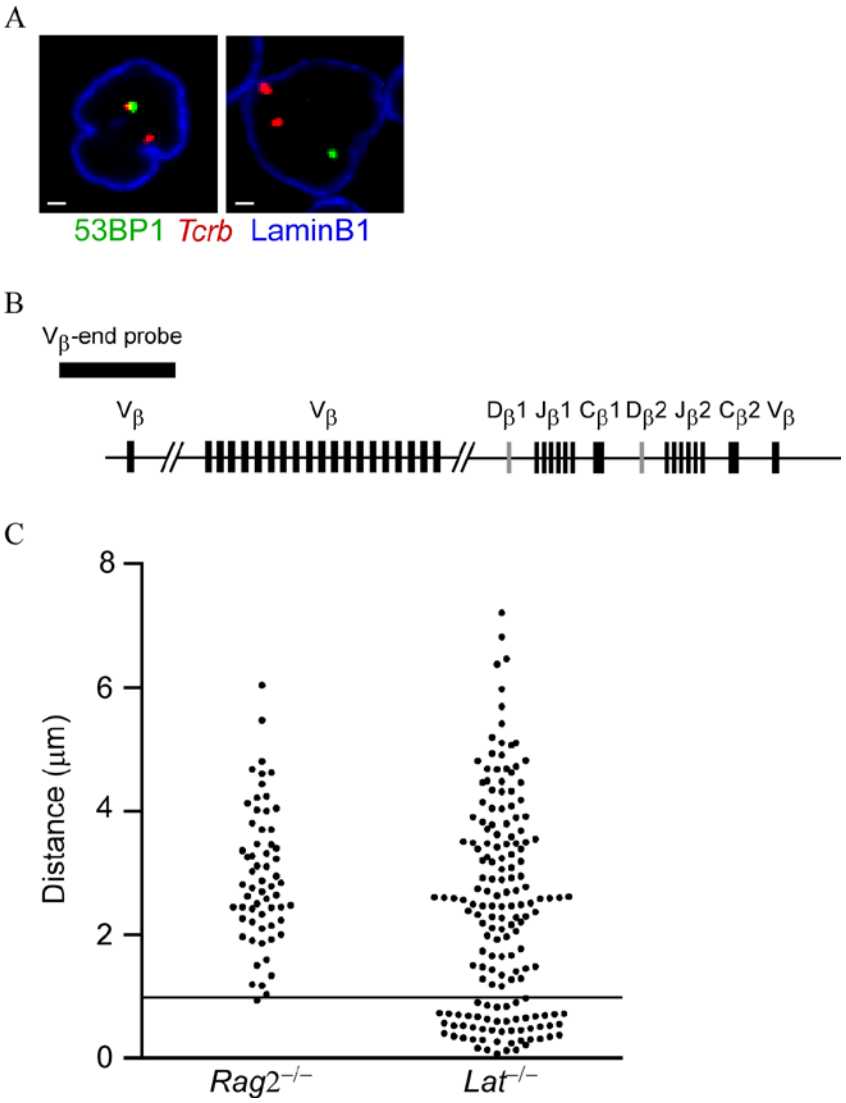

Figure 14: Identifying 53BP1^{+} *Tcr* alleles

A) Confocal immunoFISH microscopy showing single z-slices of *Lat*$^{-/-}$ DN thymocyte nuclei containing 53BP1 foci at or distant from *Tcrb* foci. Scale bar = 1 μm. B) Diagram of the *Tcrb* locus and the location of the Vβ-end probe. C) Distance of 53BP1 foci from the nearest *Tcrb* allele in 500 *Rag2*$^{-/-}$ and 500 *Lat*$^{-/-}$ DN thymocyte nuclei. *Tcrb* alleles were identified using the Vβ probe. The horizontal line at 1 μm separates presumed *Tcrb* 53BP1 foci from other 53BP1 foci.

4.2.5 *Tcrb* alleles recombine monoallelically in DN thymocytes

To directly determine whether *Tcrb* alleles undergo asynchronous *Tcrb* recombination, we analyzed the frequency of *Tcrb* alleles that were 53BP1$^+$ and the frequency of nuclei containing one or two 53BP1$^+$ *Tcrb* alleles in thymocytes from mice with WT *Tcrb* alleles on a *Lat*$^{-/-}$ background. We found that 5.1% of WT alleles on a *Lat*$^{-/-}$ background were 53BP1$^+$ (Fig. 15A), demonstrating that *Tcrb* recombination is a relatively rare event in DN thymocyte nuclei. We saw that 90% of *Lat*$^{-/-}$ DN thymocytes contained zero 53BP1$^+$ *Tcrb* alleles, 9.4% contained a single 53BP1$^+$ *Tcrb* allele, and only 0.4% contained two 53BP1$^+$ *Tcrb* alleles (Fig. 15B). A recent study demonstrated 53BP1$^+$ *Tcrb* alleles in a somewhat smaller fraction (4%) of sorted DN2/3 thymocytes from WT mice (Bowen *et al.* 2013). We conclude that *Tcrb* recombination occurs infrequently in *Lat*$^{-/-}$ DN thymocytes.

The rare *Lat*$^{-/-}$ nuclei containing two 53BP1$^+$ *Tcrb* alleles could be due to the simultaneous rearrangement of both alleles; however, since 53BP1 foci can remain at the site of a DSB for several hours (Anderson *et al.* 2001, Asaithamby and Chen 2009) they could also be explained by rearrangement events occurring hours apart.

Though 53BP1 foci located at *Tcrb* alleles could not be separated into those resulting from Dβ-to-Jβ and Vβ-to-DJβ recombination events in this experiment, the foci

likely represent a mixture of both events. Therefore, we suspect that both steps of *Tcrb* recombination occur asynchronously on *Tcrb* alleles in DN thymocytes.

To directly examine whether the two steps of recombination each occur monoallelically in DN thymocyte nuclei, we used gene-targeted mice carrying modified *Tcrb* alleles that can undergo only D_β-to-J_β or only V_β-to-DJ_β rearrangement events (Fig. 15C). The M4 *Tcrb* allele has a mutation in the 5′ $D_\beta1$ RSS and lacks the $D_\beta2J_\beta2$ cluster, and thus can undergo only D_β-to-J_β recombination (Bassing *et al.* 2000). The DJβ allele has a pre-rearranged $DJ_\beta1$ gene segment and lacks the $D_\beta2J_\beta2$ cluster, and thus can undergo only V_β-to-$DJ_\beta1$ recombination (Carpenter *et al.* 2009). The ω allele serves as a useful control since it lacks the $D_\beta2J_\beta2$ cluster but has an unmanipulated $D_\beta1J_\beta1$ cluster and thus can undergo both D_β-to-$J_\beta1$ and V_β-to-$DJ_\beta1$ recombination (Bassing *et al.* 2000). All modified alleles were crossed onto a $Lat^{-/-}$ background to allow for the direct harvest and analysis of DN thymocytes immediately *ex vivo*.

We began by determining the frequency of modified *Tcrb* alleles that were $53BP1^+$ (Fig. 15A). The frequency of ω *Tcrb* alleles that were $53BP1^+$ was roughly half that of WT *Tcrb* alleles, which is consistent with the loss of one of the two DJ_β clusters (Fig. 15A). The frequencies of M4 and DJβ alleles that were $53BP1^+$ were slightly lower than ω alleles. Though it might be expected that D_β-to-J_β rearrangements would occur at a higher frequency than long-range V_β-to-DJ_β rearrangements, the frequencies of

53BP1^{+} M4 and DJβ alleles were quite similar to each other. The relatively high frequency of DJβ alleles undergoing V_{β}-to-DJ_{β} rearrangements could be the result of V_{β}-to-DJ_{β} recombination occurring more efficiently on alleles that have already undergone D_{β}-J_{β} recombination (Carpenter *et al.* 2009).

We then evaluated the frequency of nuclei containing 0, 1, and 2 53BP1^{+} *Tcrb* alleles in mice containing the modified *Tcrb* alleles (Fig. 15B). 4.6% of DN thymocyte nuclei of ω/ω *Lat*$^{-/-}$ mice contained one 53BP1^{+} *Tcrb* allele per nucleus, roughly half the frequency of WT *Lat*$^{-/-}$ *Tcrb* nuclei. Less than 0.1% of ω/ω *Lat*$^{-/-}$ nuclei contained two 53BP1^{+} *Tcrb* alleles, as compared to the 0.4% of *Lat*$^{-/-}$ nuclei that contained two 53BP1^{+} *Tcrb* alleles (Fig. 15B). 3.8% of M4/M4 *Lat*$^{-/-}$ nuclei contained only one 53BP1^{+} *Tcrb* allele and 0.1% contained two 53BP1^{+} *Tcrb* alleles. This contradicts the previous assumption of synchronous D_{β}-to-J_{β} recombination, and suggests D_{β}-to-J_{β} recombination occurs monoallelically. 3.2% of DN thymocyte nuclei from DJβ/DJβ *Lat*$^{-/-}$ mice contained one 53BP1^{+} *Tcrb* allele, and 0% containing two 53BP1^{+} *Tcrb* alleles. As expected, this demonstrates that V_{β}-to-DJ_{β} recombination also occurs monoallelically. Taken together, we conclude that both steps of *Tcrb* recombination occur asynchronously in DN thymocyte nuclei.

Using the frequencies of *Tcrb* alleles that are 53BP1^{+} in the various genotypes, we calculated the theoretical distribution of nuclei containing 0, 1, and 2 53BP1^{+} *Tcrb* alleles

and compared those values to the observed distribution (Table 1). We found no statistically significant differences between the theoretical and observed distributions in any DN thymocyte cell type. This suggests that DSBs are limited primarily by infrequent recombination, and that there may be no additional mechanisms in place to prevent recombination on the second *Tcrb* allele when the first has recently recombined.

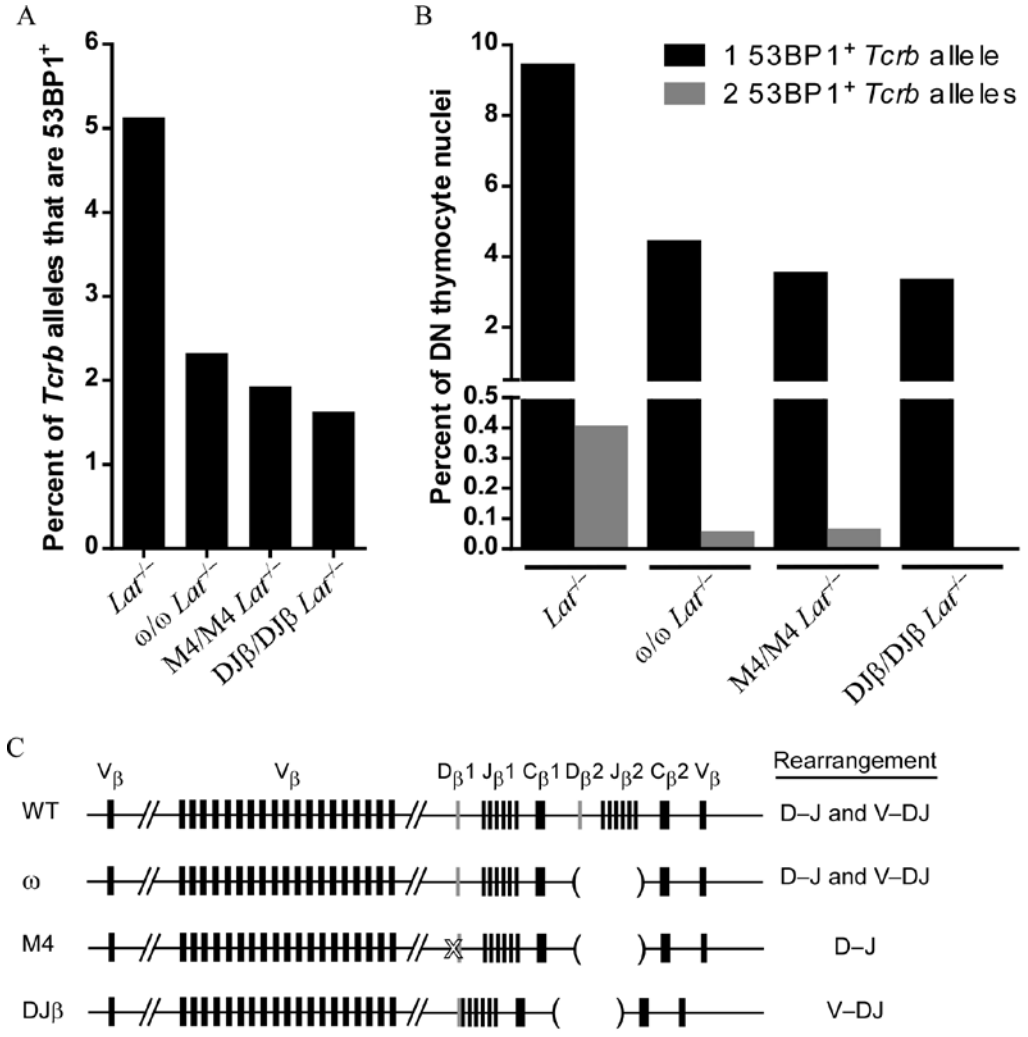

Figure 15: Both steps of *Tcrb* recombination occur monoallelically

A) Frequency of *Tcrb* alleles in 500 WT *Lat*$^{-/-}$, 1100 ω/ω *Lat*$^{-/-}$, 1525 M4/M4 *Lat*$^{-/-}$, and 394 DJβ/DJβ *Lat*$^{-/-}$ DN thymocyte nuclei that are 53BP1^{+}. B) Distribution of nuclei containing one or two 53BP1^{+} *Tcrb* alleles in the same nuclei as in panel A. Data were each compiled from 2-4 independent experiments per genotype. C) Diagram of modified *Tcrb* alleles. WT and ω alleles can undergo Dβ-to-Jβ and Vβ-to-DJβ recombination whereas M4 alleles can undergo Dβ-to-Jβ and DJβ alleles can undergo Vβ-to-DJβ recombination only.

Table 1: Observed and theoretical distributions of *Lat*$^{-/-}$ DN thymocyte nuclei containing 0, 1, and 2 53BP1^{+} *Tcrb* alleles

Cell type	Nuclei	% of 53BP1^{+} *Tcrb* alleles, p	Observed distribution (%)			Theoretical distribution (%)		
			Neither allele	One allele	Both alleles	Neither allele	One allele	Both alleles
						$(1-p)^2$	$2p(1-p)$	p^2
Lat$^{-/-}$	500	5.1	90.2	9.4	0.4	90.06	9.68	0.26
ω/ω *Lat*$^{-/-}$	1100	2.3	95.55	4.4	0.05	95.45	4.49	0.05
M4/M4 *Lat*$^{-/-}$	1525	1.9	96.44	3.5	0.06	96.24	3.73	0.04
DJβ/DJβ *Lat*$^{-/-}$	394	1.6	96.7	3.3	0.0	96.83	3.15	0.04

Statistics were performed by using Fisher's Exact Test to compare the observed frequency of events to the theoretical frequency of events. Percent of *Tcrb* alleles that are 53BP1^{+} was compiled from 2-4 independent experiments per genotype. The number of nuclei analyzed in the observed distribution was also used as the number of nuclei analyzed in the theoretical distribution for the statistical comparison. Any observed value statistically different than the theoretical has been bolded.

4.2.6 Nuclei containing two 53BP1^{+} *Tcrb* alleles accumulate in DN thymocyte nuclei unable to form coding joints

To evaluate whether 53BP1^{+} *Tcrb* alleles accumulate when RAG-mediated DSB repair is prevented, we analyzed the frequency of *Tcrb* alleles that were 53BP1^{+} and the frequency of nuclei containing one or two 53BP1^{+} *Tcrb* alleles in thymocytes from mice on an *Art*$^{-/-}$ background. We found that 27.5% of WT alleles on an *Art*$^{-/-}$ background were 53BP1^{+} (Fig. 16A), a much higher frequency than seen in repair-sufficient *Lat*$^{-/-}$ thymocyte nuclei (Fig. 15A). We saw that 54.3% of *Art*$^{-/-}$ DN thymocytes contained zero 53BP1^{+} *Tcrb* alleles, 36.4% contained a single 53BP1^{+} *Tcrb* allele, and 9.25% contained two

53BP1^{+} *Tcrb* alleles (Fig. 16B). No significant differences between the observed and theoretical frequencies of nuclei containing 0, 1, and 2 53BP1^{+} *Tcrb* alleles in *Art*$^{-/-}$ thymocyte nuclei (Table 2) supports the notion that the presence of a rearranging *Tcrb* allele does not signal to prevent additional *Tcrb* recombination.

As the two steps of recombination may be regulated differently, we wanted to specifically evaluate the impact of impaired coding joint formation on V$_{\beta}$-to-DJ$_{\beta}$ recombination. To accomplish this analysis, we crossed DJβ/DJβ mice onto an *Art*$^{-/-}$ background. We then examined DN thymocyte nuclei from these mice, which can only initiate, but not repair, V$_{\beta}$-to-DJ$_{\beta}$ recombination. We asked if the presence of a V$_{\beta}$-to-DJ$_{\beta}$ DSB at one *Tcrb* allele regulated the formation of a V$_{\beta}$-to-DJ$_{\beta}$ DSB on the second *Tcrb* allele. We began by determining the frequency of *Tcrb* alleles that were 53BP1^{+} and the frequency of nuclei containing 0, 1, and 2 53BP1^{+} *Tcrb* alleles. Only 8.3% of *Tcrb* alleles were 53BP1^{+} (Fig. 16A), and just 0.8% of nuclei contained two 53BP1^{+} *Tcrb* alleles (Fig. 16B). The observed frequencies of nuclei containing 0, 1, and 2 53BP1^{+} *Tcrb* alleles in DJβ/DJβ *Art*$^{-/-}$ thymocytes was not significantly different from the theoretical frequencies (Table 2). However, the observed frequency of nuclei containing 2 53BP1^{+} *Tcrb* alleles was also not significantly different than 0. Therefore these results are difficult to interpret, and more analyses are required in order to conclude whether the

presence of a V_β-to-DJ_β DSB signals the cell to cease V_β-to-DJ_β recombination until the DSB can be repaired.

The protein kinase ATM has been implicated in the regulation of monoallelic *Igk* locus recombination (Steinel *et al.* 2013) and monoallelic V_H-to-DJ_H recombination at *Igh* loci (Hewitt *et al.* 2009). Specifically, ATM was shown to downregulate *Rag1* and *Rag2* transcription in response to a RAG-mediated DSB at *Igk* loci (Steinel *et al.* 2013). Regarding *Igh* regulation, conclusions were based on a slight increase of nuclei containing biallelic *Igh* DSBs in the absence of ATM. However ATM is required for efficient DSB repair following V(D)J recombination (Lukas *et al.* 2011), and the above publication analyzing *Igh* recombination did not control for an increase in the time required for DSB repair in ATM-deficient nuclei. This means that the reported increase in nuclei containing two V_H-to-DJ_H recombination events could have resulted from slower repair and not more frequent biallelic RAG cleavage at *Igh* loci. To investigate this possibility at *Tcrb* loci and to control for differences in repair, we analyzed the frequency of $Atm^{+/-}$ or $Atm^{-/-}$ thymocyte nuclei on an $Art^{-/-}$ background containing two $53BP1^+$ *Tcrb* alleles. Any increase in the accumulation of biallelic *Tcrb* RAG-dependent DSBs in $Atm^{-/-}$ $Art^{-/-}$ over $Atm^{+/+}$ $Art^{-/-}$ or $Atm^{+/-}$ $Art^{-/-}$ thymocyte nuclei should be clearly visible, as $Art^{-/-}$ thymocyte nuclei are unable to repair any RAG-dependent DSBs. Thymocyte nuclei from $Atm^{+/-}$ $Art^{-/-}$ mice contained exactly the same frequency of

53BP1^{+} *Tcrb* alleles as *Atm*$^{+/+}$ *Art*$^{-/-}$ mice (Fig. 16A), and the frequencies of *Atm*$^{+/-}$ *Art*$^{-/-}$ nuclei containing 0, 1, and 2 53BP1^{+} *Tcrb* alleles were not significantly different than those of *Atm*$^{+/+}$ *Art*$^{-/-}$ mice (Fig. 16B). These results are unsurprising, as *Atm* haploinsufficiency does not affect the frequency of DSB foci formation after low-dose irradiation (Kato *et al.* 2006).

Nuclei from *Atm*$^{-/-}$ *Art*$^{-/-}$ mice displayed significantly fewer 53BP1^{+} *Tcrb* alleles than *Art*$^{-/-}$ mice (Fig. 16A), and significantly fewer nuclei containing 2 53BP1^{+} *Tcrb* alleles (Fig. 16B). The difference between the frequencies of nuclei containing 0 and 1 53BP1^{+} *Tcrb* allele fell just short of significance. As we were expecting to see either the same or a higher frequency of 53BP1^{+} *Tcrb* alleles and the same or a higher frequency of nuclei containing 2 53BP1^{+} *Tcrb* alleles, these results are uninterpretable. We suspect that the reduced frequency of 53BP1 foci resulted from less DNA DDR signaling in nuclei lacking ATM. Regardless, the frequencies of nuclei predicted to contain 0, 1, and 2 53BP1^{+} *Tcrb* alleles were very similar to the observed frequencies. Thus there appears to be a stochastic distribution of nuclei with 0, 1, and 2 53BP1^{+} *Tcrb* alleles in the presence or absence of ATM signaling.

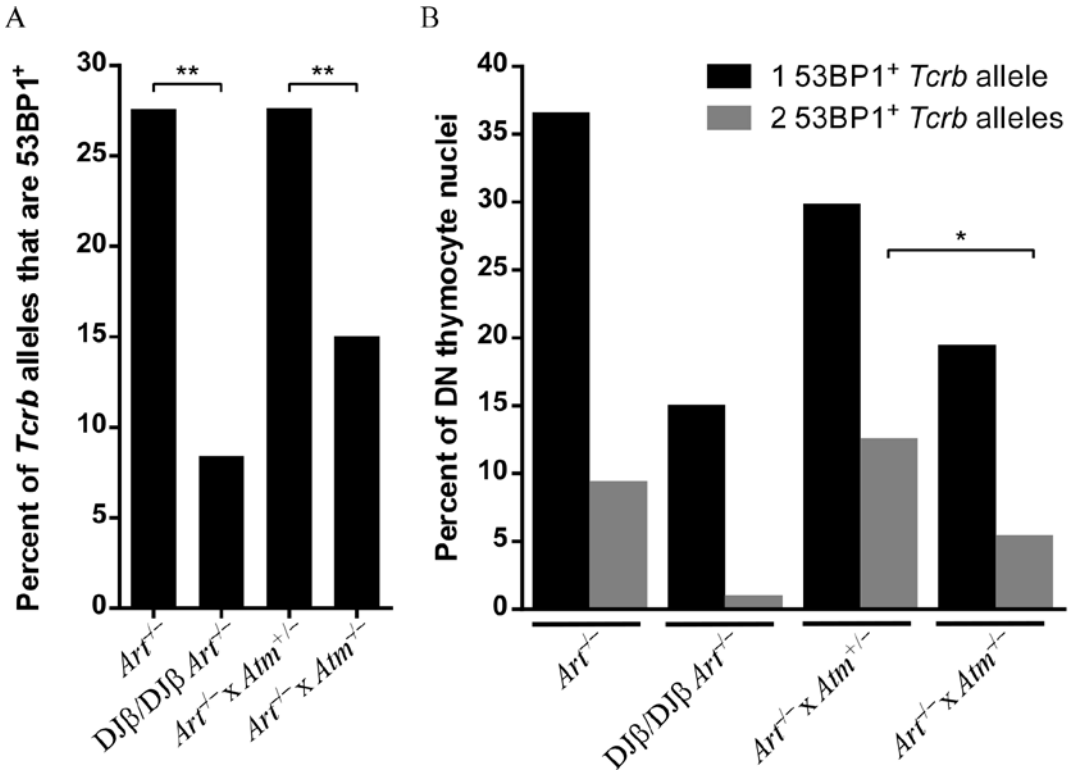

Figure 16: DN thymocyte nuclei containing two impaired 53BP1$^+$ *Tcrb* alleles accumulate in cells unable to form coding joints

A) Frequency of *Tcrb* alleles in 173 *Art*$^{-/-}$, 242 DJβ/DJβ *Art*$^{-/-}$, 209 *Art*$^{-/-}$ x *Atm*$^{+/-}$, and 228 *Art*$^{-/-}$ x *Atm*$^{-/-}$ DN thymocyte nuclei that are 53BP1$^+$. B) Distribution of nuclei containing one or two 53BP1$^+$ *Tcrb* alleles in the same nuclei as in panel A. Data were each compiled from 2-3 independent experiments. **P*<0.05; ***P*<0.01.

Table 2: Observed and theoretical distributions of *Art*$^{-/-}$ DN thymocyte nuclei containing 0, 1, and 2 53BP1^{+} *Tcrb* alleles

Cell type	Nuclei	Frequency of 53BP1^{+} *Tcrb* alleles, p (%)	Experimental distribution (%)			Theoretical distribution (%)		
			Neither allele	One allele	Both alleles	Neither allele $(1-p)^2$	One allele $2p(1-p)$	Both alleles p^2
Art$^{-/-}$	173	27.5	54.34	36.42	9.25	52.56	39.88	7.56
DJβ/DJβ *Art*$^{-/-}$	242	8.3	84.30	14.88	0.83	84.13	15.19	0.69
Art$^{-/-}$ *x* *Atm*$^{+/-}$	209	27.5	56.94	29.67	12.44	52.56	39.88	7.56
Art$^{-/-}$ *x* *Atm*$^{-/-}$	228	14.9	75.44	19.30	5.26	72.42	25.36	2.22

Statistics were performed by using Fisher's Exact Test to compare the observed frequency of events to the theoretical frequency of events. The number of nuclei analyzed in the observed distribution was also used as the number of nuclei analyzed in the theoretical distribution for the statistical comparison. Any observed value statistically different than the theoretical has been bolded.

4.2.7 Nuclei containing two 53BP1^{+} *Tcrd* and nuclei containing multilocus 53BP1^{+} *Tcr* loci accumulate in DN thymocyte when coding joint formation is blocked

We next sought to investigate whether biallelic RAG-dependent DSBs accumulate at other *Tcr* loci. We analyzed the frequency of *Tcrd* alleles that were 53BP1^{+} (Fig. 17A) and the frequencies of nuclei containing 0, 1, and 2 53BP1^{+} *Tcrd* alleles in *Lat*$^{-/-}$ and *Art*$^{-/-}$ DN thymocyte nuclei. Data from *Tcrb* analyses performed alongside *Tcrd* experiments are provided for comparison, though it should be noted that these results differ slightly from those shown in Fig 12. To identify *Tcrd* alleles, the 5′ V_{α} probe was used, which localizes to a region distanced roughly 1.5 Mb from the DJC_{δ} cluster. As the

probe targeted a region relatively far from the site of recombination, and the 5′ region and the 3′ region of unrearranged *Tcra*/*Tcrd* loci can extend up to 1.5 μm apart (Shih and Krangel 2010), we considered *Tcrd* alleles to be 53BP1$^+$ if the center of the 3D distance between an allele focus measured within 1.5 μm of the center of a 53BP1 focus. Like *Tcrb* alleles, we saw an increase in the frequency of *Tcrd* alleles that are 53BP1$^+$ (Fig. 17A), and an increase in the frequencies of nuclei containing 0, 1, and 2 53BP1$^+$ *Tcrd* alleles (Fig. 17B) in *Art*$^{-/-}$ thymocyte nuclei. We also see that the observed frequencies of nuclei containing 0, 1, and 2 53BP1$^+$ *Tcrd* alleles were quite similar to the predicted frequencies (Table 3). Moreover, the observed distributions of *Lat*$^{-/-}$ and *Art*$^{-/-}$ DN thymocyte nuclei containing at least one 53BP1$^+$ *Tcrd* allele and one 53BP1$^+$ *Tcrb* allele was not greater than the theoretical distribution (Table 4). These data indicate that the formation of RAG-dependent DSBs at other *Tcr* loci is also not restricted when a *Tcr* DSB is present.

In a similar vein, we were interested in the presence of concurrent DSBs at multiple *Tcr* loci in individual DN thymocytes unable to form coding joints. We evaluated the frequency of *Lat*$^{-/-}$ and *Art*$^{-/-}$ DN thymocyte nuclei containing at least one 53BP1$^+$ *Tcrb* allele and at least one 53BP1$^+$ *Tcrd* allele. We observed only 0.7% of *Lat*$^{-/-}$ thymocyte nuclei containing both *Tcrb* and *Tcrd* DSBs. That frequency increased to 7.9% in *Art*$^{-/-}$ thymocyte nuclei. Our results agree with a recent article that showed no

underrepresentation of WT DN2/3 nuclei containing 53BP1 foci at multiple *Tcr* loci simultaneously (Bowen *et al.* 2013).

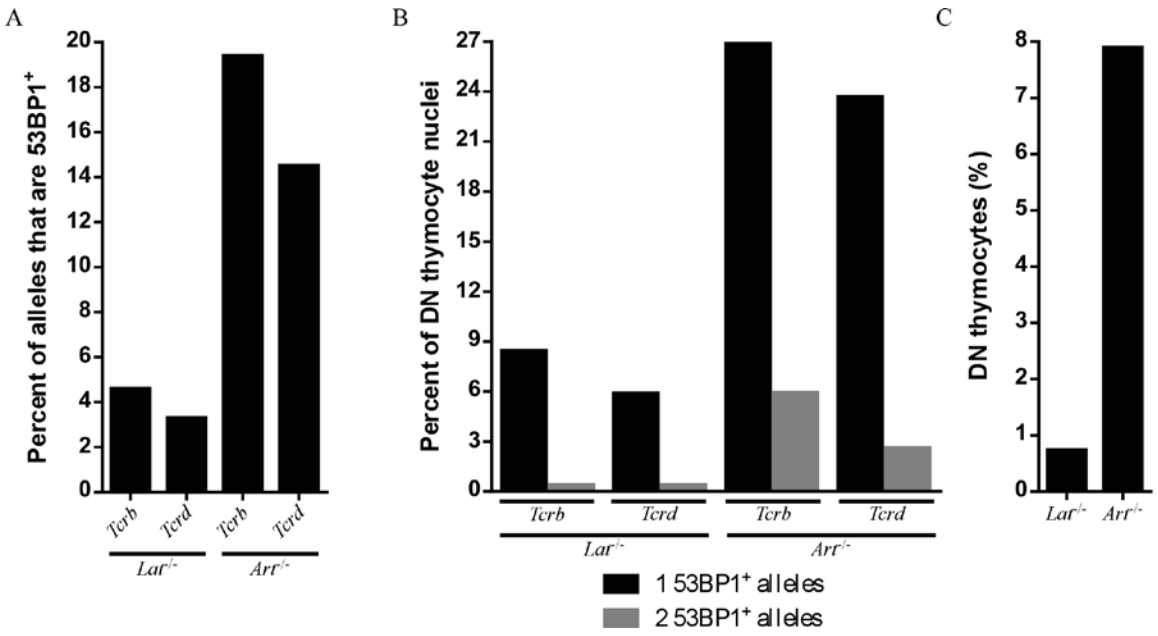

Figure 17: Nuclei containing two 53BP1$^+$ *Tcrd* alleles and nuclei containing at least one 53BP1$^+$ *Tcrd* allele and one 53BP1$^+$ *Tcrb* allele accumulate in DN thymocyte nuclei unable to form coding joints

A) Frequency of *Tcrb* and *Tcrd* alleles in 273 *Lat*$^{-/-}$ and 153 *Art*$^{-/-}$ DN thymocyte nuclei that are 53BP1$^+$. *Tcrd* alleles were considered to be 53BP1$^+$ if the 3D distance between the centers of the two foci was less than 1.5 μm. B) Distribution of nuclei containing 1 or 2 53BP1$^+$ *Tcrb* or *Tcrd* alleles from the same nuclei analyzed in panel A. C) Frequency of *Lat*$^{-/-}$ and *Art*$^{-/-}$ DN thymocyte nuclei that contain at least one 53BP1$^+$ *Tcrb* allele and at least one 53BP1$^+$ *Tcrd* allele. Data are from one experiment each.

Table 3: Observed and theoretical distributions of *Lat*$^{-/-}$ and *Art*$^{-/-}$ DN thymocyte nuclei containing 0, 1, and 2 53BP1^{+} *Tcrd* and *Tcrb* alleles

Cell type	n	Allele	Frequency of 53BP1^{+} alleles, p (%)	Experimental distribution (%)			Theoretical distribution (%)		
				Neither allele	One allele	Both alleles	Neither allele	One allele	Both alleles
							$(1-p)^2$	$2p(1-p)$	p^2
Lat$^{-/-}$	273	*Tcrb*	4.58	91.21	8.43	0.37	91.05	8.74	0.21
		Tcrd	3.30	93.77	5.86	0.37	93.51	6.38	0.11
Art$^{-/-}$	152	*Tcrb*	19.41	67.11	26.97	5.92	64.95	28.78	3.67
		Tcrd	14.43	73.69	23.68	2.63	73.22	24.70	2.08

Statistics were performed by using Fisher's Exact Test to compare the observed frequency of events to the theoretical frequency of events. The number of nuclei analyzed in the observed distribution was also used as the number of nuclei analyzed in the theoretical distribution for the statistical comparison. Any observed value statistically different than the theoretical has been bolded.

Table 4: Observed and theoretical distributions of *Lat*$^{-/-}$ and *Art*$^{-/-}$ DN thymocyte nuclei containing at least one 53BP1^{+} *Tcrd* allele and one 53BP1^{+} *Tcrb* allele

Cell type	Nuclei	Allele	Frequency of 53BP1^{+} alleles, p (%)	Experimental distribution (%)
				$p_{Tcrb} \times p_{Tcrd}$
Lat$^{-/-}$	273	*Tcrb* + *Tcrd*	0.73	0.15
Art$^{-/-}$	152	*Tcrb* + *Tcrd*	7.89	2.80

Statistics were performed by using Fisher's Exact Test to compare the observed frequency of events to the theoretical frequency of events. The number of nuclei analyzed in the observed distribution was also used as the number of nuclei analyzed in the theoretical distribution for the statistical comparison. Any observed value statistically different than the theoretical has been bolded.

4.2.8 *Tcra* alleles recombine biallelically in DP thymocytes

Though *Tcrb* alleles are allelically excluded, it is common for both *Tcra* alleles to be functionally rearranged and expressed in mature T cells (Borgulya *et al.* 1992). In addition, individual *Tcra* alleles typically undergo several rounds of recombination (Krangel *et al.* 2004, Krangel 2009). In order to determine the frequency of *Tcra* alleles that are 53BP1$^+$ and the frequencies of DP thymocyte nuclei containing 0, 1, or 2 53BP1$^+$ *Tcra* alleles, we sorted DP thymocytes from WT mice and visualized *Tcra*/*Tcrd* alleles and 53BP1 foci. 13.4% of *Tcra*/*Tcrd* alleles in WT DP thymocytes were 53BP1$^+$ (Fig. 18A), a significantly higher frequency than *Tcrb* alleles in DN thymocytes. 77.3% of WT DP thymocytes contained zero 53BP1$^+$ *Tcra*/*Tcrd* alleles, 18.5% contained a single 53BP1$^+$ *Tcra*/*Tcrd* allele, and 4.2% contained two 53BP1$^+$ *Tcra*/*Tcrd* alleles (Fig. 18B). The frequencies of WT DP thymocyte nuclei containing two 53BP1$^+$ *Tcra*/*Tcrd* alleles did not significantly differ from the expected frequencies (Table 5). Though preliminary, these results suggest that *Tcra* recombination in DP thymocyte nuclei occurs stochastically, and that *Tcra* alleles can recombine biallelically in DP thymocyte nuclei. Taken together, data presented in this chapter indicate that signaling downstream of an unrepaired *Tcrb* DSB is insufficient to ensure monoallelic RAG activity.

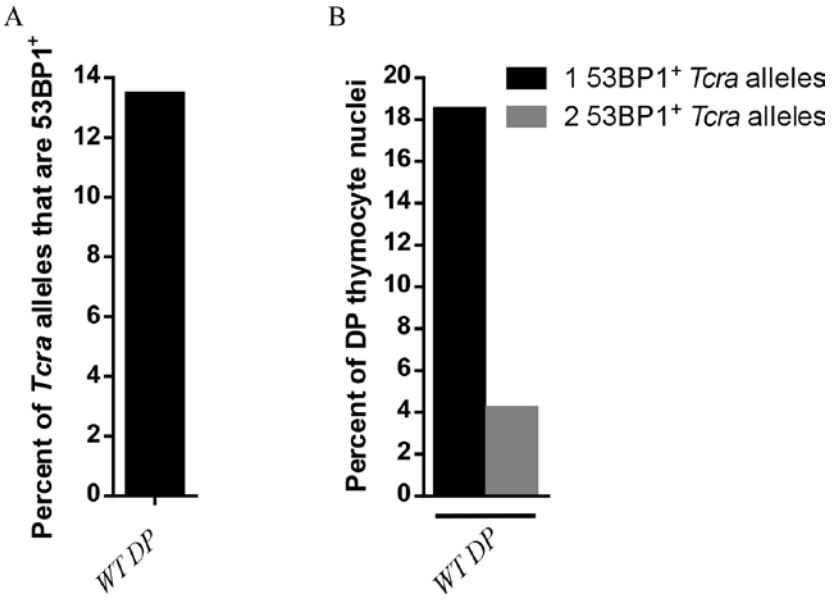

Figure 18: *Tcra* alleles recombine biallelically in DP thymocyte nuclei

A) Frequency of *Tcra* alleles in 119 sorted DP thymocytes from WT mice that are 53BP1$^+$. B) Distribution of nuclei containing 1 or 2 53BP1$^+$ *Tcra* alleles in the same nuclei as A. Data are from one experiment each.

Table 5: Observed and theoretical distributions of WT sorted DP thymocyte nuclei containing 0, 1, and 2 53BP1$^+$ *Tcra* alleles

Cell type	Nuclei	Frequency of 53BP1$^+$ *Tcra* alleles, p (%)	Observed distribution (%)			Theoretical distribution (%)		
			Neither allele	One allele	Both alleles	Neither allele	One allele	Both alleles
						$(1-p)^2$	$2p(1-p)$	p^2
WT DP	119	13.4	77.3	18.5	4.2	75.0	23.2	1.8

Statistics were performed by using Fisher's Exact Test to compare the observed frequency of events to the theoretical frequency of events. The number of nuclei analyzed in the observed distribution was also used as the number of nuclei analyzed in the theoretical distribution for the statistical comparison. Any observed value statistically different than the theoretical has been bolded.

4.3 Discussion

RAG-dependent DSBs may occur stochastically at a very low frequency, or they may be regulated so that once a recombination event occurs in a nucleus all additional rearrangements are halted. Here we show that *Tcr* loci in thymocyte nuclei recombine in a stochastic manner, with no reduction in the likelihood of a RAG-dependent DSB occurring in a nucleus that already contains a RAG-dependent DSB.

Though the observed distribution of nuclei containing 2 53BP1$^+$ alleles did not significantly differ from the theoretical distribution in any of our analyses, sometimes the observed distribution also did not significantly differ from 0. An example of this occurred when analyzing DJβ/DJβ *Lat*$^{-/-}$ thymocyte nuclei, which contain a pre-rearranged DJβ gene segments and can only undergo V_β-to-DJ_β recombination. Because we were unable to conclude that there were significantly more than 0 nuclei containing 2 53BP1$^+$ *Tcrb* alleles in our experimental sample, it is possible that V_β-to-DJ_β recombination is regulated so that once a V_β-to-DJ_β DSB is present, signals are sent to prevent additional V_β-to-DJ_β recombination. However we are unaware of any potential mechanisms that would be selectively activated following V_β-to-DJ_β recombination, but not following D_β-to-J_β recombination.

One mechanism that could inhibit the generation of additional RAG-dependent DSBs in nuclei in which a DSB is present would be ATM signaling. RAG-induced DSBs

activate the ATM kinase, which aids in efficient DSB repair (Bednarski and Sleckman 2012). ATM was recently shown to help enforce allelic exclusion at *Igk* loci by downregulating *Rag1* and *Rag2* transcription in response to a RAG-induced DSB (Steinel *et al.* 2013). Transient suppression of recombination by this mechanism could guarantee asynchronous recombination by preventing recombination on the second allele while the first allele is being repaired and tested for functionality. Should such a mechanism function in DN thymocytes, stringent regulation of *Tcrb* recombination would predict uniformly monoallelic *Tcrb* 53BP1 foci in Art-deficient thymocytes, since these thymocytes cannot repair RAG-induced coding ends and would continuously signal to suppress *Tcrb* recombination on the other allele. However, we found that nearly 10% of Art-deficient DN thymocyte nuclei contained two $53BP1^{+}$ *Tcrb* alleles. Moreover, if such a mechanism were active, it should also prevent concurrent rearrangement events at different TCR loci in DN thymocytes. However, nuclei with 53BP1 foci at two or three *Tcr* loci do not appear to be underrepresented in wild-type DN thymocytes (Bowen *et al.* 2013). We conclude that signaling downstream of an unrepaired *Tcrb* DSB is insufficient to ensure monoallelic RAG activity, perhaps because RAG protein expression cannot be downregulated rapidly enough to guarantee this outcome. It remains unclear whether this insufficiency applies selectively to D_{β}-to-J_{β} recombination, which likely predominates in Art-deficient DN thymocyte nuclei, or applies to V_{β}-to-DJ_{β}

recombination as well. However we believe a mechanism that uniquely suppresses V_β-to-DJ_β recombination is unlikely to exist.

A recent publication reported monoallelic recombination of *Tcra* alleles in DP thymocyte nuclei (Chaumeil *et al.* 2013). The authors of that publication concluded that *Tcra* alleles recombine one at a time, though they actually observed 14% of DP nuclei containing DSB repair foci at both *Tcra* alleles. As one DSB focus in each of these nuclei was weaker than the other and they saw relatively weak foci at *Tcra* alleles in *Rag*$1^{-/-}$ x *Tcrb* tg mice, they reasoned that the weak foci were RAG-independent. However, we consider the presence of DSB foci at *Tcra* alleles in *Rag*$1^{-/-}$ x *Tcrb* tg mice to be an indication of a very high background that would invalidate their conclusions.

5. Analysis of the role of subnuclear positioning in the regulation of V(D)J recombination

5.1 Introduction

Antigen receptor V, D, and J gene segments are assembled by V(D)J recombination in immature T and B lymphocytes to generate diverse repertoires of TCRs and BCRs, respectively (Schatz and Swanson 2011). V(D)J recombination is initiated by the RAG1/2 proteins, which bind to and induce DSBs at recombination signal sequences that flank V, D, and J segments. V(D)J recombination at antigen receptor loci is regulated according to cell lineage and developmental stage (Schatz and Ji 2011). In addition, at some loci V(D)J recombination is regulated to enforce allelic exclusion, such that a complete antigen receptor protein is produced by only one allele (Brady *et al.* 2010, Vettermann and Schlissel 2010). However, the mechanisms that establish allelic exclusion are poorly understood.

Allelic exclusion occurs in two phases. The first phase, initiation, is presumed to result from asynchronous recombination, so that only one allele per cell rearranges at a time (Brady *et al.* 2010). The initiation of allelic exclusion applies to V-to-DJ, but not to D-to-J, rearrangements at *Tcrb* and *Igh* loci, as mature T and B cells often contain functional D-to-J rearrangements on both alleles (Khor and Sleckman 2002, Vettermann and Schlissel 2010). The second step, maintenance, prevents additional recombination once a functional rearrangement has occurred. Together, the two steps of allelic

exclusion lead to most T cells and B cells containing only one completely and functionally rearranged *Tcrb* allele and *Igh* allele, respectively (Khor and Sleckman 2002, Mostoslavsky *et al.* 2004, Jackson and Krangel 2006, Jung *et al.* 2006).

Though RAG accessibility, transcriptional repression, and locus decontraction all likely play a role in the maintenance of allelically excluded loci (Tripathi *et al.* 2002, Skok *et al.* 2007, Abarrategui and Krangel 2009), it is thought that both *Tcrb* alleles in DN thymocyte nuclei are actively transcribing, and are contracted (Jia *et al.* 2007, Skok *et al.* 2007). Therefore the mechanism behind the initiation phase of recombination remains poorly understood.

Two models have been proposed to explain asynchronous recombination (Khor and Sleckman 2002, Mostoslavsky *et al.* 2004, Jackson and Krangel 2006). In the regulated model, one allele is predetermined to recombine first or more efficiently than the other allele. It is thought that allellic exclusion at *Igk* loci is governed by the regulated model, as the early replicating allele is predisposed to rearrange first (Mostoslavsky *et al.* 1998, Mostoslavsky *et al.* 2001). On the other hand if a stochastic model were to exist, both alleles would rearrange infrequently so that the likelihood of simultaneous rearrangement of alleles is low. Additionally a combination of both models is possible. It is not currently known if allelic exclusion at *Tcrb* loci results from a stochastic or regulated mechanism.

The subnuclear localization of *Igh* and *Tcrb* alleles has been implicated as a potential mechanism leading to the initiation of allelic exclusion (Skok *et al.* 2001, Roldan *et al.* 2005, Skok *et al.* 2007, Schlimgen *et al.* 2008). For example, association with PCH has been linked to the process of allelic exclusion. *Igh* loci were shown to associate with PCH monoallelically in roughly 70% of pre-B cells. Moreover, the recruited alleles were decontracted, suggesting that they had not undergone V_H–DJ_H rearrangement (Roldan *et al.* 2005). *Tcrb* alleles have been shown to associate with PCH in a regulated (Skok *et al.* 2007) or stochastic (Schlimgen *et al.* 2008) fashion in different studies. Direct analysis of rearrangement status revealed that PCH-associated *Tcrb* alleles tend not to have undergone V_β rearrangement (Schlimgen *et al.* 2008).

The positioning of TCR and BCR alleles at the nuclear periphery may also suppress V(D)J recombination. Most *Igh* and *Igk* alleles are located at the nuclear periphery in non-B-lineage cells, whereas in pro-B cells during rearrangement they are more centrally located (Kosak *et al.* 2002). This relocalization is thought to occur as a prelude to expression and V(D)J recombination. *Tcrb* alleles localize stochastically to the nuclear periphery in DN thymocytes, with most nuclei having either one or two associated alleles (Schlimgen *et al.* 2008). *Tcrb* alleles are uniquely regulated, in that they are the only antigen receptor loci in which a large portion of alleles are positioned at the nuclear periphery during the developmental stage in which their rearrangement occurs

(Schlimgen *et al.* 2008). All other antigen receptor alleles relocate from the nuclear periphery to the nuclear interior prior to recombination (Kosak *et al.* 2002, Schlimgen *et al.* 2008).

Analysis of the recombination status of peripheral *Tcrb* alleles showed that they were less likely to have undergone V_β-to-DJ_β rearrangement than more central alleles (Schlimgen *et al.* 2008), suggesting that association with the nuclear periphery may suppress recombination and contribute to allelic exclusion. However, this analysis tracked already rearranged *Tcrb* alleles, allowing for the possibility that recombination occurs freely at the nuclear periphery, with rearranged alleles subsequently relocating away from this compartment. Direct analysis of the suppressive nature of the nuclear periphery on *Tcrb* alleles has yet to be performed.

Additionally, it is possible that positioning of alleles with respect to their CT may alter the efficiency of V(D)J recombination. Previous studies have demonstrated that certain transcriptionally active genes are more likely to be positioned at the surface or external to their respective CTs (Chambeyron and Bickmore 2004, Morey *et al.* 2009). As transcriptional activation is required for V(D)J recombination to proceed (Abarrategui and Krangel 2009), it is possible that V(D)J recombination preferentially occurs on *Tcr* alleles that are located outside their CT. Additionally, positioning of alleles within their CT could function to separate antigen receptor alleles from recombination factors, if

factors required for recombination were excluded from CTs. Therefore positioning of *Tcrb* alleles internal to their CT could serve as a mechanism of reducing the frequency of *Tcrb* recombination, and ultimately as a means of ensuring asynchronous *Tcrb* recombination.

Here we provide evidence that *Tcrb* alleles situated at the nuclear periphery are less frequently marked by DNA DSB repair foci. Moreover, the repair foci that were detected on *Tcrb* alleles positioned at the nuclear periphery tended to occur on alleles oriented to allow for partial dissociation from this compartment.

5.2 Results

5.2.1 *Tcrb* recombination is suppressed on alleles positioned at the nuclear periphery

Previous work showed that ~45% of DN thymocyte nuclei contain two lamin-associated *Tcrb* alleles and an equal number contain one lamin-associated and one free allele. Within the latter subset, fully rearranged *Tcrb* alleles were substantially underrepresented at the lamina (Schlimgen *et al.* 2008). To more directly address whether association with nuclear lamina may suppress ongoing *Tcrb* recombination, we assessed the locations of recently rearranged *Tcrb* alleles in $Lat^{-/-}$ nuclei containing a single $53BP1^{+}$ *Tcrb* allele and a single *Tcrb* allele in contact with the nuclear lamina. We scored contact when two adjacent pixels were positive for both laminB1 staining and

Tcrb hybridization. When association with the lamina was assessed using a probe hybridizing with the Vβ-end of the *Tcrb* locus (Fig. 19A), there was no significant underrepresentation of 53BP1^{+} foci on wild-type (WT) *Tcrb* alleles in *Lat*$^{-/-}$ thymocytes (Fig. 19B).

The Dβ-to-Jβ and Vβ-to-DJβ steps of *Tcrb* recombination could be differentially impacted by Vβ-end contact with the lamina. Therefore, a specific effect on one step of recombination could have been masked in the above experiment. To distinguish 53BP1 foci arising from the two steps of recombination, we again utilized gene-targeted mice carrying modified *Tcrb* alleles that can undergo Dβ-to-Jβ or Vβ-to-DJβ recombination events only (Fig. 19A).

Similar to the results obtained with *Lat*$^{-/-}$ thymocytes, we found no evidence that 53BP1 foci were underrepresented on *Tcrb* alleles anchored to the nuclear lamina by the Vβ-end in either ω/ω *Lat*$^{-/-}$ or M4/M4 *Lat*$^{-/-}$ thymocytes (Fig. 19B). However, DJβ/DJβ *Lat*$^{-/-}$ thymocytes behaved differently, as only 26% of 53BP1 foci occurred on *Tcrb* alleles in contact with the nuclear lamina, and 74% occurred on free alleles. This result implies that Vβ-end association with the nuclear lamina suppresses the Vβ-to-DJβ but not the Dβ-to-Jβ step of *Tcrb* recombination.

Given the selective impact of Vβ-end association on Vβ-to-DJβ recombination, we hypothesized that recombination could be differentially influenced depending on the

nature of *Tcrb* locus contact with the nuclear lamina. Therefore, we also scored *Tcrb*-lamin colocalization using a probe that detects the Cβ-end of the *Tcrb* locus (Fig. 19A and C). We observed substantially reduced frequencies of 53BP1^{+} foci on Cβ-end associated *Tcrb* alleles in *Lat*$^{-/-}$, M4/M4 *Lat*$^{-/-}$ and DJβ/DJβ *Lat*$^{-/-}$ thymocytes (Fig. 19C). We also observed a similar trend in ω/ω *Lat*$^{-/-}$ thymocytes, although the result fell short of statistical significance (Fig. 19C). These results imply that Cβ-end association with the nuclear lamina suppresses both the Dβ-to-Jβ and Vβ-to-DJβ steps of *Tcrb* recombination. We conclude that the Vβ- and Cβ-ends of the locus may associate independently with the nuclear lamina. Tethering by the Vβ-end selectively inhibits Vβ-to-DJβ recombination because the distant Dβ and Jβ segments may remain free of the nuclear lamina and available for recombination. In contrast, tethering by the Cβ-end inhibits both Dβ-to-Jβ and Vβ-to-DJβ recombination because only the distant Vβ segments may remain free of the lamina on these alleles.

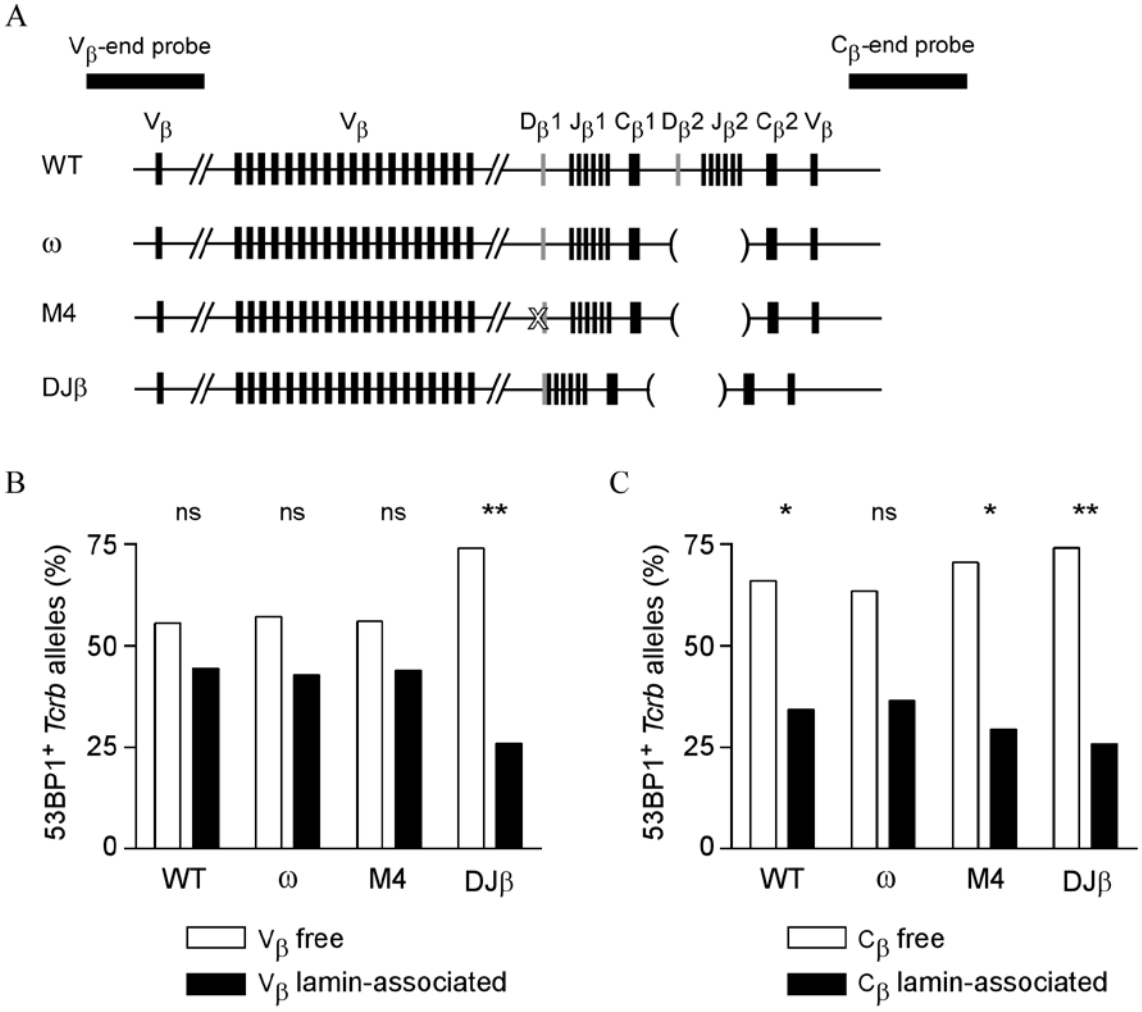

Figure 19: *Tcrb* recombination is suppressed at the nuclear periphery

A) Frequencies of lamin-associated and free 53BP1$^+$ *Tcrb* alleles in *Lat*$^{-/-}$ DN thymocyte nuclei having a single 53BP1$^+$ *Tcrb* allele and monoallelic *Tcrb* association with the nuclear lamina. *Tcrb* association with the lamina was scored using a Vβ-end probe on 63 WT, 56 ω, 61 M4, and 54 DJβ nuclei (5-8 slides per genotype). B) *Tcrb* association with the lamina was scored using a Cβ-end probe on 70 WT, 52 ω, 51 M4 and 58 DJβ nuclei (4-8 slides per genotype). Fisher's exact two-tailed contingency tables were used to compare frequencies of lamin-associated 53BP1$^+$ *Tcrb* alleles to the frequency of total lamin-associated *Tcrb* alleles (50%). *, P<0.05; **, P<0.01; ns, not significant.

5.2.2 *Tcrb* alleles positioned at the nuclear periphery adopt distinct conformations that likely regulate recombination

Independent interactions of the Vβ- and Cβ-ends suggest that lamin-associated *Tcrb* alleles may adopt distinct conformations relative to the nuclear lamina that may be suppressive or permissive for recombination. To assess this more directly, we evaluated the orientation of lamin-associated 53BP1^{+} and total *Tcrb* alleles by deconvolving 3D images and measuring the distances between the nearest point on the inner surface of the nuclear lamina and the centers of *Tcrb* and 53BP1 foci.

We first analyzed the conformations of peripheral *Tcrb* alleles by comparing the locations of the Vβ- and Cβ-ends of individual *Tcrb* alleles relative to the nuclear lamina in *Lat*$^{-/-}$ thymocytes (Fig. 20A, left). We then calculated the extent to which one end of the *Tcrb* locus was more embedded in the lamina or more nucleoplasmic than the other end (Fig. 20B). Alleles anchored to the lamina via the Vβ-end displayed a spectrum of conformations. On most alleles the Cβ-end was displaced less than 100nm relative to the Vβ-end (Fig. 20C, left). However, on some alleles the Cβ-end was substantially more nucleoplasmic than the Vβ-end. Similar conclusions were reached for Vβ-end displacement when the Cβ-end was positioned at the lamina (Fig. 20D, left). These data suggest that the entire lengths of most peripheral *Tcrb* loci interact with the lamina, whereas on some alleles one end may be free of the lamina. These observations held

true for the modified *Tcrb* alleles as well, showing that none of the modifications substantially influence *Tcrb* locus conformation relative to the lamina.

We then analyzed the displacement of 53BP1 foci relative to the lamin-associated V_β-end of the *Tcrb* locus (Fig. 20A, middle; Fig. 20C, right). 53BP1 foci were almost always farther from the lamina than the lamin-associated V_β-end, averaging 150-230 nm more nucleoplasmic in the different genotypes. This suggests that although V(D)J recombination is suppressed by the nuclear lamina, V_β-to-DJ_β and D_β-to-J_β recombination may occur on *Tcrb* alleles that have partially dissociated on the C_β-end.

Similarly, 53BP1 foci were farther from the lamina than the lamin-associated C_β-end of the *Tcrb* locus, averaging 87-126 nm more nucleoplasmic in the different genotypes (Fig. 20A, right; Fig. 20D, right). That 53BP1 foci tended to be less well separated from the C_β-end than from the V_β-end makes sense, since the C_β-end probe is centered 140kb downstream of the Dβ and Jβ segments, whereas the V_β-end is centered approximately 325kb upstream of the center of the V_β array (Fig. 10A). We conclude that the full lengths of most *Tcrb* alleles are in contact with the nuclear lamina, but that V(D)J recombination preferentially occurs on the subset of peripheral alleles that have partially dissociated from the lamina.

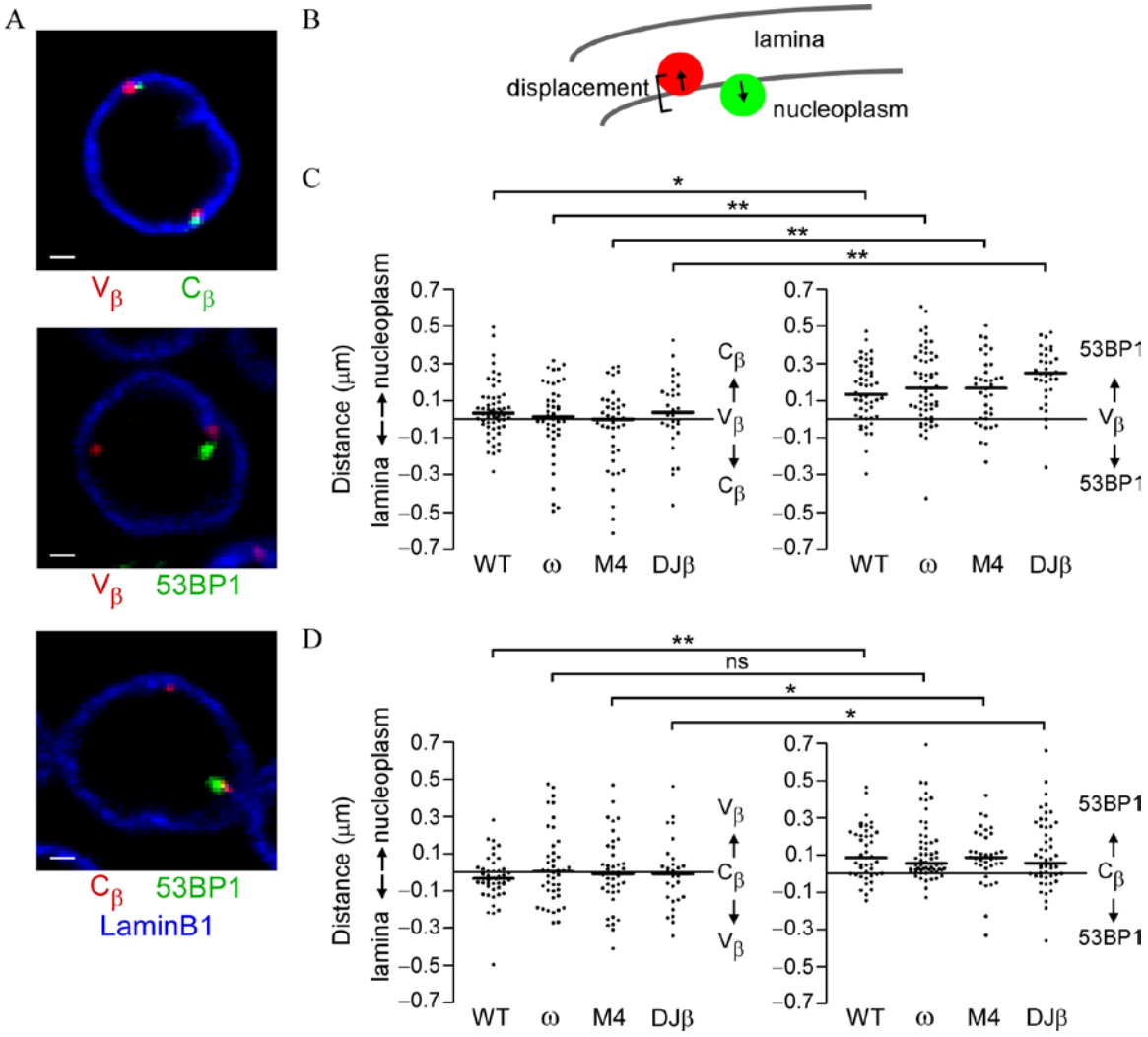

Figure 20: Orientation of peripheral *Tcrb* alleles

A) Confocal immunoFISH microscopy showing single z-slices of *Lat*$^{-/-}$ DN thymocyte nuclei containing lamin-associated *Tcrb* alleles. *Tcrb* alleles were characterized using the Vβ-end probe, the Cβ-end probe, and anti-53BP1. Scale bars = 1 μm. (B) Schematic of methodology to determine the displacement of one focus (Vβ, Cβ, or 53BP1) from the defined lamin-associated focus (Vβ or Cβ). (C) Left, Vβ-end and Cβ-end DNA probes were used to determine the relative location of the Cβ-end when the Vβ-end is positioned at the lamina. Positive values indicate that the Cβ-end is farther from the lamina than the Vβ-end; negative values indicate that the Cβ-end is more deeply embedded in the lamina than the Vβ-end. Right, a Vβ-end probe and anti-53BP1were

used to determine the relative location of 53BP1 foci when the Vβ-end is positioned at the lamina. Positive values indicate that 53BP1 is farther from the lamina than the Vβ-end; negative values indicate that 53BP1 is more deeply embedded in the lamina than the Vβ-end. (D) Left, Vβ-end and Cβ-end DNA probes were used to determine the relative location of the Vβ-end when Cβ-end is positioned at the lamina. Positive values indicate that the Vβ-end is farther from the lamina than the Cβ-end; negative values indicate that the Vβ-end is more deeply embedded in the lamina than the Cβ-end. Right, a Cβ-end probe and anti-53BP1 were used to determine the relative location of 53BP1 foci when the Cβ-end is positioned at the lamina. Positive values indicate that 53BP1 is farther from the lamina than the Cβ-end; negative values indicate that 53BP1 is more deeply embedded in the lamina than the Cβ-end. All alleles were analyzed on a $Lat^{-/-}$ background. Each Vβ-Cβ analysis was conducted on one slide per genotype; Vβ-53BP1 and Cβ-53BP1 analyses were conducted on 2-5 slides per genotype. Heavy black lines denote median displacement. *, P<0.05; **, P<0.01; ns, not significant, by unpaired, two-tailed t-tests.

5.2.3 *Tcrb* and *Tcra* recombination are not suppressed on alleles positioned within their chromosome territory

To investigate whether the positioning of *Tcrb* alleles relative to their chromosome territories affects the frequency at which the alleles undergo V(D)J recombination, we used 3D immunoFISH to visualize *Tcrb* alleles, murine chromosome 6, and 53BP1 simultaneously in $Lat^{-/-}$ DN thymocyte nuclei (Fig. 21A). We also visualized *Tcra* alleles, murine chromosome 14, and 53BP1 in WT thymocyte nuclei, to ask the same questions about *Tcra* alleles (Fig. 21B). We assessed the positioning of total *Tcr* alleles and $53BP1^{+}$ *Tcr* alleles as internal, at the surface, or external to their respective CTs. We found no significant differences between the frequency of total *Tcrb* alleles and the frequency of $53BP1^{+}$ *Tcrb* alleles at any of the three positions (Fig. 21C). Similarly,

we saw no significant differences between the frequency of total *Tcra* alleles and the frequency of 53BP1^{+} *Tcra* alleles at any of the positions. Though both *Tcrb* and *Tcra* alleles were most commonly located at the surface of their respective CT (Figs. 21C and D), there seems to be no reduction of recombination at any of the three locations. These results suggest that the location of *Tcrb* and *Tcra* alleles relative to their CTs does not influence the frequency of V(D)J recombination.

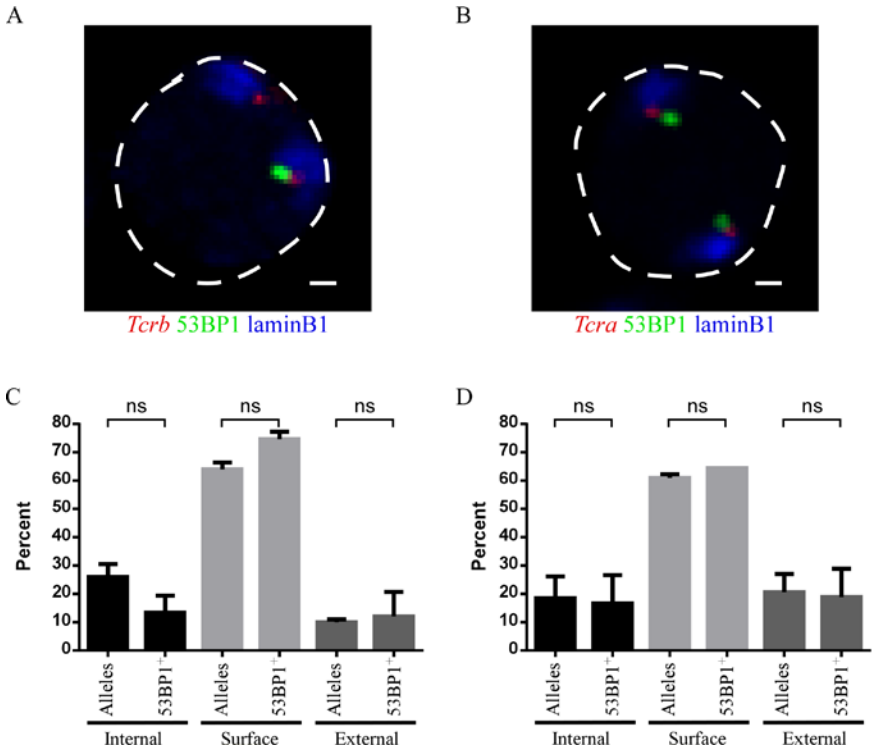

Figure 21: Recombination is not suppressed on alleles positioned within their chromosome territory

A) Confocal immunoFISH microscopy showing a 53BP1$^+$ *Tcrb* allele and CT6 from a single z-slice of a *Lat*$^{-/-}$ thymocyte nucleus. The edge of the nucleus is demarcated by a dashed white line. Scale bars = 1 μm. B) Confocal immunoFISH microscopy showing 2 53BP1$^+$ *Tcra* alleles and CT14 from a single z-slice of a WT thymocyte nucleus. The edge of the nucleus is demarcated by a dashed white line. Scale bars = 1 μm. C) Distribution of the location of *Tcrb* alleles and 53BP1$^+$ *Tcrb* alleles relative to their respective CT in *Lat*$^{-/-}$ DN thymocyte nuclei. Allele foci were considered to be internal to the CT if all but one pixel colocalized with the CT signal. Foci were considered to be at the CT surface if at least two pixels colocalized with CT signal and at least two pixels did not. Foci were considered to be external to the CT if no more than one pixel colocalized with CT signal. *Tcrb* location was scored using a V_β-end probe on 1300 *Tcrb* alleles and 56 53BP1$^+$ *Tcrb* alleles over 2 slides. D) Distribution of the location of *Tcra* alleles and 53BP1$^+$ *Tcra* alleles relative to their respective CT in WT thymocyte nuclei. Colocalization was performed as described in A. *Tcra* location was scored using the V_α-probe that localizes to the 5' region of the *Tcra* locus on 692 *Tcra* alleles and 90 53BP1$^+$ *Tcra* alleles over 2 slides. ns, not significant, by unpaired, two-tailed t-tests.

5.3 Discussion

The mechanism leading to *Tcrb* allelic exclusion remains poorly understood. It has been proposed that *Tcrb* alleles may be positioned at repressive subnuclear compartments so as to reduce the frequency of recombination. Here we analyzed the effect of subnuclear positioning on the recombination frequency of *Tcr* alleles. Though we saw no suppression of recombination on *Tcr* alleles positioned within their CTs, we did show suppression of recombination on *Tcrb* alleles positioned at the nuclei periphery in DN thymocyte nuclei.

Our conformational analysis of the *Tcrb* locus further supported the notion that location at the nuclear periphery suppresses recombination, by demonstrating that rearrangement almost always occurs on alleles that are partially dissociated from the nuclear lamina. The orientation experiments showed that on most peripheral *Tcrb* alleles, the V_β- and C_β-ends of the locus were both associated with the nuclear lamina. However, on 53BP1$^+$ *Tcrb* alleles, the 53BP1 focus was generally farther from the nuclear lamina than the lamin-associated V_β- and C_β-end of the locus. Our interpretation was that one end of the locus had dissociated from the lamina and was therefore permissive for recombination. However an alternate interpretation of our results would be that 53BP1$^+$ *Tcrb* alleles are anchored to the lamina via both ends of the locus, with 53BP1 accumulating on central *Tcrb* locus DNA that loops away from the periphery. We could

not analyze this directly, because technical limitations prevented us from performing 4-color 3D immunoFISH analysis in which the nuclear lamina, 53BP1, the V_β-end, and the C_β-end of the *Tcrb* locus could be simultaneously and distinctly labeled. However, our observation that D_β-to-J_β recombination is inhibited on alleles anchored to the lamina via their C_β- but not their V_β-end argues, at a minimum, that these must represent two conformationally distinct subsets of alleles.

A recent publication showed that *Tcra* alleles located internal to their CT were transcriptionally silent and did not often colocalize with DSB repair proteins (Chaumeil *et al.* 2013), suggesting that positioning of alleles within their CT does suppress V(D)J recombination. This directly conflicts with our findings described above. It is possible that the two analyses differ because of the location of the probes used to identify the gene loci. We used a probe that targets a 5′ region of the *Tcra* locus which localizes to a region 1.6 Mb upstream of the J_α array, whereas the aforementioned publication used a 3′ *Tcra* probe. This possibility is supported by our previous data showing a suppression of *Tcrb* recombination at the periphery using the C_β-end probe, but not the V_β-end probe, in *Lat*$^{-/-}$ thymocyte nuclei. If suppression of recombination can only be observed when a 3′ probe is used, we should also re-evaluate the effect of positioning *Tcrb* alleles within their CT, as those analyses were also performed using the 5′ V_β-end probe.

However there was a problem with the publication suggesting that positioning of *Tcra* alleles within their CT suppresses recombination in DP thymocyte nuclei. The authors often found DSB repair foci unassociated with a *Tcra* allele. As only *Tcra* loci recombine in DP thymocye nuclei, the presence of non-*Tcra* DSBs or more than two total DSBs in single nucleus may suggest that the cell is undergoing apoptosis. Therefore it is unconvincing that the DSB foci analyzed in this publication truly reflect V(D)J recombination.

6. Analysis of the role of RAG2 subnuclear distribution in the regulation of recombination at the nuclear periphery

6.1 Introduction

We have so far shown that V(D)J recombination of antigen receptor alleles, including *Tcrb* alleles, is initiated stochastically. Additionally, positioning of alleles at the transcriptionally-repressive nuclear periphery can reduce the frequency at which recombination occurs. We are therefore interested in understanding the mechanism by which positioning of *Tcrb* alleles at the periphery serves to reduce the frequency of recombination.

As V(D)J recombination requires transcription, which leads to RAG accessibility, recombination at the periphery is most likely to be suppressed by either: 1) transcriptional silencing, or 2) segregation from RAG proteins. The first option, inhibiting transcription and accessibility of *Tcrb* alleles, could function to suppress V(D)J recombination by contact of the *Tcrb* locus with the nuclear lamina. However, prior work has indicated that V_β segments are transcribed biallelically in all DN thymocytes (Jia *et al.* 2007), making this possibility unlikely.

The second option, that peripheral *Tcrb* loci might be inhibited from undergoing V(D)J recombination due to their segregation from RAG1/2 proteins, is more probable. A recent publication demonstrated that the histone H3 lysine 4 trimethylation

(H3K4me3) modification is sequestered to the nuclear interior (Yao *et al.* 2011). Because RAG2 contains a plant homeodomain (PHD) finger that interacts with H3K4me3 (Elkin *et al.* 2005, Liu *et al.* 2007, Matthews *et al.* 2007), functional RAG proteins may be similarly sequestered.

In order to understand the reason why DNA repair foci are underrepresented on peripheral *Tcrb* alleles, we proceeded to investigate the subnuclear distribution of RAG2 relative to *Tcrb* alleles and the nuclear lamina. We found that peripheral *Tcrb* alleles reside in a region of relatively low RAG2. This suggests that the nuclear periphery helps to suppress V(D)J recombination by segregating *Tcrb* alleles from functional RAG proteins.

6.2 Results

6.2.1 Visualizing RAG2 in the nuclei of developing T and B cells

We used an anti-RAG2 monoclonal antibody (Coster *et al.* 2012) to visualize endogenous RAG2 in $Lat^{-/-}$ DN thymocyte nuclei. We began by characterizing the fraction of nuclei in which RAG2 is expressed. Out of all nuclei analyzed, punctate RAG2 staining of variable intensity was seen in about 70% of $Lat^{-/-}$ nuclei, but not in control $Rag2^{-/-}$ nuclei (Fig. 22). We also co-stained with anti-Ki67, because this protein marks cycling cells (Kubbutat *et al.* 1994) and RAG2 is degraded in a cell-cycle-

dependent fashion (Li *et al.* 1996). As expected, RAG2 staining was generally low in the Ki67^{+} subset (~15%) of *Lat*$^{-/-}$ nuclei but was readily detected in most Ki67^{lo} non-dividing nuclei (Fig. 22).

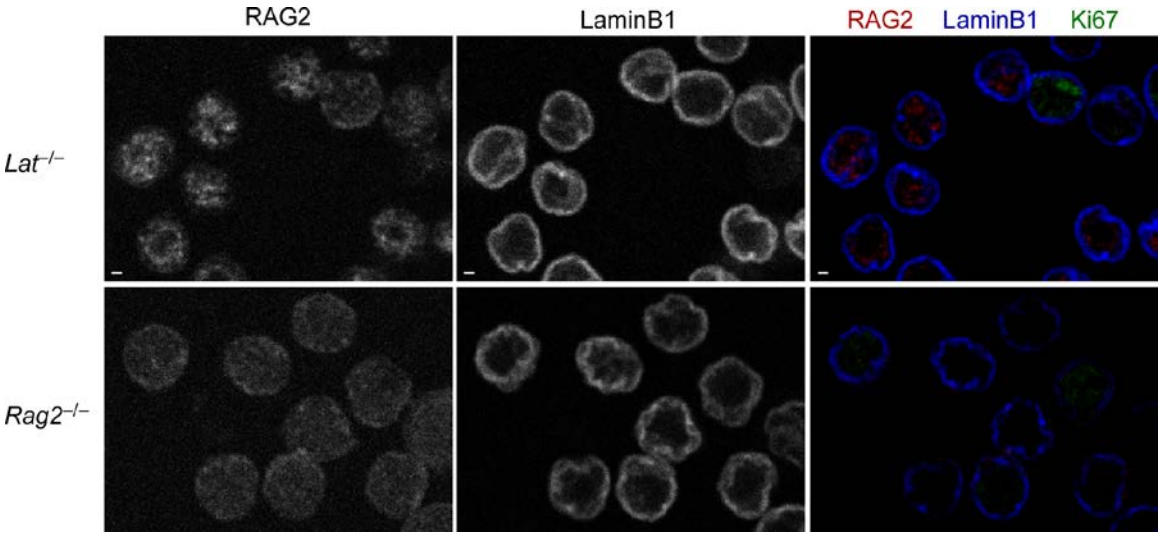

Figure 22: Subnuclear distribution of RAG2 in *Lat*$^{-/-}$ DN thymocyte nuclei

Confocal immunofluorescence microscopy showing the subnuclear localization of RAG2 relative to laminB1 in a single z-slice of both *Lat*$^{-/-}$ and *Rag2*$^{-/-}$ DN thymocyte nuclei. Ki67 staining was used to identify cycling cells. Raw laminB1, RAG2 and Ki67 images were background-subtracted and merged (right). Scale bars = 1 μm.

We then evaluated the overall subnuclear distribution of RAG2. Looking at RAG2^{+} nuclei, we compared the subnuclear location of RAG2 to areas of heterochromatin, defined by concentrated DAPI staining (Fig. 23). RAG2 staining was excluded from regions of heterochromatin.

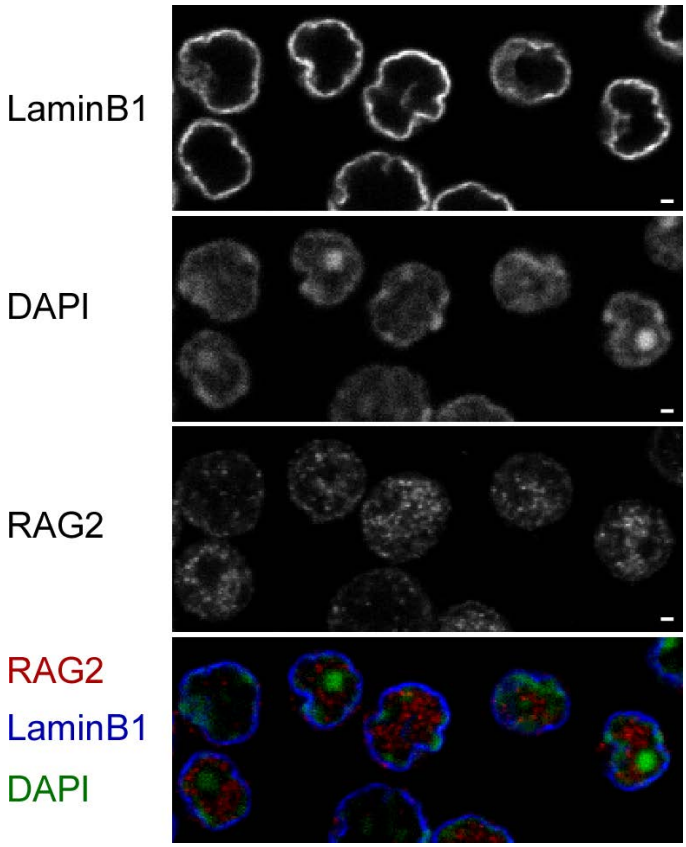

Figure 23: RAG2 is excluded from heterochromatin

Localization of laminB1, RAG2, and DAPI in nuclei of *Lat*$^{-/-}$ DN thymocytes. Raw laminB1, RAG2, and DAPI images were background-subtracted and merged (bottom).

To provide further evidence for RAG2 staining specificity, we examined additional populations of T and B cells for RAG2 signal. As expected from the known expression characteristics of RAG2 protein, staining with anti-RAG2 was detected in DP thymocyte nuclei undergoing *Tcra* recombination, but not in more mature $CD4^{+}CD8^{-}$ thymocyte nuclei (Fig. 24A). Staining was also observed in pro B cell nuclei undergoing *Igh* recombination, but not in mature peripheral B cell nuclei (Fig. 24B). The punctate staining distributions in DP thymocyte and pro B cell nuclei were similar to those observed in DN thymocyte nuclei.

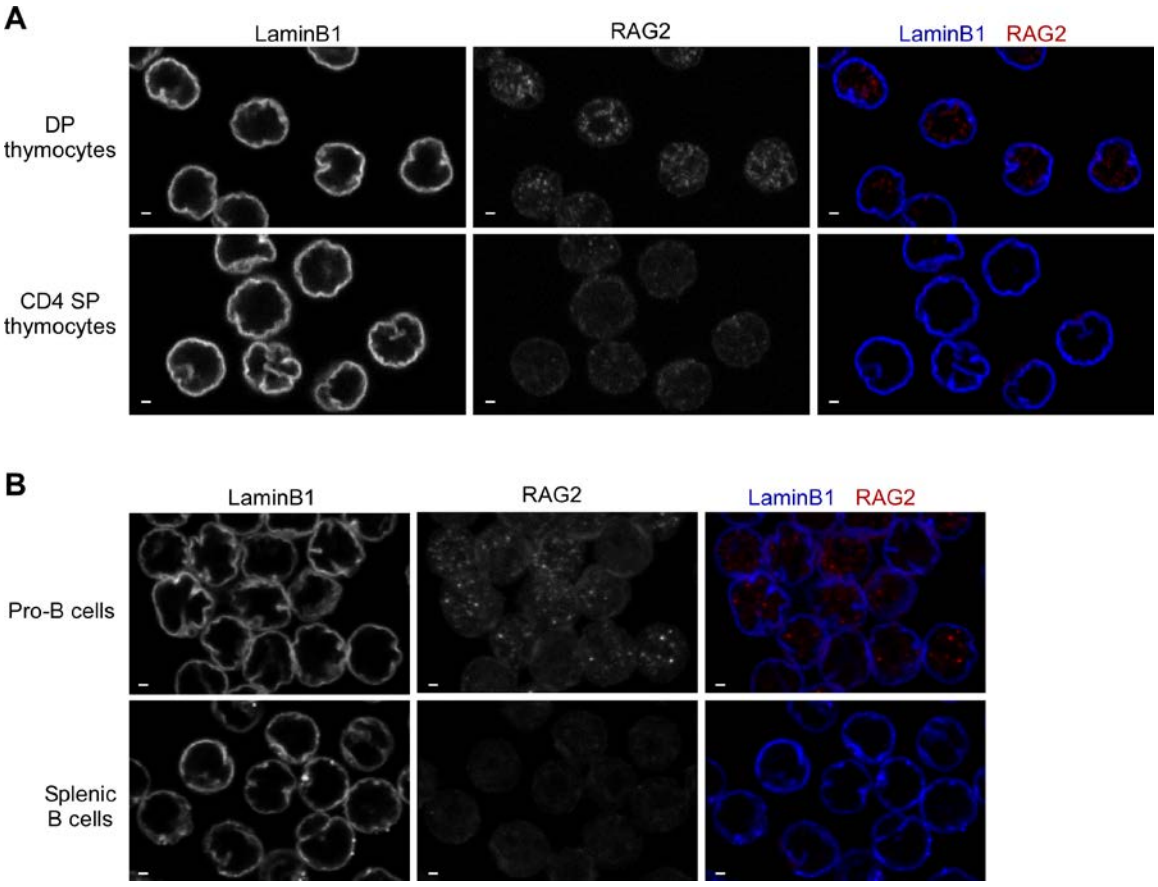

Figure 24: RAG2 staining of additional T- and B-cell populations

A) Confocal immunofluorescence microscopy showing subnuclear localization of RAG2 in nuclei of DP and $CD4^{+}CD^{-}$ thymocytes. Raw laminB1 (left) and RAG2 (center) images were background-subtracted and merged (right). Scale bars = 1 μm. B) Confocal immunofluorescence microscopy showing subnuclear localization of RAG2 in nuclei of pro-B and splenic B-cells. Raw laminB1 (left) and RAG2 (center) images were background-subtracted and merged (right). Scale bars = 1 μm.

6.2.2 RAG2 levels are reduced at the nuclear periphery

After confirming that the RAG2 signal is specific to cells in which RAG2 is expressed, we went on to ask whether RAG2 protein can localize to the nuclear periphery, where a large proportion of *Tcrb* alleles reside. To evaluate RAG2 distribution relative to the nuclear periphery, we deconvolved 3D images and obtained fluorescence intensity traces across the diameter of individual thymocyte nuclei. These traces revealed peaks of RAG2 staining between laminB1 peaks in $Lat^{-/-}$ but not $Rag2^{-/-}$ control nuclei (Fig. 25A). We then summed fluorescence intensity plots from 40 nuclear edges per experiment to obtain average distributions of RAG2 in $Lat^{-/-}$ and $Rag2^{-/-}$ nuclei relative to peak lamin intensity (Fig. 25B). These results revealed that RAG2 staining did not reach maximum intensity until nearly 1 μm from peak lamin staining, suggesting that RAG2 is excluded from the nuclear periphery.

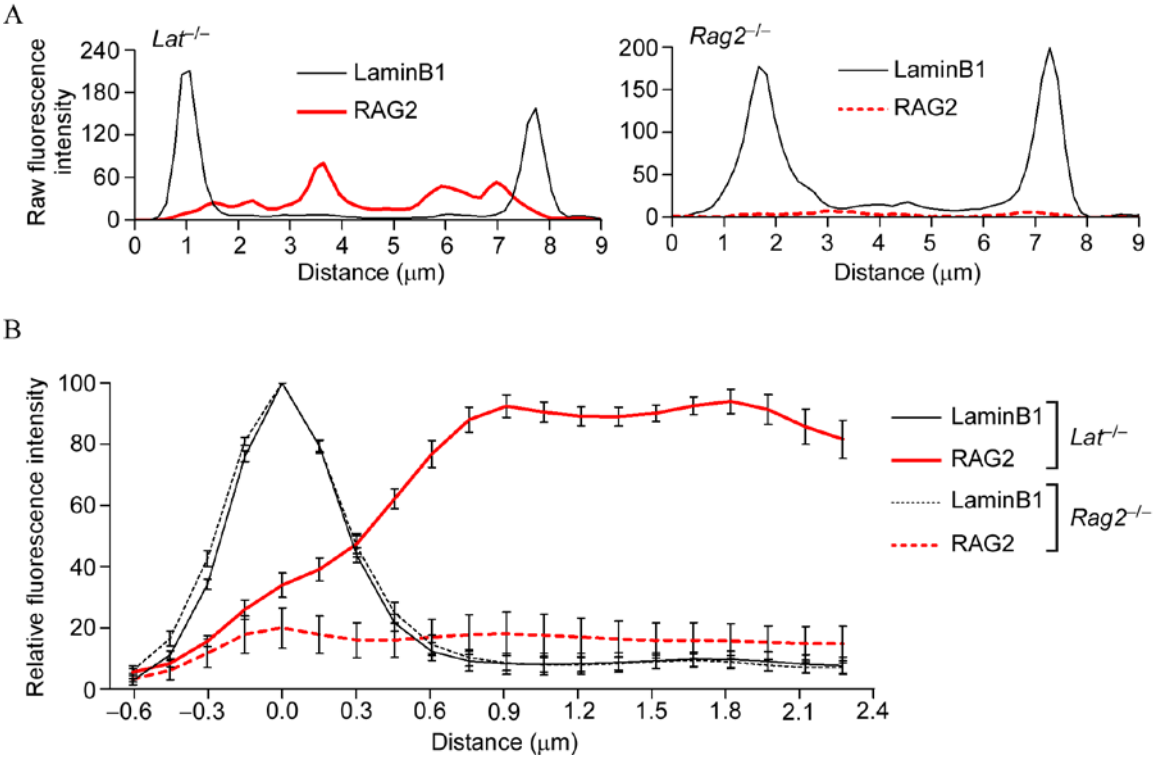

Figure 25: RAG2 protein is reduced at the nuclear periphery

A) Sample RAG2 and laminB1 fluorescence intensity plots across the diameter of a single z-slice of a *Lat*$^{-/-}$ and a *Rag2*$^{-/-}$ DN thymocyte nucleus. Slides were co-stained with anti-RAG2 and anti-laminB1. Slides containing *Lat*$^{-/-}$ and a *Rag2*$^{-/-}$ nuclei were simultaneously stained and imaged under identical conditions to allow evaluation of relative fluorescence intensities. B) Normalized RAG2 and laminB1 fluorescence intensity distributions across *Lat*$^{-/-}$ and a *Rag2*$^{-/-}$ DN thymocyte nuclei. Traces across individual nuclei were aligned at the point of peak laminB1 staining (x=0). Data were collected and summed for 40 nuclear edges per experiment. For *Lat*$^{-/-}$ nuclei, maximal laminB1 and RAG2 staining in each experiment was normalized to 100. For *Rag2*$^{-/-}$ nuclei, laminB1 staining was similarly normalized, but RAG2 staining was normalized to the maximum fluorescence intensity in the corresponding *Lat*$^{-/-}$ experiment. Each trace represents the mean±SEM of 5 independent experiments.

6.2.3 *Tcrb* alleles positioned at the nuclear periphery are segregated from RAG2

To understand the distribution of *Tcrb* alleles relative to the nuclear periphery and RAG2, we obtained traces measuring the shortest distance between peak intensities of *Tcrb* foci and the nuclear lamina. *Tcrb* alleles, on average, distributed very close to the nuclear lamina (Fig. 26A). In fact, they were as close to the lamina as the most peripheral DNA, defined by DAPI staining. In this position, most *Tcrb* alleles were segregated from the highest concentrations of RAG2. In contrast *Tcra*/*Tcrd* alleles, which are not allelically excluded, were distributed more centrally in the nucleus, in an environment characterized by high levels of RAG2 (Fig. 26A). This is not surprising, as *Tcra*/*Tcrd* alleles have been previously shown to be positioned away from the nuclear periphery (Schlimgen *et al.* 2008).

To further analyze the spatial relationship between *Tcrb* alleles and RAG2, we simultaneously visualized *Tcrb* alleles and RAG2 protein in individual DN thymocyte nuclei (Fig. 26B). The vast majority of *Tcrb* alleles embedded within the nuclear lamina did not colocalize with RAG2 foci (Fig. 26B, panel i; Fig. 26C, right bar). Moreover, *Tcrb* alleles in contact with the nuclear lamina (Fig. 26B, panels ii, iii, iv and v; Fig. 26C, middle bar) colocalized with RAG2 foci less frequently than did free *Tcrb* alleles (Fig. 26B, panels vi, vii, viii; Fig. 26C, left bar). Taken together, these data suggest that

positioning at the nuclear periphery reduces the frequency with which *Tcrb* alleles interact with RAG2.

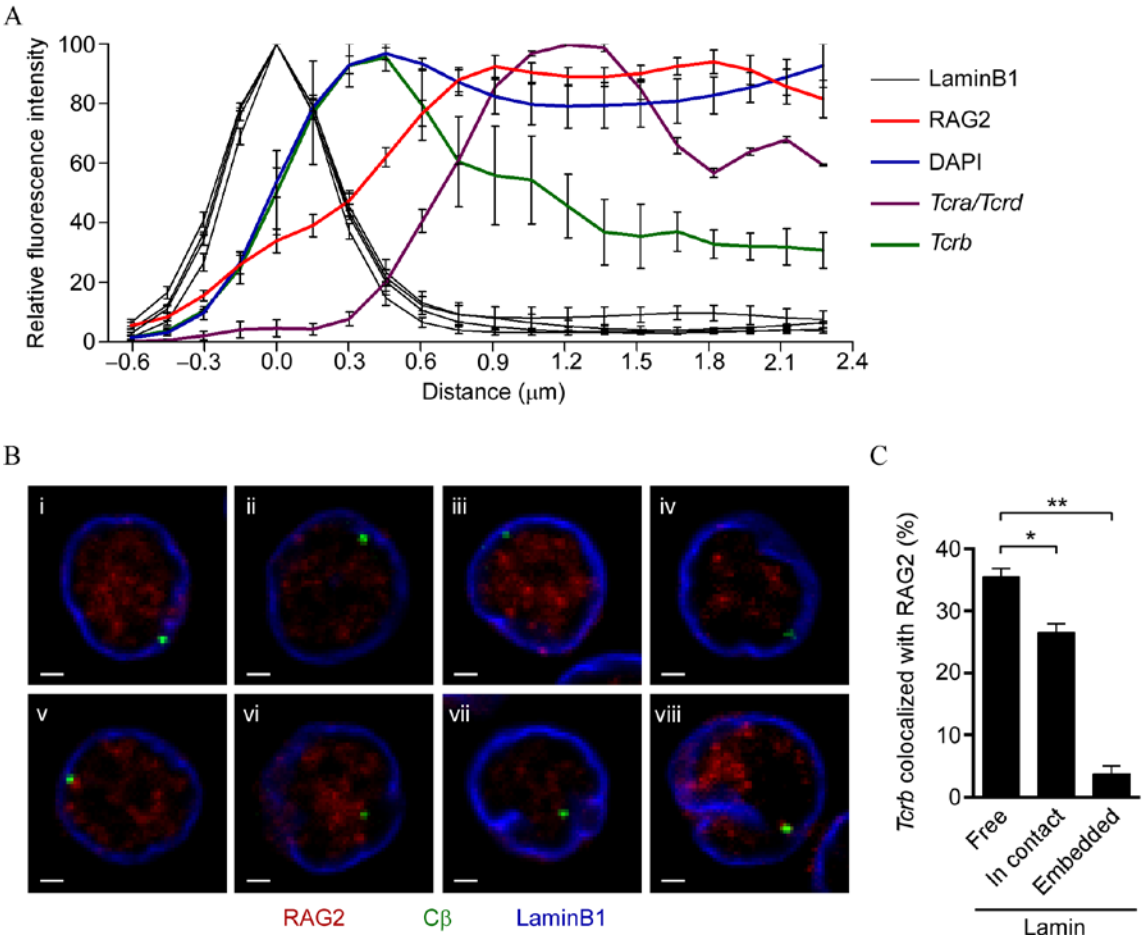

Figure 26: Peripheral *Tcrb* alleles are physically separated from RAG2 proteins

A) Normalized *Tcrb*, *Tcra/Tcrd*, DAPI, RAG2, and laminB1 fluorescence intensity distributions across $Lat^{-/-}$ DN thymocyte nuclei. The RAG2 fluorescence intensity plot and the corresponding laminB1 fluorescence intensity plot are the same as in Fig. 25B. *Tcrb*, *Tcra/Tcrd* and DAPI stains were conducted independently, each with a corresponding laminB1 stain. Traces across individual nuclei were aligned at the point of peak laminB1 staining (x=0). DAPI staining was collected and summed for 40 nuclear

edges per experiment and *Tcrb* and *Tcra*/*Tcrd* for 50 alleles per experiment, with the point of maximal staining normalized to 100 in each experiment. Data for DAPI is presented as mean±SEM of 3 independent experiments and for *Tcrb* and *Tcra*/*Tcrd* are presented as mean±SEM of 2 independent experiments. B) Confocal immunoFISH microscopy showing the relative locations of *Tcrb* foci, RAG2, and laminB1 in single z-slice images of $Lat^{-/-}$ DN thymocyte nuclei. *Tcrb* alleles were identified by hybridization with the C_β-end probe. Scale bars = 1 μm. C) Frequencies with which *Tcrb* alleles that are free of, in contact with, or embedded in the nuclear lamina colocalize with RAG2. *Tcrb* foci were considered to be lamin-free if fewer than two adjacent pixels colocalized with lamin signal. Foci were considered to be lamin-embedded if ≥ 90% of all *Tcrb* pixels colocalized with lamin signal; they were considered to be in contact with the lamina if >2 adjacent pixels but <90% of all pixels colocalized with lamin signal. Data were collected from 289 lamin-free, 318 lamin-contacting, and 99 lamin-embedded *Tcrb* alleles in 4 independent experiments. *, $P<0.05$ and **, $P<0.01$, by unpaired, two-tailed t-tests.

6.2.4. The subnuclear distribution of RAG2 is distinct from the distributions of both RNA polymerase II and H3K4me3

The above experiments raise the question of what determines the subnuclear distribution of RAG2 proteins. A previous publication used ChIP to show that *in vivo*, RAG2 proteins bind to thousands of sites throughout the genome containing the H3K4me3 histone modification (Ji *et al.* 2010). H3K4me3 is a mark of active and poised promoters (Kouzarides 2007), which could suggest that RAG2 is recruited to sites of transcription. We therefore wanted to determine whether RAG2 colocalized with H3K4me3 and/or PolII in DN thymocyte nuclei. We characterized the subnuclear distributions of H3K4me3 and PolII in $Lat^{-/-}$ DN thymocyte nuclei by staining with specific antibodies and comparing fluorescence intensity plots to those for the nuclear lamina, RAG2 and DAPI staining (Fig. 27). Antibodies used for H3K4me3 and PolII

staining were judged to be specific based the relative signal intensity following blocking with the respective immunogenic peptides (Fig. 27). Neither H3K4me3 nor PolII fluorescence intensity extended as close to the nuclear lamina as total DNA, in agreement with the idea that the nuclear periphery is generally transcriptionally repressive. However, H3K4me3 and PolII staining appeared to peak slightly closer to the nuclear lamina than RAG2 staining, suggesting that the RAG2 distribution may not be defined by either factor.

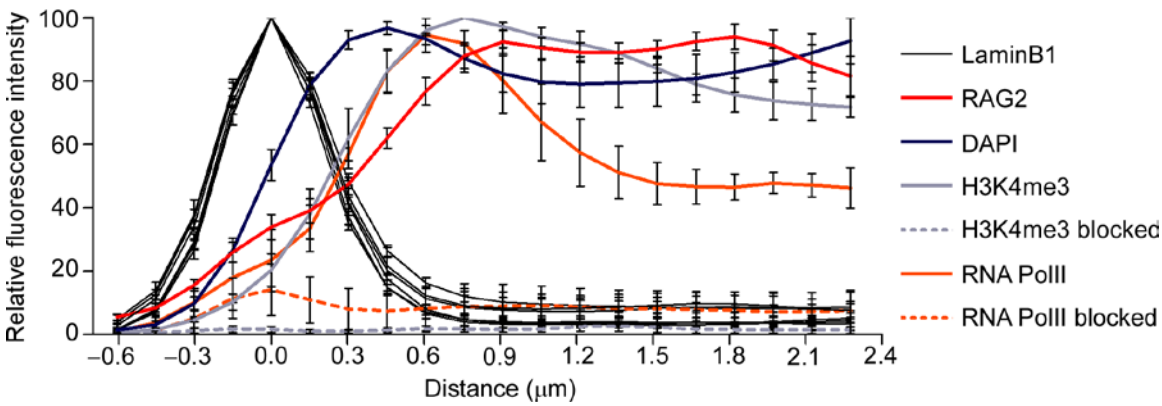

Figure 27: RAG2 distribution may not be defined by H3K4me3 or PolII

Normalized PolII, peptide immunogen-blocked PolII, H3K4me3, peptide immunogen-blocked H3K4me3, DAPI, RAG2, and laminB1 fluorescence intensity distributions across *Lat*$^{-/-}$ DN thymocyte nuclei. The RAG2 and DAPI fluorescence intensity plots and their corresponding laminB1 fluorescence intensity plots are the same as Fig. 26A. Slides for H3K4me3 and blocked H3K4me3 were simultaneously stained and imaged under identical conditions to allow evaluation of relative fluorescence intensity. Slides for PolII and blocked PolII were treated similarly. Staining was collected and summed for 40 nuclear edges per experiment. Maximal H3K4me3 and PolII staining was normalized to 100 in each experiment. In each case, control (blocked) staining was normalized to the maximum fluorescence intensity in the corresponding experimental (unblocked) staining. Corresponding laminB1 traces are presented for all experiments. Data for H3K4me3, blocked H3K4me3, PolII and blocked PolII each represent the mean±SEM of 3 independent experiments.

To better evaluate the subnuclear relationship between RAG2 and PolII, we simultaneously visualized both proteins in individual thymocyte nuclei (Fig. 28A). We calculated the average colocalization of RAG2 and PolII within individual nuclei containing both signals to determine the Pearson's correlation coefficient *r*. The distributions of the two proteins overlapped only partially, with minimal correlation

between the two fluorescence intensity signals in individual thymocyte nuclei (Fig. 28B, top) and as averaged over many nuclei in several independent experiments (Fig. 28C). Hence RAG2 protein does not primarily localize to transcription factories.

Technical limitations prevented us from directly comparing the RAG2 distribution to that of H3K4me3. However, we were able to co-visualize H3K4me3 and PolII (Fig. 28D). We observed substantially overlapping and highly correlated distributions (Fig. 28B, bottom; Fig. 28C), consistent with the localization of H3K4me3 near the promoters of actively transcribed genes (Vermeulen *et al.* 2010). Thus, although RAG2 has a PHD domain that binds H3K4me3 (Liu *et al.* 2007, Matthews *et al.* 2007) and chromatin-bound RAG2 colocalizes with H3K4me3 genome-wide (Ji *et al.* 2010), we infer that the distribution of total RAG2 protein in DN thymocyte nuclei is unlikely to correspond well to the distribution of H3K4me3.

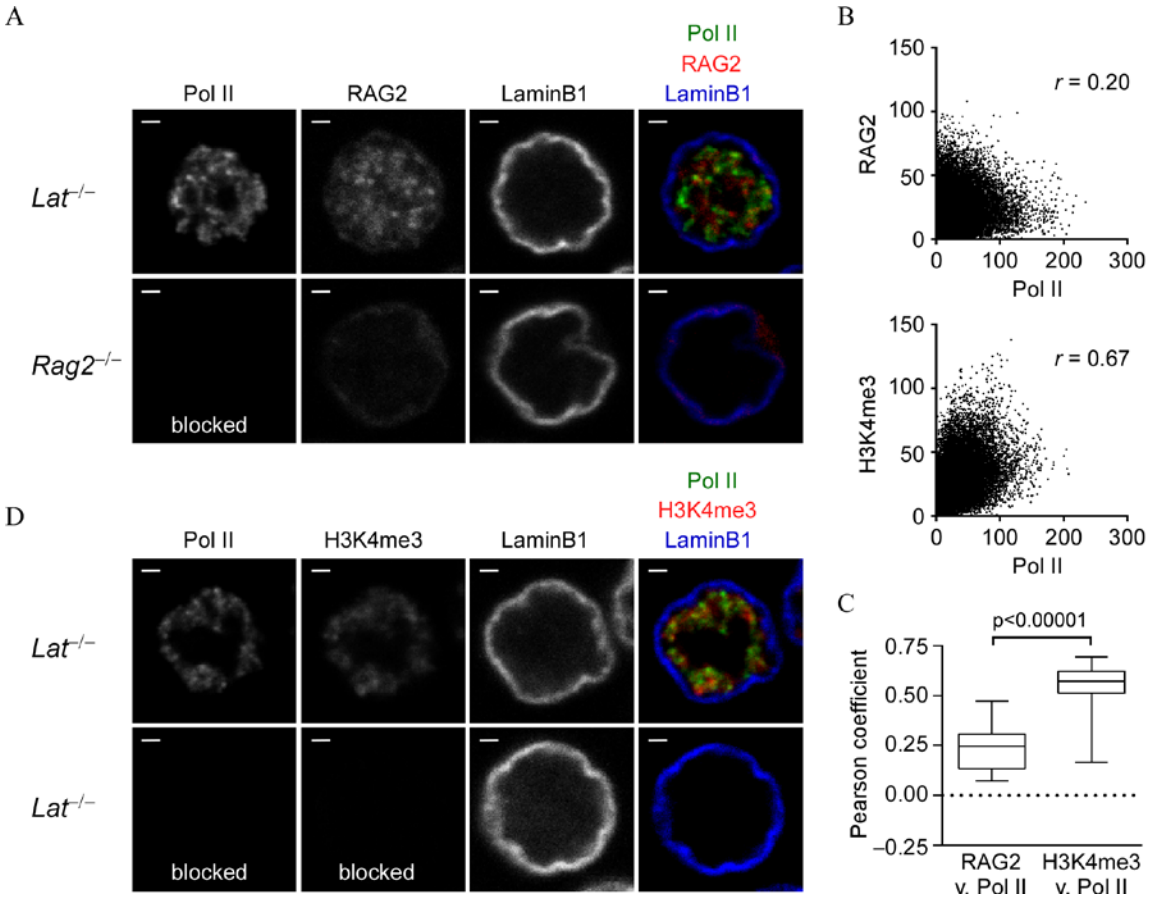

Figure 28: RAG2 protein distribution is distinct from that of PolII and H3K4me3

A) Confocal immunofluorescence microscopy showing subnuclear localization of PolII, RAG2 and laminB1 in nuclei of *Lat*$^{-/-}$ and *Rag2*$^{-/-}$ DN thymocytes. Raw PolII, RAG2, and laminB1 images were background-subtracted and merged (right-most panels). Scale bars = 1 μm. B) Correlation analysis of RAG2 and PolII fluorescence intensity (top) and of H3K4me3 and PolII fluorescence intensity (bottom) in all voxels of single *Lat*$^{-/-}$ DN thymocyte nuclei. *r*, Pearson correlation coefficient. C) Box and whisker plots of Pearson correlation coefficients for distributions of RAG2 v. PolII (total of 43 nuclei in two independent experiments) and H3K4me3 v. PolII (total of 61 nuclei in two independent experiments). Statistical significance was evaluated by unpaired t-test. (D) Confocal immunofluorescence microscopy showing subnuclear localization of PolII, H3K4me3 and laminB1 in nuclei of *Lat*$^{-/-}$ DN thymocytes. Raw PolII, RAG2, and laminB1 images were background-subtracted and merged (right-most panels). Scale bars = 1 μm.

To address the role of H3K4me3 in determining the subnuclear distribution of RAG2 protein independently, we analyzed the RAG2 distribution in DN thymocytes of mice expressing a truncated RAG2 protein that lacks its C-terminal region. This truncation removes the PHD domain, which disrupts RAG2 recruitment to H3K4me3 (Liang *et al.* 2002). Comparison of the subnuclear distributions of truncated RAG2 in $Rag^{\Delta/\Delta}$ $Lat^{-/-}$ thymocyte nuclei to full length RAG2 in $Lat^{-/-}$ DN thymocyte nuclei revealed indistinguishable distributions of RAG2 protein relative to the nuclear lamina in the two cell populations (Fig. 29). This result indicates that binding to H3K4me3 does not limit RAG2 protein from the nuclear periphery, and reinforces the notion that binding to H3K4me3 does not dictate the subnuclear distribution of total RAG2 protein.

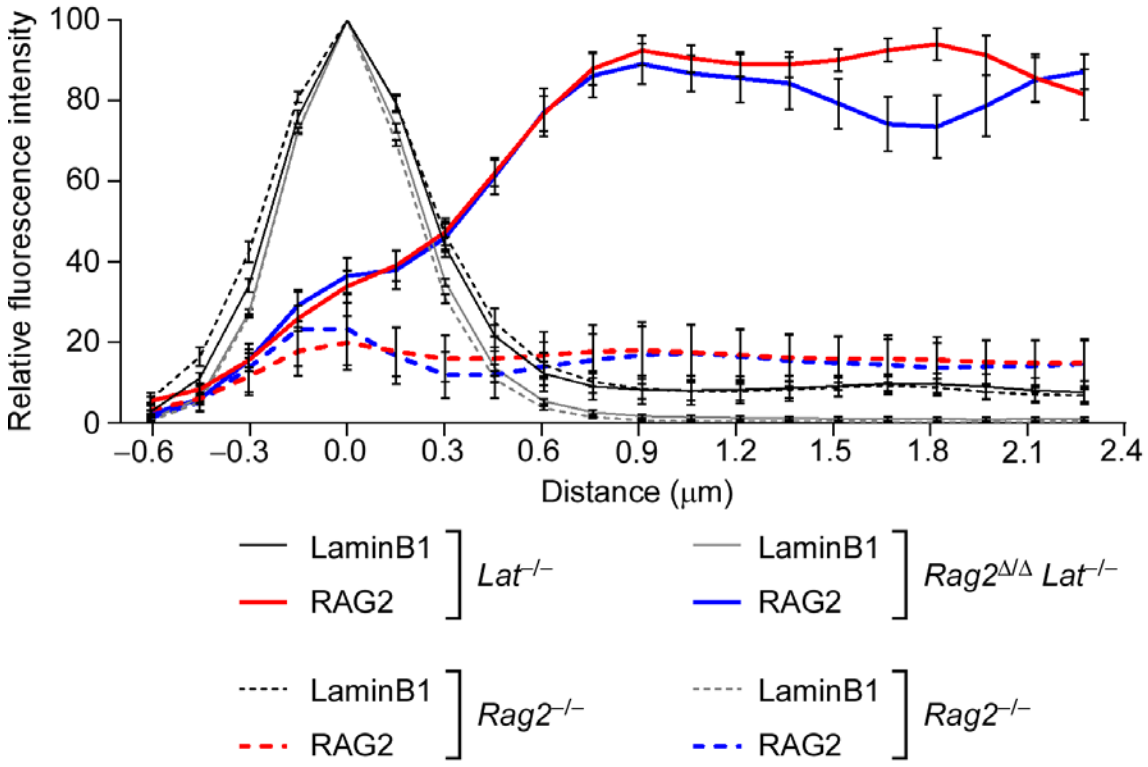

Figure 29: The RAG2 PHD domain is not required for RAG2 localization to the nuclear interior

Normalized RAG2 and laminB1 fluorescence intensity distributions across *Lat*$^{-/-}$, Rag2$^{\Delta/\Delta}$ and *Rag2*$^{-/-}$ DN thymocyte nuclei. The RAG2 (red) and laminB1 fluorescence intensity plots (black) for *Lat*$^{-/-}$ and its corresponding *Rag2*$^{-/-}$ staining are from Fig. 26B. Slides containing Rag2$^{\Delta/\Delta}$ *Lat*$^{-/-}$ nuclei were stained and imaged together with an additional set of slides containing *Rag2*$^{-/-}$ nuclei to allow evaluation of relative fluorescence intensities (RAG2, blue; laminB1, gray). Traces were aligned and normalized as in Fig. 26B. Data were collected for 40 nuclear edges per experiment. Each trace represents the mean±SEM of 4-5 independent experiments.

6.2.5 Nearly all *Tcrb* alleles colocalize with RNA polymerase II

Because the nuclear lamina is thought to be repressive for transcription, the inhibition of V(D)J recombination on peripheral *Tcrb* alleles could reflect, in part, segregation from RNA PolII and reduced transcription and accessibility to RAG proteins. To address this point, we simultaneously visualized *Tcrb* alleles and PolII in DN thymocyte nuclei (Fig. 30A). Almost all *Tcrb* alleles colocalized with PolII signal, regardless of their peripheral localization (Fig. 30A and B). Notably, *Tcrb* alleles were almost always positioned at the edge of regions of PolII staining, and we often observed finger-like projections of PolII extending to *Tcrb* alleles at the nuclear lamina (Fig. 30A, panels i and vii). Moreover, in most nuclei, both *Tcrb* alleles were in contact with PolII (panels i, ii, iii, iv and vi). Thus, our results are consistent with previous work demonstrating that V_β gene segments are transcribed biallelically in DN thymocyte nuclei (Jia *et al.* 2007). We originally hypothesized that the suppression of *Tcrb* recombination at the nuclear periphery resulted from either RAG2 segregation and/or transcriptional repression. As we see no segregation of *Tcrb* alleles from PolII, we conclude that the peripheral location of many *Tcrb* alleles may limit recombination primarily by impacting the supply of RAG2 to accessible *Tcrb* alleles.

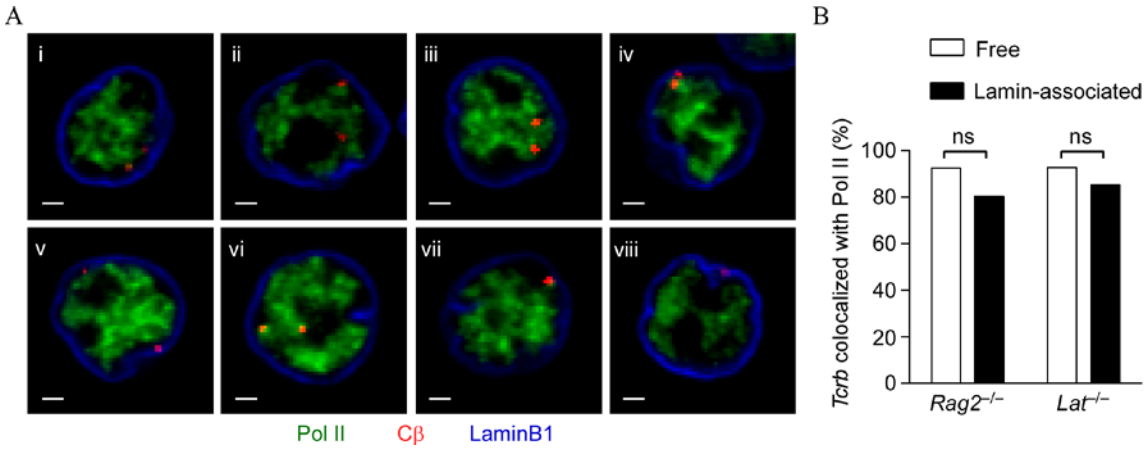

Figure 30: Nearly all *Tcrb* alleles colocalize with PolII

A) Confocal immunoFISH microscopy showing the relative locations of *Tcrb*, PolII, and laminB1 in single z-slice images of $Lat^{-/-}$ DN thymocyte nuclei. *Tcrb* alleles were identified by hybridization with the Cβ-end probe. Scale bars = 1 μm. B) Frequencies of lamin-associated and free *Tcrb* alleles that colocalize with PolII. Data were collected from 160 alleles in $Rag2^{-/-}$ and 186 alleles in $Lat^{-/-}$ DN thymocytes; ns, not significant using Fisher's exact two-tailed contingency tables.

6.2.6 The majority of RAG2 is unbound or weakly bound to chromatin

Although we could not directly compare the subnuclear distributions of RAG2 and H3K4me3, our data do argue that the overall RAG2 distribution is not defined by that of H3K4me3. This could be thought to conflict with the publication demonstrating that RAG2 is located at sites containing H3K4me3 genome-wide (Ji *et al.* 2010). However this apparent discrepancy may reflect the fact that ChIP-seq results come from a population of cells, and cannot determine whether RAG2 is present on all or only some alleles, or if the interaction is dynamic and/or transient.

We propose that DN thymocyte nuclei may contain both chromatin-bound and -free pools of RAG2. To test this, we briefly incubated *Lat*$^{-/-}$ and *Rag2*$^{-/-}$ thymocytes with a standard Triton X-100 wash buffer prior to fixation, in order to extract nucleoplasmic proteins that were weakly associated or unassociated with chromatin. RAG2 staining in the Triton X-100 extracted nuclei was greatly diminished, but the PolII staining was not (Fig. 31). This suggests that most nuclear RAG2 is either weakly-associated or unassociated with chromatin.

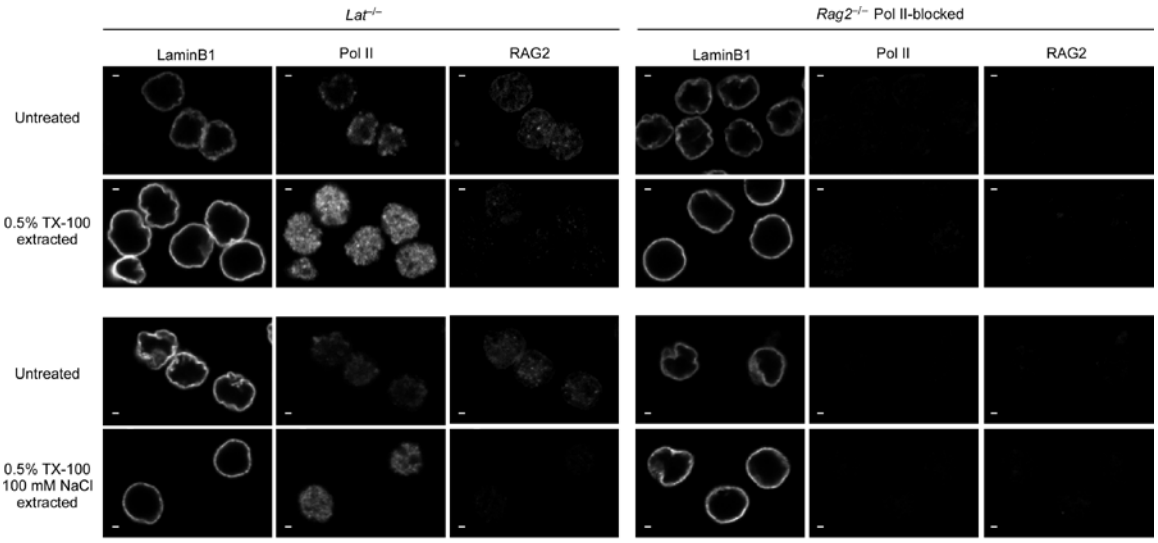

Figure 31: Diminished RAG2 staining following extraction of nucleoplasmic proteins

Confocal immunofluorescence microscopy showing the subnuclear localization of laminB1, PolII and RAG2 in untreated and Triton X-100 (TX-100)-extracted *Lat*$^{-/-}$ and *Rag2*$^{-/-}$ DN thymocyte nuclei. The *Rag2*$^{-/-}$ DN thymocyte nuclei were incubated with PolII peptide immunogen-blocked anti-RNA PolII antibody. For each experimental condition, the *Rag2*$^{-/-}$ and PolII peptide immunogen-blocked control slides were background subtracted to eliminate PolII and RAG2 signals and this background subtraction was applied equally to the *Lat*$^{-/-}$ experimental slides. Signals shown for *Lat*$^{-/-}$ nuclei represent staining above this background. Results are representative of 3-4 independent experiments for each treatment group. Scale bars = 1 μm.

6.3 Discussion

Here we demonstrate that RAG2 levels are reduced at the nuclear periphery, suggesting that *Tcrb* alleles are positioned at this subnuclear location so that the frequency of V(D)J recombination is reduced. This could be useful to prevent the simultaneous V_β-to-DJ_β recombination of both *Tcrb* alleles within a single cell, especially

since both *Tcrb* alleles appear to be contracted (Skok *et al.* 2007) and actively transcribing (Jia *et al.* 2007) in DN thymocytes.

Although we found that the majority of *Tcrb* alleles are present at the nuclear periphery in an environment characterized by reduced levels of RAG2, chromatin immunoprecipitation (ChIP) analysis has demonstrated abundant RAG2 binding to D_β and J_β segments in DN thymocytes (Ji *et al.* 2010). Although these results seem contradictory, it is important to consider that ChIP only provides a population analysis that cannot discriminate heterogeneity of RAG2 binding on different alleles. We suggest that the RAG2 ChIP signals reflect RAG2 binding on the subset of *Tcrb* alleles that are free of the nuclear lamina and the subset of peripheral *Tcrb* alleles whose D_β and J_β segments are dissociated from the lamina.

Although we have documented reduced RAG2 levels at the nuclear periphery, we cannot formally rule out that the nuclear periphery may also inhibit *Tcrb* recombination by other mechanisms. For example, the nuclear periphery could exclude other components of the V(D)J recombination machinery, including RAG1 and DSB repair factors. Moreover, because the nuclear periphery is generally suppressive for gene expression, it remains possible that the nuclear periphery suppresses *Tcrb* recombination by regulating locus transcription and accessibility. One argument against this was a study in which a knock-in reporter of V_β8.2 expression was shown to be

biallelically transcribed in all DN thymocytes (Jia *et al.* 2007). However it could not formally be excluded that $V_{\beta}8.2$ has atypical expression characteristics or that its expression was perturbed by introduction of the reporter. Consistent with the notion of biallelic transcription irrespective of subnuclear localization, we detected PolII at 80-90% of lamin-associated and free *Tcrb* alleles in DN thymocyte nuclei. However, colocalization with PolII is insufficient information from which to conclude active transcription. Thus, it will be important in future studies to evaluate by RNA FISH whether germline transcription is equivalent on lamin-associated and free *Tcrb* alleles.

The molecular basis for the RAG2 distribution in DN thymocyte nuclei remains unknown. RAG2 is known to interact with the active histone modification H3K4me3 (Liu *et al.* 2007, Matthews *et al.* 2007) and ChIP-seq analysis has revealed very high concordance between RAG2 binding and H3K4me3 islands genome wide (Ji *et al.* 2010). Our data suggest that the overall RAG2 distribution is not defined by that of H3K4me3. We also showed that the majority of RAG2 in DN thymocyte nuclei is weakly-bound or unbound to chromatin. We take these data to suggest that DN thymocyte nuclei may contain both chromatin-bound and -free pools of RAG2, that may move in and out of transcription factories (which themselves appear to be quite dynamic (Cisse *et al.* 2013)) interacting with only a subset of actively transcribed genes at any moment in individual nuclei. We contend that the subnuclear distribution of the free pool of RAG2 is highly

relevant for the regulation of V(D)J recombination, because this pool would serve as the local source of RAG2 that becomes functionally associated with antigen receptor loci.

7. Discussion and Future Directions

Antigen receptor diversity results from highly controlled V(D)J recombination at *Tcr* and *Bcr* gene loci. Recombination is also regulated to ensure that each lymphocyte expresses a single unique receptor. While lineage- and stage-specific RAG expression and RSS accessibility are partially responsible for the regulation of recombination, additional mechanisms have been recently discovered. One of the potential regulatory mechanisms is the localization of antigen receptor alleles to repressive subnuclear compartments, in order to reduce the frequency of V(D)J recombination. However, at the onset of this study, there was a lack of direct evidence that positioning at certain compartments represses recombination.

7.1 Additional questions regarding the regulation of V(D)J recombination in developing thymocytes

Igh alleles in pro-B cell nuclei, like *Tcrb* alleles in DN thymocyte nuclei, are subject to allelic exclusion at the V-to-DJ step of recombination. Recombination at *Igh* alleles has been suggested to be regulated so that recombination at one allele sends a signal to stop additional rearrangement events, through the DSB repair factor ATM (Hewitt *et al.* 2009). The authors came to this conclusion after observing a slight increase of the frequency of nuclei containing DSB repair foci at both *Igh* alleles in WT pro B cells

(0.1%) as compared to *Atm*$^{-/-}$ pro B cells (0.8%). If true, this theory would support the idea that asynchronous recombination of *Igh* alleles is achieved through a directed model.

However there are several problems with this conclusion. Most importantly, the authors did not take into consideration that the amount of time required for DSB repair to be completed in ATM-deficient cells will increase (Kato *et al.* 2006). This alone could account for the increased frequency of nuclei containing DSB repair foci at both *Igh* alleles. Additionally, the immunofluorescence staining in this paper was questionable, as some of the representative images showed more than 3 DSB repair foci per pro-B cell nucleus, and one image contained more than 10 DSB repair foci. Finally, there is no direct evidence that pairing of *Igh* alleles has any functional effect. As an aside, our lab analyzed the location of *Tcrb* alleles in DN thymocyte nuclei and found that they do not pair (Schlimgen *et al.* 2008).

To evaluate how recombination is regulated at *Tcr* loci, we characterized *Tcr* recombination events in developing thymocyte nuclei. We analyzed *Tcrb* and *Tcra* recombination in DN and DP thymocytes, respectively, and examined the two steps of *Tcrb* recombination (D_β-to-J_β and V_β-to-DJ_β) individually. In order to determine whether thymocytes are regulated so that the presence of a DSB prevents additional V(D)J recombination, we blocked the NHEJ-mediated repair of DSBs in DN thymocyte

nuclei. In cells capable of DSB repair, the frequency of rearrangements was quite low. However, no cell types or developmental stages analyzed deviated from the expected frequencies of cells containing 0, 1, and 2 53BP1^{+} *Tcr* alleles. In contrast, nuclei unable to repair RAG-dependent DSBs exhibited a dramatic increase in the frequency of nuclei containing 2 53BP1^{+} *Tcr* alleles. Therefore we concluded that the presence of a RAG-dependent DSB does not signal to prevent the generation of additional RAG-dependent DSBs.

Though we analyzed *Tcrb* and *Tcra*/*Tcrd* alleles, we did not analyze *Tcrg* alleles. It is therefore possible that *Tcrg* alleles are regulated differently than *Tcrb* and *Tcrd* alleles in DN thymocyte nuclei. However, a recent study visualized 53BP1 and all three *Tcr* alleles (*Tcrb*, *Tcrd*, and *Tcrg*) in WT and *Atm*$^{-/-}$ DN2/3 thymocytes. While they did not distinguish between nuclei containing 1 and 2 53BP1^{+} *Tcrg* alleles, they found roughly the same frequency of nuclei containing at least one 53BP1^{+} *Tcrg* allele as either 53BP1^{+} *Tcrb* or 53BP1^{+} *Tcra*/*Tcrd* alleles (Bowen *et al.* 2013). Together, these data suggest that all *Tcr* loci are regulated similarly, in a stochastic manner, but confirmation of this at *Tcrg* alleles is still needed.

7.2 Mechanism by which Tcrb *alleles are positioned at the nuclear periphery*

A relatively large proportion of *Tcrb* alleles are frequently located at the nuclear periphery in pro-B cells, DN thymocytes, and DP thymocytes (Schlimgen *et al.* 2008). However, the mechanism by which the *Tcrb* locus is positioned at the nuclear lamina remains an important unresolved question. Potential mechanisms include both DNA sequence-independent and dependent mechanisms. One DNA sequence-independent possibility is the histone modification H3K9me, which has been shown to mediate peripheral anchoring of heterochromatin (Towbin *et al.* 2013). Indeed, the 3′ trypsinogen region of the *Tcrb* locus is enriched in the H3K9me2 modification (Carabana *et al.* 2011), making this mechanism of peripheral localization intriguing.

DNA content may also direct the subnuclear localization of genes. For example, the ratio of As and Ts to guanines and cytosines in the DNA sequence may influence positioning of genes at the nuclear periphery, as high A/T-content (>60%) is a defining feature of constitutive LADs (Meuleman *et al.* 2013). However, a brief survey of the *Tcrb* locus did not reveal high A/T content.

Genes containing specific DNA sequences may also mediator peripheral localization. For example, two genes frequently positioned at the nuclear periphery were recently shown to contain DNA sequences that recruit heterologous genes to the lamina in NIH3T3 cells (Zullo *et al.* 2012). These DNA sequence fragments contained

multiple binding motifs for the transcriptional repressor cKrox. Additionally, both cKrox and its interaction partner HDAC3 were shown to be significant mediators of *Igh* and *Cyp3a* lamin-association.

We suspect that the *Tcrb* locus may be positioned at the nuclear periphery due to a sequence-dependent mechanism. If this is true, identifying which discrete regions of the *Tcrb* locus are most frequently associated with the periphery could provide insight into which regions of the *Tcrb* locus are responsible for positioning the locus at the periphery. Our analysis of the conformation of *Tcrb* alleles at the periphery did not strongly suggest that either the V_β or C_β end of the locus is preferentially located at the periphery (Fig. 20C, left and 20D, left). This could suggest that both ends of the locus are equally likely to localize to the periphery, or that a central region of the locus is responsible for peripheral positioning. We next performed preliminary experiments to evaluate whether *Tcrb* loci physically associate with the nuclear lamina, and to determine which regions of the locus most frequently associate with the lamina. We collaborated with Joseph Zullo and Harinder Singh to perform an alternative to ChIP known as DNA adenine methyltransferase identification (DamID) (Greil *et al.* 2006) to identify genomic sequences associating with the nuclear periphery. The DamID protocol involves first fusing the protein of interest (in our case laminB1) to the bacterial methyltransferase Dam, and then expressing the fusion protein in the appropriate cell

lines or cultured cells. The Dam methyltransferase marks all DNA in the genome that interacts with the protein of interest. Dam-only plasmids were also expressed in a separate set of cells, to account for nonspecific methylation resulting from accessible chromatin. Genomic DNA from transfected cells was isolated, and DNA sequences marked by methylation were specifically amplified and identified using microarray analysis.

Joseph Zullo provided two independently amplified DNA samples for DamID analysis. The first was processed by Youngjoo Oh and the second by Han-Yu Shih. The relative interaction frequency along the entirety of the *Tcrb* locus in NIH3T3 cells with laminB1 in NIH3T3 cells was analyzed by hybridization to a custom microarray generated by Han-Yu Shih. Dam-laminB1 values were normalized to dam-only values and shown as an interaction profile where more frequent interaction is shown above the x-axis. Both interaction profiles were similar, and a representative example is shown in Fig. 32. The average interaction frequency sharply increases a few hundred kb 5′ of the *Tcrb* locus and remains relatively high throughout the locus (Fig. 32). Interestingly, we see relative increases in laminB1 association at both the 5′ and 3′ trypsinogen regions, as compared to laminB1 association in the V_β region. These results suggest that the trypsinogen regions of the *Tcrb* locus may be responsible for localizing the locus to the nuclear periphery, at least in the NIH3T3 fibroblast cell line.

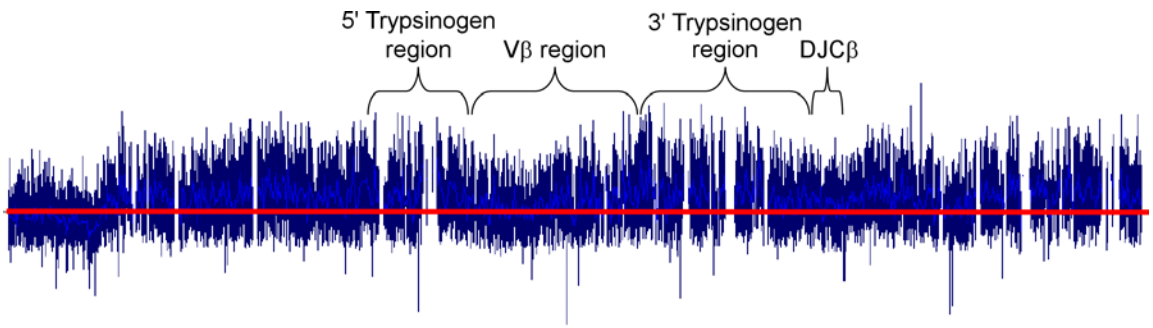

Figure 32: The *Tcrb* locus interacts with laminB1 in NIH3T3 cells

A microarray was used to analyze the association of the *Tcrb* locus with laminB1 in NIH3T3 fibroblast cells. The microarray covered 1.2 Mb of chromosome 6, which included the entire *Tcrb* locus, and used probes ranging between 50-75 bp with a 10 bp interval between each probe. The y-axis depicts the $\log_2$ transformed dam-laminB1 over the dam-only methylation ratio. The locations of the main V_β region, the DJC_β cluster, and the 5′ and 3′ trypsinogen regions are shown.

In the future, we hope to experimentally determine whether certain fragments of the *Tcrb* sequence mediate peripheral localization in developing thymocyte nuclei. One way to accomplish this would be to take small portions of the locus and insert them randomly into the genome, followed by 3D DNA immunoFISH to evaluate whether these inserted regions localize the nearby chromatin to the nuclear periphery. By continuing to reduce the size of the transfected sequence, we could potentially identify discrete DNA regions that associate chromatin with the nuclear periphery.

CTCF is known to regulate the 3D structure of chromatin and bring DNA strands together to form loops (Phillips and Corces 2009). However, CTCF was recently found to position the inactive human cystic fibrosis transmembrane conductance regulator

(*Cftr*) gene (Muck *et al.* 2012) and a subtelomeric element (Ottaviani *et al.* 2009) at the nuclear periphery. Upon CTCF knock-down, approximately 10% of *Cftr* alleles relocated from the outer shell of nuclei to a more interior nuclear region (Muck *et al.* 2012), suggesting that CTCF may tether *Ctfr* alleles to the nuclear periphery. Therefore CTCF is a candidate for mediating the peripheral positioning of *Tcrb* alleles.

To test whether CTCF plays a role in *Tcrb* positioning at the nuclear periphery, we visualized the location of *Tcrb* alleles relative to the nuclear periphery in developing thymocyte nuclei lacking CTCF, supplied by Han-Yu Shih. *Ctcf* was deleted by the expression of the Cre recombinase, which specifically excises the DNA sequence between two similarly oriented loxP sites. In the genome of $Ctcf^{f/f}$ mice, the *Ctcf* gene is flanked by loxP sites in the same orientation. $Ctcf^{f/f}$ mice were crossed to mice expressing Cre recombinase under control of the *Lck* promoter, which induces expression only in developing thymocytes, beginning at the DN stage. As Cre expression begins at the DN stage, *Ctcf* was not completely deleted from the genome until the DP stage of development. Because *Tcrb* alleles remain positioned at the nuclear periphery in DP thymocyte nuclei and slides containing DP thymocytes prepared from Cre^{+} and Cre^{-} $Ctcf^{f/f}$ mice were readily available, we used CTCF-deficient DP thymocytes for our initial analysis.

We began by visualizing *Tcrb* alleles, the nuclear lamina, and CTCF in *Ctcf*$^{fl/fl}$ *Lck*-Cre^{+} and *Lck*-Cre^{-} thymocyte nuclei (Fig. 33A). We assessed the subnuclear location of *Tcrb* alleles relative to the nuclear lamina in DP thymocyte nuclei sufficient or deficient for CTCF (Fig. 33A). Though there was a slight reduction of peripheral *Tcrb* alleles in CTCF-deficient DP thymocytes, the change was statistically insignificant (Fig. 33B). There was also no significant change in the frequencies of nuclei containing 0, 1, and 2 peripheral *Tcrb* alleles; though again a slight reduction in the frequency of nuclei containing 2 in the periphery was observed (Fig. 33C). Theoretical distributions of nuclei containing 0, 1, and 2 peripheral *Tcrb* alleles also closely resembled the observed frequencies (Table 6). These results suggest that CTCF may be dispensable for peripheral subnuclear positioning of *Tcrb* alleles in developing thymocyte nuclei.

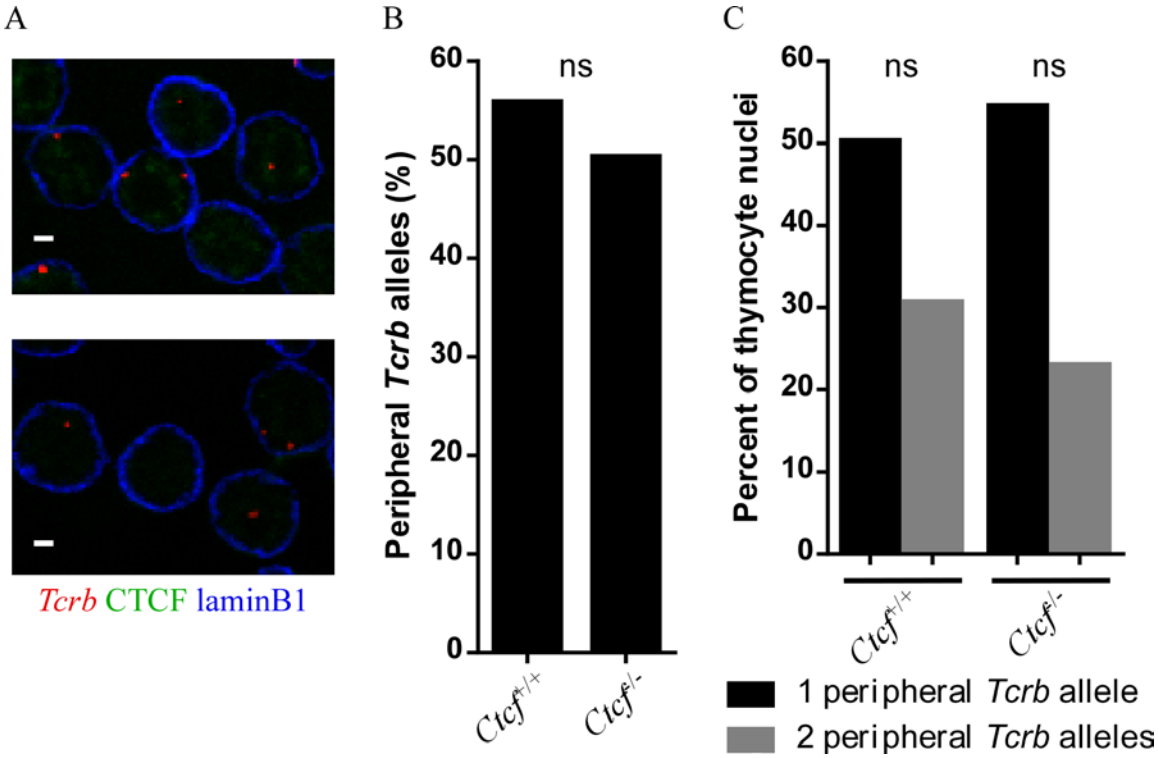

Figure 33: CTCF is dispensable for peripheral *Tcrb* positioning in DP thymocyte nuclei

A) Top, Confocal immunoFISH microscopy showing the subnuclear localization of *Tcrb* alleles in single z-slices of sorted DP Ctcf$^{f/f}$ Lck-Cre^{-} thymocyte nuclei. Bottom, Confocal immunoFISH microscopy showing the subnuclear localization of *Tcrb* alleles in single z-slices of sorted DP DP Ctcf$^{f/f}$ Lck-Cre^{+} thymocyte nuclei. Scale bars = 1 μm. B) Frequency of *Tcrb* alleles in 153 DP Ctcf$^{f/f}$ Lck-Cre^{-} and 152 Ctcff/f Lck-Cre^{+} thymocyte nuclei that are positioned at the nuclear periphery from 1 slide per genotype. C) Distribution of nuclei containing one or two peripheral *Tcrb* alleles in DP Ctcf$^{f/f}$ Lck-Cre^{-} and Ctcf$^{f/f}$ Lck-Cre^{+} thymocyte nuclei. Data were compiled from 1 slide of each genotype. C) The experimental frequencies of peripheral and central *Tcrb* alleles in DP Ctcf$^{f/f}$ Lck-Cre^{-} and 152 Ctcf$^{f/f}$ Lck-Cre^{+} thymocyte nuclei is quite similar to the theoretical distribution predicted based on probability. ns, not significant by unpaired, two-tailed t-tests.

Table 6: Observed and theoretical distributions of Ctcf$^{f/f}$ *Lck*-Cre^{-} and Ctcf$^{f/f}$ *Lck*-Cre^{+} sorted DP thymocyte nuclei containing 0, 1, and 2 peripheral *Tcrb* alleles

Cell type	n	Frequency of peripheral *Tcrb* alleles, p (%)	Experimental distribution (%)			Theoretical distribution (%)		
			Both alleles central	One allele central, one peripheral	Both alleles peripheral	Both alleles central	One allele central, one peripheral	Both alleles peripheral
						$(1-p)^2$	$2p(1-p)$	p^2
Ctcf$^{f/f}$ *Lck*-Cre^{-}	153	55.9	19	50.3	30.7	19.4	49.3	31.2
Ctcf$^{f/f}$ *Lck*-Cre^{+}	152	50.3	22.4	54.6	23	24.7	50.0	25.3

Statistics were performed by using Fisher's Exact Test to compare the observed frequency of events to the theoretical frequency of events. The number of nuclei analyzed in the observed distribution was also used as the number of nuclei analyzed in the theoretical distribution for the statistical comparison. Any observed value statistically different than the theoretical has been bolded.

Though we found no significant difference in the location of *Tcrb* alleles in the absence of CTCF, we observed a trend toward slightly fewer *Tcrb* alleles at the nuclear periphery in CTCF-deficient nuclei. If the analysis was repeated and more nuclei were analyzed, there may be a small, but significant, change in *Tcrb* localization without CTCF. Also, as we only assessed *Tcrb* localization in DP thymocytes, it would be interesting to evaluate positioning in DN thymocyte nuclei that lack CTCF.

7.3 Confirmation that positioning at the nuclear periphery is a mechanism by which Tcrb *recombination is suppressed*

Correlations between peripheral subnuclear positioning and less frequent V(D)J recombination of *Tcrb* alleles do not prove that subnuclear localization causes the

suppression of recombination. It is therefore important to formally demonstrate that positioning at the nuclear periphery is a mechanism by which recombination is suppressed. This could be shown by relocalizing an endogenous antigen receptor locus to the nuclear periphery. For example, if the centrally located *Tcra*/*Tcrd* locus were positioned at the nuclear periphery, we could ask whether this change reduces the frequency of *Tcra*/*Tcrd* recombination. We attempted this by generating a targeting construct that would insert 256 lactose operator (lacO) sequence repeats between the $V_{\alpha/\delta}$ array and the DJC cluster of the murine *Tcra*/*Tcrd* locus. As lacO is bound by the lactose repressor (lacI), genomic regions containing lacO repeats can be relocalized to the nuclear periphery in cells after transfection with a fusion protein containing lacI and a protein component of the inner nuclear membrane. The Duke Transgenic Facility was unable to successfully insert the lacO array into the *Tcra*/*Tcrd* locus using traditional homologous recombination techniques, likely due to the large number of repetitive sequence present in the construct. However if targeting had been successful, thymocytes containing the lacO repeats in the *Tcra*/*Tcrd* locus would have been relocated to the nuclear periphery in the presence of isopropyl β-D-1-thiogalactopyranoside (IPTG), which inhibits lacI from binding lacO. Following IPTG removal and peripheral relocalization, recombination frequency of the *Tcra*/*Tcrd* locus would have been assessed.

Using a different experimental technique, Beth Jones-Mason similarly attempted to assess the effect of peripheral localization on V(D)J recombination by building a reporter construct. The reporter construct contained (from 5′ to 3′) 128 lacO repeats, a selection cassette, a promoter, a red fluorescent protein (DsRed) gene, a recombination substrate, and a HS4 chicken beta-globin transcription insulator (HS4) (Fig. 34). The construct was transfected into a *Bcl2*-containing Abelson virus-transformed pre B cell line, and stable clones were transduced with a retrovirus encoding an enhanced green fluorescent protein and a lacI-emerin fusion protein. A preliminary immunoFISH analysis found that in the presence of IPTG ~6% of reporter construct foci were in contact with the nuclear laminB1, whereas that frequency increased to ~41% following IPTG withdrawal. This suggests that the recombination substrate is brought to the nuclear periphery upon IPTG removal.

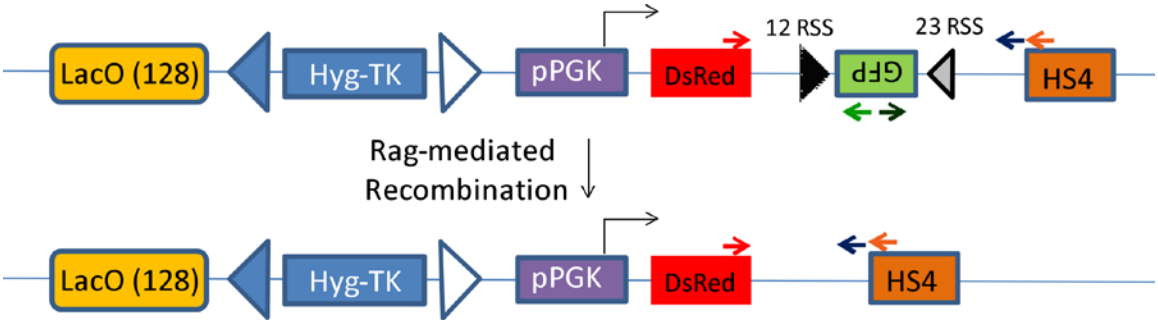

Figure 34: Diagram of the reporter construct used to test for rearrangement at the nuclear periphery

Recombination was induced by STI treatment, which stops Abelson cells from cycling and induces RAG expression (Muljo and Schlissel 2003). Recombination frequency was measured by PCR analysis of the loss of the region between DsRed and HS4. Though no difference in the frequency of substrate recombination between tethered and untethered constructs was found, many aspects of this experiment could differ from that of peripheral antigen receptor loci. For example, the genomic location in which the construct was inserted is unknown. It is possible that the recombination substrate ended up nearby a strong promoter that cannot be repressed by the nuclear periphery.

Many new techniques now exist that could potentially be used to relocate specific loci to the nuclear periphery. For example, zinc-finger (ZF) proteins and transcription activator-like effectors (TALE) (Carlson *et al.* 2012) are DNA-binding proteins that can be engineered to target nearly any DNA sequence. Currently, Shiwei Chen is using TALE-technology in an attempt to target the *Tcra*/*Tcrd* locus to the nuclear periphery. The TALE will be inserted into the genome as a tg, under control of a T-lineage specific promoter. The TALE will be fused to emerin, which should relocate the endogenous *Tcra*/*Tcrd* locus to the nuclear periphery. Thymocytes will be obtained from mice containing the tg, and 3D DNA immunoFISH analysis will be used to confirm

peripheral localization of the locus as well as determine whether the frequency of recombination is affected by positioning at the nuclear periphery.

7.4 To determine whether recombination is suppressed on Tcrb *alleles positioned at other repressive subnuclear compartments*

There may be additional subnuclear compartments that reduce the frequency of V(D)J recombination in thymocyte nuclei, such as PCH and CTs. *Tcrb* alleles are frequently located at PCH (Schlimgen *et al.* 2008), and it has been suggested that association with PCH plays a role in the maintenance of allelic exclusion at *Igh* loci (Roldan *et al.* 2005). It has been proposed that after pairing, recombination at the *Igh* allele that was not selected to undergo recombination is prevented by positioning at PCH. If positioning at PCH can suppress recombination at *Igh* alleles, it may also contribute to the asynchronous recombination of *Tcrb* alleles positioned at PCH in DN thymocytes. Therefore it would be interesting to perform an analysis of 53BP1^{+} *Tcrb* alleles positioned at PCH, similar to our examination of 53BP1^{+} *Tcrb* alleles located at the nuclear periphery.

The position of antigen receptor alleles relative to their CTs could function as an additional layer of V(D)J recombination regulation. Although we have conducted the CT analysis using 5′ *Tcrb* and *Tcra* probes, in order to draw conclusions from our findings, it would be necessary to reprise this analysis using 3′ probes.

7.5 Transcription and recombination of peripheral Tcrb *alleles*

We saw that most *Tcrb* alleles, regardless of their subnuclear location, colocalize with PolII. However this finding alone is insufficient to conclude that peripheral and central *Tcrb* alleles transcribe at similar levels. It is important to measure transcription levels, because if transcription is suppressed on peripheral *Tcrb* alleles reduced transcription and accessibility could be the mechanism by which recombination is suppressed. One way to evaluate transcription occurring on differentially-positioned *Tcrb* alleles would be to perform RNA FISH analysis on single-cells and quantify transcript abundance.

We demonstrated that *Tcrb* alleles are physically segregated from high concentrations of RAG2 when positioned at the nuclear periphery. However, additional mechanisms may also contribute to the suppression of *Tcrb* recombination at the nuclear periphery. For example, the exclusion of other components required for recombination, such as RAG1 or DSB repair factors, could also reduce recombination at the periphery.

It is possible that the subnuclear distribution of RAG1 also plays a role in regulating V(D)J recombination. We attempted to visualize RAG1 in developing thymocyte nuclei to ascertain if it is also excluded from the nuclear periphery. We were unsuccessful, which could be explained if RAG1 protein abundance is lower than RAG2 abundance in DN thymocyte nuclei. However, new highly sensitive technologies could

allow for the visualization of locations within the nucleus in which individual RAG1 and RAG2 proteins interact with each other and where in the nucleus a single RAG2 protein interacts with *Tcrb* alleles. One such technique is the *in situ* proximity ligation assay (PLA) (Leuchowius *et al.* 2011), which can detect, localize, and quantify single-molecules undergoing protein-protein and protein-DNA interactions. The PLA protocol uses antibodies to identify two molecules. If the two molecules are within 40 nm of each other, secondary antibodies conjugated to a unique short DNA strand will initiate a polymerase-mediated DNA amplification reaction. Fluorescently-labeled oligonucleotides, complementary to the amplified DNA, form foci at the site of the interaction.

7.6 Mechanism of RAG2 subnuclear localization

The mechanism dictating RAG2 subnuclear distribution has yet to be elucidated. While the distribution of RAG2 does not reflect that of H3K4me3 or PolII, we did not compare RAG2 to other known subnuclear compartments. Visualizing RAG2 and markers of nuclear speckles, Cajal bodies, gems, and promyelocytic leukaemia nuclear bodies could reveal whether RAG2 localizes to these subnuclear regions and potentially suggest additional functions of RAG2 in developing lymphocytes. Additionally, performing mass spectrometry on RAG2 after an antibody pull-down could identify

which proteins RAG2 is interacting with and potentially give clues as to where RAG2 localizes in developing B- and T-cell nuclei.

7.7 Conclusions

In closing, this dissertation expanded our understanding of V(D)J recombination events occurring in developing thymocyte nuclei. We demonstrated that recombination occurs in a stochastic manner, as no inhibition of recombination was observed in cells that contain a RAG-dependent DSB. Furthermore, we showed that positioning of *Tcrb* alleles at the nuclear periphery suppresses recombination, and that V_β-to-DJ_β recombination could be suppressed if either end of the locus was located at the periphery. Finally, we were able to put forth a model by which positioning at the nuclear periphery suppresses recombination. We propose that because endogenous RAG2 levels were reduced at the nuclear periphery in developing thymocyte nuclei and peripheral *Tcrb* alleles colocalized with RAG2 less frequently than central alleles, *Tcrb* alleles localize to the nuclear periphery in order to reduce their exposure to RAG2. This could serve to reduce the frequency of *Tcrb* recombination, and possibly support *Tcrb* allelic exclusion.

References

Abarrategui, I. and M. S. Krangel **Nat Immunol**. **2006**. 7; (10): 1109-1115. Regulation of T cell receptor-α gene recombination by transcription.

Abarrategui, I. and M. S. Krangel **EMBO J**. **2007**. 26; (20): 4380-4390. Noncoding transcription controls downstream promoters to regulate T-cell receptor α recombination.

Abarrategui, I. and M. S. Krangel **Adv Exp Med Biol**. **2009**. 650; 93-102. Germline transcription: a key regulator of accessibility and recombination.

Adolfsson, J., R. Mansson, N. Buza-Vidas, A. Hultquist, K. Liuba, C. T. Jensen, D. Bryder, L. Yang, O. J. Borge, L. A. Thoren, K. Anderson, E. Sitnicka, Y. Sasaki, M. Sigvardsson and S. E. Jacobsen **Cell**. **2005**. 121; (2): 295-306. Identification of $Flt3^+$ lympho-myeloid stem cells lacking erythro-megakaryocytic potential a revised road map for adult blood lineage commitment.

Afshar, R., S. Pierce, D. J. Bolland, A. Corcoran and E. M. Oltz **J Immunol**. **2006**. 176; (4): 2439-2447. Regulation of *Igh* gene assembly: role of the intronic enhancer and 5'DQ52 region in targeting D_HJ_H recombination.

Agata, Y., N. Tamaki, S. Sakamoto, T. Ikawa, K. Masuda, H. Kawamoto and C. Murre **Immunity**. **2007**. 27; (6): 871-884. Regulation of T cell receptor β gene rearrangements and allelic exclusion by the helix-loop-helix protein, E47.

Alam, S. M., I. N. Crispe and N. R. Gascoigne **Immunity**. **1995**. 3; (4): 449-458. Allelic exclusion of mouse T cell receptor α chains occurs at the time of thymocyte TCR up-regulation.

Allman, D. and S. Pillai **Curr Opin Immunol**. **2008**. 20; (2): 149-157. Peripheral B cell subsets.

Amin, R. H., D. Cado, H. Nolla, D. Huang, S. A. Shinton, Y. Zhou, R. R. Hardy and M. S. Schlissel **Proc Natl Acad Sci U S A**. **2009**. 106; (2): 522-527. Biallelic, ubiquitous transcription from the distal germline Igk locus promoter during B cell development.

Anderson, L., C. Henderson and Y. Adachi **Mol Cell Biol**. **2001**. 21; (5): 1719-1729. Phosphorylation and rapid relocalization of 53BP1 to nuclear foci upon DNA damage.

Asaithamby, A. and D. J. Chen **Nucleic Acids Res**. **2009**. 37; (12): 3912-3923. Cellular responses to DNA double-strand breaks after low-dose γ-irradiation.

Baker, J. E., D. Cado and D. H. Raulet **Immunity**. **1998**. 9; (2): 159-168. Developmentally programmed rearrangement of T cell receptor Vγ genes is controlled by sequences immediately upstream of the Vγ genes.

Balomenos, D., R. S. Balderas, K. P. Mulvany, J. Kaye, D. H. Kono and A. N. Theofilopoulos **J Immunol**. **1995**. 155; (7): 3308-3312. Incomplete T cell receptor Vβ allelic exclusion and dual Vβ-expressing cells.

Barlow, C., S. Hirotsune, R. Paylor, M. Liyanage, M. Eckhaus, F. Collins, Y. Shiloh, J. N. Crawley, T. Ried, D. Tagle and A. Wynshaw-Boris **Cell**. **1996**. 86; (1): 159-171. ATM-deficient mice: a paradigm of ataxia telangiectasia.

Bassing, C. H., F. W. Alt, M. M. Hughes, M. D'Auteuil, T. D. Wehrly, B. B. Woodman, F. Gartner, J. M. White, L. Davidson and B. P. Sleckman **Nature**. **2000**. 405; (6786): 583-586. Recombination signal sequences restrict chromosomal V(D)J recombination beyond the 12/23 rule.

Bednarski, J. J. and B. P. Sleckman **Cell Cycle**. **2012**. 11; (22): 4129-4134. Integrated signaling in developing lymphocytes: the role of DNA damage responses.

Bhandoola, A., H. von Boehmer, H. T. Petrie and J. C. Zuniga-Pflucker **Immunity**. **2007**. 26; (6): 678-689. Commitment and developmental potential of extrathymic and intrathymic T cell precursors: plenty to choose from.

Birshtein, B. K. **Front Genet**. **2012**. 3; 251. The role of CTCF binding sites in the 3' immunoglobulin heavy chain regulatory region.

Borgulya, P., H. Kishi, Y. Uematsu and H. von Boehmer **Cell**. **1992**. 69; (3): 529-537. Exclusion and inclusion of α and β T cell receptor alleles.

Bories, J. C., J. Demengeot, L. Davidson and F. W. Alt **Proc Natl Acad Sci U S A**. **1996**. 93; (15): 7871-7876. Gene-targeted deletion and replacement mutations of the T-cell

receptor β-chain enhancer: the role of enhancer elements in controlling V(D)J recombination accessibility.

Bossen, C., R. Mansson and C. Murre **Annu Rev Immunol**. **2012**. 30; 337-356. Chromatin topology and the regulation of antigen receptor assembly.

Bowen, S., D. Wangsa, T. Ried, F. Livak and R. J. Hodes **Nucleic Acids Res**. **2013**. 41; (8): 4535-4548. Concurrent V(D)J recombination and DNA end instability increase interchromosomal trans-rearrangements in ATM-deficient thymocytes.

Brady, B. L., N. C. Steinel and C. H. Bassing **J Immunol**. **2010**. 185; (7): 3801-3808. Antigen receptor allelic exclusion: an update and reappraisal.

Bredemeyer, A. L., G. G. Sharma, C. Y. Huang, B. A. Helmink, L. M. Walker, K. C. Khor, B. Nuskey, K. E. Sullivan, T. K. Pandita, C. H. Bassing and B. P. Sleckman **Nature**. **2006**. 442; (7101): 466-470. ATM stabilizes DNA double-strand-break complexes during V(D)J recombination.

Brekke, K. M. and W. T. Garrard **Immunogenetics**. **2004**. 56; (7): 490-505. Assembly and analysis of the mouse immunoglobulin κ gene sequence.

Brickner, D. G., S. Ahmed, L. Meldi, A. Thompson, W. Light, M. Young, T. L. Hickman, F. Chu, E. Fabre and J. H. Brickner **Dev Cell**. **2012**. 22; (6): 1234-1246. Transcription factor binding to a DNA zip code controls interchromosomal clustering at the nuclear periphery.

Bridger, J. M., N. Foeger, I. R. Kill and H. Herrmann **FEBS J**. **2007**. 274; (6): 1354-1361. The nuclear lamina. Both a structural framework and a platform for genome organization.

Brown, K. E., J. Baxter, D. Graf, M. Merkenschlager and A. G. Fisher **Mol Cell**. **1999**. 3; (2): 207-217. Dynamic repositioning of genes in the nucleus of lymphocytes preparing for cell division.

Brown, K. E., S. S. Guest, S. T. Smale, K. Hahm, M. Merkenschlager and A. G. Fisher **Cell**. **1997**. 91; (6): 845-854. Association of transcriptionally silent genes with Ikaros complexes at centromeric heterochromatin.

Buhler, M., W. Haas, S. P. Gygi and D. Moazed **Cell**. **2007**. 129; (4): 707-721. RNAi-dependent and -independent RNA turnover mechanisms contribute to heterochromatic gene silencing.

Busse, C. E., A. Krotkova and K. Eichmann **J Immunol**. **2005**. 175; (5): 3067-3074. The TCRβ enhancer is dispensable for the expression of rearranged TCRβ genes in thymic DN2/DN3 populations but not at later stages.

Caccia, N., M. Kronenberg, D. Saxe, R. Haars, G. A. Bruns, J. Goverman, M. Malissen, H. Willard, Y. Yoshikai, M. Simon and et al. **Cell**. **1984**. 37; (3): 1091-1099. The T cell receptor β chain genes are located on chromosome 6 in mice and chromosome 7 in humans.

Carabana, J., A. Watanabe, B. Hao and M. S. Krangel **J Immunol**. **2011**. 186; (6): 3556-3562. A barrier-type insulator forms a boundary between active and inactive chromatin at the murine TCRβ locus.

Carlson, D. F., S. C. Fahrenkrug and P. B. Hackett **Mol Ther Nucleic Acids**. **2012**. 1; e3. Targeting DNA With Fingers and TALENs.

Carpenter, A. C., K. S. Yang-Iott, L. H. Chao, B. Nuskey, S. Whitlow, F. W. Alt and C. H. Bassing **J Immunol**. **2009**. 182; (9): 5586-5595. Assembled DJβ complexes influence TCRβ chain selection and peripheral Vβ repertoire.

Carter, N. P. **Cytometry**. **1994**. 18; (1): 2-10. Cytogenetic analysis by chromosome painting.

Casanova, J. L., P. Romero, C. Widmann, P. Kourilsky and J. L. Maryanski **J Exp Med**. **1991**. 174; (6): 1371-1383. T cell receptor genes in a series of class I major histocompatibility complex-restricted cytotoxic T lymphocyte clones specific for a *Plasmodium berghei* nonapeptide: implications for T cell allelic exclusion and antigen-specific repertoire.

Casolari, J. M., C. R. Brown, S. Komili, J. West, H. Hieronymus and P. A. Silver **Cell**. **2004**. 117; (4): 427-439. Genome-wide localization of the nuclear transport machinery couples transcriptional status and nuclear organization.

Chakraborty, T., T. Perlot, R. Subrahmanyam, A. Jani, P. H. Goff, Y. Zhang, I. Ivanova, F. W. Alt and R. Sen **J Exp Med**. **2009**. 206; (5): 1019-1027. A 220-nucleotide deletion of the intronic enhancer reveals an epigenetic hierarchy in immunoglobulin heavy chain locus activation.

Chambeyron, S. and W. A. Bickmore **Genes Dev**. **2004**. 18; (10): 1119-1130. Chromatin decondensation and nuclear reorganization of the HoxB locus upon induction of transcription.

Chattopadhyay, S., C. E. Whitehurst, F. Schwenk and J. Chen **J Immunol**. **1998**. 160; (3): 1256-1267. Biochemical and functional analyses of chromatin changes at the TCR-β gene locus during $CD4^{-}CD8^{-}$ to $CD4^{+}CD8^{+}$ thymocyte differentiation.

Chaumeil, J., M. Micsinai, P. Ntziachristos, L. Deriano, J. M. Wang, Y. Ji, E. P. Nora, M. J. Rodesch, J. A. Jeddeloh, I. Aifantis, Y. Kluger, D. G. Schatz and J. A. Skok **Cell Rep**. **2013**. 3; (2): 359-370. Higher-order looping and nuclear organization of *Tcra* facilitate targeted Rag cleavage and regulated rearrangement in recombination centers.

Chen, B. P., N. Uematsu, J. Kobayashi, Y. Lerenthal, A. Krempler, H. Yajima, M. Lobrich, Y. Shiloh and D. J. Chen **J Biol Chem**. **2007**. 282; (9): 6582-6587. Ataxia telangiectasia mutated (ATM) is essential for DNA-PKcs phosphorylations at the Thr-2609 cluster upon DNA double strand break.

Chen, H. T., A. Bhandoola, M. J. Difilippantonio, J. Zhu, M. J. Brown, X. Tai, E. P. Rogakou, T. M. Brotz, W. M. Bonner, T. Ried and A. Nussenzweig **Science**. **2000**. 290; (5498): 1962-1965. Response to RAG-mediated VDJ cleavage by NBS1 and γ-H2AX.

Cheung, A. Y. and A. S. Reddy **Plant Physiol**. **2012**. 158; (1): 23-25. Nuclear architecture and dynamics: territories, nuclear bodies, and nucleocytoplasmic trafficking.

Chinenov, Y. and T. K. Kerppola **Oncogene**. **2001**. 20; (19): 2438-2452. Close encounters of many kinds: Fos-Jun interactions that mediate transcription regulatory specificity.

Chowdhury, D. and R. Sen **Immunity**. **2003**. 18; (2): 229-241. Transient IL-7/IL-7R signaling provides a mechanism for feedback inhibition of immunoglobulin heavy chain gene rearrangements.

Cisse, II, I. Izeddin, S. Z. Causse, L. Boudarene, A. Senecal, L. Muresan, C. Dugast-Darzacq, B. Hajj, M. Dahan and X. Darzacq **Science**. **2013**. 341; (6146): 664-667. Real-time dynamics of RNA polymerase II clustering in live human cells.

Clements, L., S. Manilal, D. R. Love and G. E. Morris **Biochem Biophys Res Commun**. **2000**. 267; (3): 709-714. Direct interaction between emerin and lamin A.

Cobb, R. M., K. J. Oestreich, O. A. Osipovich and E. M. Oltz **Adv Immunol**. **2006**. 91; 45-109. Accessibility control of V(D)J recombination.

Cook, P. R. **J Mol Biol**. **2010**. 395; (1): 1-10. A model for all genomes: the role of transcription factories.

Corneo, B., R. L. Wendland, L. Deriano, X. Cui, I. A. Klein, S. Y. Wong, S. Arnal, A. J. Holub, G. R. Weller, B. A. Pancake, S. Shah, V. L. Brandt, K. Meek and D. B. Roth **Nature**. **2007**. 449; (7161): 483-486. Rag mutations reveal robust alternative end joining.

Cortelli, P., R. Terlizzi, S. Capellari and E. Benarroch **Neurology**. **2012**. 79; (16): 1726-1731. Nuclear lamins: functions and clinical implications.

Cosgrove, D., S. H. Chan, C. Waltzinger, C. Benoist and D. Mathis **Int Immunol**. **1992**. 4; (6): 707-710. The thymic compartment responsible for positive selection of $CD4^+$ T cells.

Coster, G., A. Gold, D. Chen, D. G. Schatz and M. Goldberg **J Biol Chem**. **2012**. 287; (43): 36488-36498. A dual interaction between the DNA damage response protein MDC1 and the RAG1 subunit of the V(D)J recombinase.

Couez, D., M. Malissen, M. Buferne, A. M. Schmitt-Verhulst and B. Malissen **Int Immunol**. **1991**. 3; (7): 719-729. Each of the two productive T cell receptor α-gene rearrangements found in both the A10 and BM 3.3 T cell clones give rise to an α chain which can contribute to the constitution of a surface-expressed $\alpha\beta$ dimer.

Coussens, M. A., R. L. Wendland, L. Deriano, C. R. Lindsay, S. M. Arnal and D. B. Roth **Cell Rep**. **2013**. 4; (5): 870-878. RAG2's acidic hinge restricts repair-pathway choice and promotes genomic stability.

Cremer, T., M. Cremer, S. Dietzel, S. Muller, I. Solovei and S. Fakan **Curr Opin Cell Biol**. **2006**. 18; (3): 307-316. Chromosome territories--a functional nuclear landscape.

Cui, X. and K. Meek **Proc Natl Acad Sci U S A**. **2007**. 104; (43): 17046-17051. Linking double-stranded DNA breaks to the recombination activating gene complex directs repair to the nonhomologous end-joining pathway.

Curry, J. D., J. K. Geier and M. S. Schlissel **Nat Immunol**. **2005**. 6; (12): 1272-1279. Single-strand recombination signal sequence nicks *in vivo*: evidence for a capture model of synapsis.

Daley, J. M., Y. Kwon, H. Niu and P. Sung **Yale J Biol Med**. **2013**. 86; (4): 453-461. Investigations of Homologous Recombination Pathways and Their Regulation.

Degner, S. C., J. Verma-Gaur, T. P. Wong, C. Bossen, G. M. Iverson, A. Torkamani, C. Vettermann, Y. C. Lin, Z. Ju, D. Schulz, C. S. Murre, B. K. Birshtein, N. J. Schork, M. S. Schlissel, R. Riblet, C. Murre and A. J. Feeney **Proc Natl Acad Sci U S A**. **2011**. 108; (23): 9566-9571. CCCTC-binding factor (CTCF) and cohesin influence the genomic architecture of the *Igh* locus and antisense transcription in pro-B cells.

Dudley, D. D., J. Sekiguchi, C. Zhu, M. J. Sadofsky, S. Whitlow, J. DeVido, R. J. Monroe, C. H. Bassing and F. W. Alt **J Exp Med**. **2003**. 198; (9): 1439-1450. Impaired V(D)J recombination and lymphocyte development in core RAG1-expressing mice.

Ebert, A., S. McManus, H. Tagoh, J. Medvedovic, G. Salvagiotto, M. Novatchkova, I. Tamir, A. Sommer, M. Jaritz and M. Busslinger **Immunity**. **2011**. 34; (2): 175-187. The distal V(H) gene cluster of the *Igh* locus contains distinct regulatory elements with Pax5 transcription factor-dependent activity in pro-B cells.

Eccles, S., N. Sarner, M. Vidal, A. Cox and F. Grosveld **New Biol**. **1990**. 2; (9): 801-811. Enhancer sequences located 3' of the mouse immunoglobulin λ locus specify high-level expression of an immunoglobulin λ gene in B cells of transgenic mice.

Edry, E. and D. Melamed **J Immunol**. **2004**. 173; (7): 4265-4271. Receptor editing in positive and negative selection of B lymphopoiesis.

Elkin, S. K., D. Ivanov, M. Ewalt, C. G. Ferguson, S. G. Hyberts, Z. Y. Sun, G. D. Prestwich, J. Yuan, G. Wagner, M. A. Oettinger and O. P. Gozani **J Biol Chem**. **2005**. 280; (31): 28701-28710. A PHD finger motif in the C terminus of RAG2 modulates recombination activity.

Engel, H., A. Rolink and S. Weiss **Eur J Immunol**. **1999**. 29; (7): 2167-2176. B cells are programmed to activate κ and λ for rearrangement at consecutive developmental stages.

Eyquem, S., K. Chemin, M. Fasseu and J. C. Bories **Proc Natl Acad Sci U S A**. **2004**. 101; (44): 15712-15717. The Ets-1 transcription factor is required for complete pre-T cell receptor function and allelic exclusion at the T cell receptor β locus.

Farago, M., C. Rosenbluh, M. Tevlin, S. Fraenkel, S. Schlesinger, H. Masika, M. Gouzman, G. Teng, D. Schatz, Y. Rais, J. H. Hanna, A. Mildner, S. Jung, G. Mostoslavsky, H. Cedar and Y. Bergman **Nature**. **2012**. 490; (7421): 561-565. Clonal allelic predetermination of immunoglobulin-κ rearrangement.

Felsenfeld, G., D. Clark and V. Studitsky **Biophys Chem**. **2000**. 86; (2-3): 231-237. Transcription through nucleosomes.

Ferrai, C., S. Q. Xie, P. Luraghi, D. Munari, F. Ramirez, M. R. Branco, A. Pombo and M. P. Crippa **PLoS Biol**. **2010**. 8; (1): e1000270. Poised transcription factories prime silent uPA gene prior to activation.

Finlan, L. E., D. Sproul, I. Thomson, S. Boyle, E. Kerr, P. Perry, B. Ylstra, J. R. Chubb and W. A. Bickmore **PLoS Genet**. **2008**. 4; (3): e1000039. Recruitment to the nuclear periphery can alter expression of genes in human cells.

Fitzsimmons, S. P., R. M. Bernstein, E. E. Max, J. A. Skok and M. A. Shapiro **J Immunol**. **2007**. 179; (8): 5264-5273. Dynamic changes in accessibility, nuclear positioning, recombination, and transcription at the Igκ locus.

Fuxa, M., J. Skok, A. Souabni, G. Salvagiotto, E. Roldan and M. Busslinger **Genes Dev**. **2004**. 18; (4): 411-422. Pax5 induces V-to-DJ rearrangements and locus contraction of the immunoglobulin heavy-chain gene.

Gallinari, P., S. Di Marco, P. Jones, M. Pallaoro and C. Steinkuhler **Cell Res**. **2007**. 17; (3): 195-211. HDACs, histone deacetylation and gene transcription: from molecular biology to cancer therapeutics.

Gant, T. M., C. A. Harris and K. L. Wilson **J Cell Biol**. **1999**. 144; (6): 1083-1096. Roles of LAP2 proteins in nuclear assembly and DNA replication: truncated LAP2β proteins alter

lamina assembly, envelope formation, nuclear size, and DNA replication efficiency in Xenopus laevis extracts.

Garrett, F. E., A. V. Emelyanov, M. A. Sepulveda, P. Flanagan, S. Volpi, F. Li, D. Loukinov, L. A. Eckhardt, V. V. Lobanenkov and B. K. Birshtein **Mol Cell Biol**. **2005**. 25; (4): 1511-1525. Chromatin architecture near a potential 3' end of the *Igh* locus involves modular regulation of histone modifications during B-cell development and in vivo occupancy at CTCF sites.

Gascoigne, N. R. and S. M. Alam **Semin Immunol**. **1999**. 11; (5): 337-347. Allelic exclusion of the T cell receptor α-chain: developmental regulation of a post-translational event.

Gellert, M. **Annu Rev Biochem**. **2002**. 71; 101-132. V(D)J recombination: RAG proteins, repair factors, and regulation.

Gerace, L. and M. D. Huber **J Struct Biol**. **2012**. 177; (1): 24-31. Nuclear lamina at the crossroads of the cytoplasm and nucleus.

Ghamari, A., M. P. van de Corput, S. Thongjuea, W. A. van Cappellen, W. van Ijcken, J. van Haren, E. Soler, D. Eick, B. Lenhard and F. G. Grosveld **Genes Dev**. **2013**. 27; (7): 767-777. *In vivo* live imaging of RNA polymerase II transcription factories in primary cells.

Giallourakis, C. C., A. Franklin, C. Guo, H. L. Cheng, H. S. Yoon, M. Gallagher, T. Perlot, M. Andzelm, A. J. Murphy, L. E. Macdonald, G. D. Yancopoulos and F. W. Alt **Proc Natl Acad Sci U S A**. **2010**. 107; (51): 22207-22212. Elements between the *Igh* variable (V) and diversity (D) clusters influence antisense transcription and lineage-specific V(D)J recombination.

Godfrey, D. I. and A. Zlotnik **Immunol Today**. **1993**. 14; (11): 547-553. Control points in early T-cell development.

Goldman, R. D., Y. Gruenbaum, R. D. Moir, D. K. Shumaker and T. P. Spann **Genes Dev**. **2002**. 16; (5): 533-547. Nuclear lamins: building blocks of nuclear architecture.

Goldmit, M. and Y. Bergman **Immunol Rev**. **2004**. 200; 197-214. Monoallelic gene expression: a repertoire of recurrent themes.

Goldmit, M., Y. Ji, J. Skok, E. Roldan, S. Jung, H. Cedar and Y. Bergman **Nat Immunol**. **2005**. 6; (2): 198-203. Epigenetic ontogeny of the *Igk* locus during B cell development.

Gonzalez-Garcia, S., M. Garcia-Peydro, J. Alcain and M. L. Toribio **Curr Top Microbiol Immunol**. **2012**. 360; 47-73. Notch1 and IL-7 receptor signalling in early T-cell development and leukaemia.

Goodarzi, A. A. and P. A. Jeggo **Adv Genet**. **2013**. 82; 1-45. The repair and signaling responses to DNA double-strand breaks.

Gorman, J. R., N. van der Stoep, R. Monroe, M. Cogne, L. Davidson and F. W. Alt **Immunity**. **1996**. 5; (3): 241-252. The *Igk* enhancer influences the ratio of *Igk* versus *Igl* B lymphocytes.

Greil, F., C. Moorman and B. van Steensel **Methods Enzymol**. **2006**. 410; 342-359. DamID: mapping of *in vivo* protein-genome interactions using tethered DNA adenine methyltransferase.

Grewal, S. I. and D. Moazed **Science**. **2003**. 301; (5634): 798-802. Heterochromatin and epigenetic control of gene expression.

Grundy, G. J., S. Ramon-Maiques, E. K. Dimitriadis, S. Kotova, C. Biertumpfel, J. B. Heymann, A. C. Steven, M. Gellert and W. Yang **Mol Cell**. **2009**. 35; (2): 217-227. Initial stages of V(D)J recombination: the organization of RAG1/2 and RSS DNA in the postcleavage complex.

Gubitz, A. K., W. Feng and G. Dreyfuss **Exp Cell Res**. **2004**. 296; (1): 51-56. The SMN complex.

Guelen, L., L. Pagie, E. Brasset, W. Meuleman, M. B. Faza, W. Talhout, B. H. Eussen, A. de Klein, L. Wessels, W. de Laat and B. van Steensel **Nature**. **2008**. 453; (7197): 948-951. Domain organization of human chromosomes revealed by mapping of nuclear lamina interactions.

Guenatri, M., D. Bailly, C. Maison and G. Almouzni **J Cell Biol**. **2004**. 166; (4): 493-505. Mouse centric and pericentric satellite repeats form distinct functional heterochromatin.

Guo, C., T. Gerasimova, H. Hao, I. Ivanova, T. Chakraborty, R. Selimyan, E. M. Oltz and R. Sen **Cell**. **2011**. 147; (2): 332-343. Two forms of loops generate the chromatin conformation of the immunoglobulin heavy-chain gene locus.

Guo, C., H. S. Yoon, A. Franklin, S. Jain, A. Ebert, H. L. Cheng, E. Hansen, O. Despo, C. Bossen, C. Vettermann, J. G. Bates, N. Richards, D. Myers, H. Patel, M. Gallagher, M. S. Schlissel, C. Murre, M. Busslinger, C. C. Giallourakis and F. W. Alt **Nature**. **2011**. 477; (7365): 424-430. CTCF-binding elements mediate control of V(D)J recombination.

Hagman, J., C. M. Rudin, D. Haasch, D. Chaplin and U. Storb **Genes Dev**. **1990**. 4; (6): 978-992. A novel enhancer in the immunoglobulin λ locus is duplicated and functionally independent of NFκB.

Hampsey, M., B. N. Singh, A. Ansari, J. P. Laine and S. Krishnamurthy **Adv Enzyme Regul**. **2011**. 51; (1): 118-125. Control of eukaryotic gene expression: gene loops and transcriptional memory.

Hao, B. and M. S. Krangel **J Immunol**. **2011**. 187; (5): 2484-2491. Long-distance regulation of fetal Vδ gene segment TRDV4 by the *Tcrd* enhancer.

Haralick, R. M. and L. G. Shapiro (1992). Computer and robot vision. Reading, Mass., Addison-Wesley Pub. Co.

Hawwari, A. and M. S. Krangel **J Exp Med**. **2005**. 202; (4): 467-472. Regulation of TCRδ and α repertoires by local and long-distance control of variable gene segment chromatin structure.

Heath, H., C. Ribeiro de Almeida, F. Sleutels, G. Dingjan, S. van de Nobelen, I. Jonkers, K. W. Ling, J. Gribnau, R. Renkawitz, F. Grosveld, R. W. Hendriks and N. Galjart **EMBO J**. **2008**. 27; (21): 2839-2850. CTCF regulates cell cycle progression of $\alpha\beta$ T cells in the thymus.

Helmink, B. A. and B. P. Sleckman **Annu Rev Immunol**. **2012**. 30; 175-202. The response to and repair of RAG-mediated DNA double-strand breaks.

Helmink, B. A., A. T. Tubbs, Y. Dorsett, J. J. Bednarski, L. M. Walker, Z. Feng, G. G. Sharma, P. J. McKinnon, J. Zhang, C. H. Bassing and B. P. Sleckman **Nature**. **2011**. 469;

(7329): 245-249. H2AX prevents CtIP-mediated DNA end resection and aberrant repair in G1-phase lymphocytes.
Hernandez-Munain, C., B. P. Sleckman and M. S. Krangel **Immunity**. **1999**. 10; (6): 723-733. A developmental switch from TCRδ enhancer to TCR*α* enhancer function during thymocyte maturation.

Hesslein, D. G. and D. G. Schatz **Adv Immunol**. **2001**. 78; 169-232. Factors and forces controlling V(D)J recombination.

Hewitt, S. L., D. Farmer, K. Marszalek, E. Cadera, H. E. Liang, Y. Xu, M. S. Schlissel and J. A. Skok **Nat Immunol**. **2008**. 9; (4): 396-404. Association between the *Igk* and *Igh* immunoglobulin loci mediated by the 3' *Igk* enhancer induces 'decontraction' of the *Igh* locus in pre-B cells.

Hewitt, S. L., F. A. High, S. L. Reiner, A. G. Fisher and M. Merkenschlager **Eur J Immunol**. **2004**. 34; (12): 3604-3613. Nuclear repositioning marks the selective exclusion of lineage-inappropriate transcription factor loci during T helper cell differentiation.

Hewitt, S. L., B. Yin, Y. Ji, J. Chaumeil, K. Marszalek, J. Tenthorey, G. Salvagiotto, N. Steinel, L. B. Ramsey, J. Ghysdael, M. A. Farrar, B. P. Sleckman, D. G. Schatz, M. Busslinger, C. H. Bassing and J. A. Skok **Nat Immunol**. **2009**. 10; (6): 655-664. RAG-1 and ATM coordinate monoallelic recombination and nuclear positioning of immunoglobulin loci.

Hiom, K. and M. Gellert **Mol Cell**. **1998**. 1; (7): 1011-1019. Assembly of a 12/23 paired signal complex: a critical control point in V(D)J recombination.

Ho, A. D. and W. Wagner **Curr Opin Hematol**. **2007**. 14; (4): 330-336. The beauty of asymmetry: asymmetric divisions and self-renewal in the haematopoietic system.

Hoeijmakers, J. H. **Nature**. **2001**. 411; (6835): 366-374. Genome maintenance mechanisms for preventing cancer.

Honjo, T., F. W. Alt and M. S. Neuberger (2004). Molecular biology of B cells. Amsterdam ; Boston, Elsevier.

Huesmann, M., B. Scott, P. Kisielow and H. von Boehmer **Cell**. **1991**. 66; (3): 533-540. Kinetics and efficacy of positive selection in the thymus of normal and T cell receptor transgenic mice.

Iborra, F. J., A. Pombo, D. A. Jackson and P. R. Cook **J Cell Sci**. **1996**. 109 (Pt 6); 1427-1436. Active RNA polymerases are localized within discrete transcription "factories' in human nuclei.

Ichii, M., T. Shimazu, R. S. Welner, K. P. Garrett, Q. Zhang, B. L. Esplin and P. W. Kincade **Immunol Rev**. **2010**. 237; (1): 10-21. Functional diversity of stem and progenitor cells with B-lymphopoietic potential.

Iliev, A., L. Spatz, S. Ray and B. Diamond **J Immunol**. **1994**. 153; (8): 3551-3556. Lack of allelic exclusion permits autoreactive B cells to escape deletion.

Inlay, M., F. W. Alt, D. Baltimore and Y. Xu **Nat Immunol**. **2002**. 3; (5): 463-468. Essential roles of the κ light chain intronic enhancer and 3' enhancer in κ rearrangement and demethylation.

Jackson, A., H. D. Kondilis, B. Khor, B. P. Sleckman and M. S. Krangel **Nat Immunol**. **2005**. 6; (2): 189-197. Regulation of T cell receptor β allelic exclusion at a level beyond accessibility.

Jackson, A. M. and M. S. Krangel **Immunol Rev**. **2006**. 209; 129-141. Turning T-cell receptor β recombination on and off: more questions than answers.

Janeway, C. (2005). Immunobiology : the immune system in health and disease. New York, Garland Science.

Jhunjhunwala, S., M. C. van Zelm, M. M. Peak, S. Cutchin, R. Riblet, J. J. van Dongen, F. G. Grosveld, T. A. Knoch and C. Murre **Cell**. **2008**. 133; (2): 265-279. The 3D structure of the immunoglobulin heavy-chain locus: implications for long-range genomic interactions.

Ji, Y., W. Resch, E. Corbett, A. Yamane, R. Casellas and D. G. Schatz **Cell**. **2010**. 141; (3): 419-431. The in vivo pattern of binding of RAG1 and RAG2 to antigen receptor loci.

Jia, J., M. Kondo and Y. Zhuang **EMBO J**. **2007**. 26; (9): 2387-2399. Germline transcription from T-cell receptor Vβ gene is uncoupled from allelic exclusion.

Johnston, C. M., A. L. Wood, D. J. Bolland and A. E. Corcoran **J Immunol**. **2006**. 176; (7): 4221-4234. Complete sequence assembly and characterization of the C57BL/6 mouse *Ig* heavy chain V region.

Jones, J. M. and M. Gellert **Immunol Rev**. **2004**. 200; 233-248. The taming of a transposon: V(D)J recombination and the immune system.

Jung, D., C. Giallourakis, R. Mostoslavsky and F. W. Alt **Annu Rev Immunol**. **2006**. 24; 541-570. Mechanism and control of V(D)J recombination at the immunoglobulin heavy chain locus.

Kalhor, R., H. Tjong, N. Jayathilaka, F. Alber and L. Chen **Nat Biotechnol**. **2012**. 30; (1): 90-98. Genome architectures revealed by tethered chromosome conformation capture and population-based modeling.

Kato, T. A., H. Nagasawa, M. M. Weil, P. C. Genik, J. B. Little and J. S. Bedford **Radiat Res**. **2006**. 166; (1 Pt 1): 47-54. γ-H2AX foci after low-dose-rate irradiation reveal ATM haploinsufficiency in mice.

Khanna, K. K. and S. P. Jackson **Nat Genet**. **2001**. 27; (3): 247-254. DNA double-strand breaks: signaling, repair and the cancer connection.

Khor, B. and B. P. Sleckman **Curr Opin Immunol**. **2002**. 14; (2): 230-234. Allelic exclusion at the TCRβ locus.

Kind, J., L. Pagie, H. Ortabozkoyun, S. Boyle, S. S. de Vries, H. Janssen, M. Amendola, L. D. Nolen, W. A. Bickmore and B. van Steensel **Cell**. **2013**. 153; (1): 178-192. Single-cell dynamics of genome-nuclear lamina interactions.

Kisielow, P., H. Bluthmann, U. D. Staerz, M. Steinmetz and H. von Boehmer **Nature**. **1988**. 333; (6175): 742-746. Tolerance in T-cell-receptor transgenic mice involves deletion of nonmature $CD4^{+}8^{+}$ thymocytes.

Kitamura, D., J. Roes, R. Kuhn and K. Rajewsky **Nature**. **1991**. 350; (6317): 423-426. A B cell-deficient mouse by targeted disruption of the membrane exon of the immunoglobulin μ chain gene.

Kondilis-Mangum, H. D., R. M. Cobb, O. Osipovich, S. Srivatsan, E. M. Oltz and M. S. Krangel **J Immunol**. **2010**. 184; (12): 6970-6977. Transcription-dependent mobilization of nucleosomes at accessible TCR gene segments *in vivo*.

Kondilis-Mangum, H. D., H. Y. Shih, G. Mahowald, B. P. Sleckman and M. S. Krangel **J Immunol**. **2011**. 187; (12): 6374-6381. Regulation of TCRβ allelic exclusion by gene segment proximity and accessibility.

Kornberg, R. D. **Proc Natl Acad Sci U S A**. **2007**. 104; (32): 12955-12961. The molecular basis of eukaryotic transcription.

Kosak, S. T., J. A. Skok, K. L. Medina, R. Riblet, M. M. Le Beau, A. G. Fisher and H. Singh **Science**. **2002**. 296; (5565): 158-162. Subnuclear compartmentalization of immunoglobulin loci during lymphocyte development.

Kouzarides, T. **Cell**. **2007**. 128; (4): 693-705. Chromatin modifications and their function.

Krangel, M. S. **Nat Immunol**. **2007**. 8; (7): 687-694. T cell development: better living through chromatin.

Krangel, M. S. **Curr Opin Immunol**. **2009**. 21; (2): 133-139. Mechanics of T cell receptor gene rearrangement.

Krangel, M. S., J. Carabana, I. Abbarategui, R. Schlimgen and A. Hawwari **Immunol Rev**. **2004**. 200; 224-232. Enforcing order within a complex locus: current perspectives on the control of V(D)J recombination at the murine T-cell receptor α/δlocus.

Kranz, D. M., H. Saito, C. M. Disteche, K. Swisshelm, D. Pravtcheva, F. H. Ruddle, H. N. Eisen and S. Tonegawa **Science**. **1985**. 227; (4689): 941-945. Chromosomal locations of the murine T-cell receptor α-chain gene and the T-cell γ gene.

Kreslavsky, T., M. Gleimer, A. I. Garbe and H. von Boehmer **Immunol Rev**. **2010**. 238; (1): 169-181. αβ versus γδ fate choice: counting the T-cell lineages at the branch point.

Kubbutat, M. H., G. Key, M. Duchrow, C. Schluter, H. D. Flad and J. Gerdes **J Clin Pathol**. **1994**. 47; (6): 524-528. Epitope analysis of antibodies recognising the cell proliferation associated nuclear antigen previously defined by the antibody Ki-67 (Ki-67 protein).

Kuida, K., M. Furutani-Seiki, T. Saito, H. Kishimoto, K. Sano and T. Tada **Int Immunol**. **1991**. 3; (1): 75-82. Post-translational attainment of allelic exclusion of the T cell receptor α chain in a T cell clone.

Kumaran, R. I. and D. L. Spector **J Cell Biol**. **2008**. 180; (1): 51-65. A genetic locus targeted to the nuclear periphery in living cells maintains its transcriptional competence.

Kuo, T. C. and M. S. Schlissel **Curr Opin Immunol**. **2009**. 21; (2): 173-178. Mechanisms controlling expression of the RAG locus during lymphocyte development.

Lande-Diner, L., J. Zhang and H. Cedar **Mol Cell**. **2009**. 34; (6): 767-774. Shifts in replication timing actively affect histone acetylation during nucleosome reassembly.

Landree, M. A., J. A. Wibbenmeyer and D. B. Roth **Genes Dev**. **1999**. 13; (23): 3059-3069. Mutational analysis of RAG1 and RAG2 identifies three catalytic amino acids in RAG1 critical for both cleavage steps of V(D)J recombination.

Leduc, I., W. M. Hempel, N. Mathieu, C. Verthuy, G. Bouvier, F. Watrin and P. Ferrier **J Immunol**. **2000**. 165; (3): 1364-1373. T cell development in TCR β enhancer-deleted mice: implications for $\alpha\beta$ T cell lineage commitment and differentiation.

Lees-Miller, S. P. and K. Meek **Biochimie**. **2003**. 85; (11): 1161-1173. Repair of DNA double strand breaks by non-homologous end joining.

Leuchowius, K. J., I. Weibrecht and O. Soderberg **Curr Protoc Cytom**. **2011**. Chapter 9; Unit 9 36. *In situ* proximity ligation assay for microscopy and flow cytometry.

Lewis, J. D., R. R. Meehan, W. J. Henzel, I. Maurer-Fogy, P. Jeppesen, F. Klein and A. Bird **Cell**. **1992**. 69; (6): 905-914. Purification, sequence, and cellular localization of a novel chromosomal protein that binds to methylated DNA.

Li, B. and T. de Lange **Mol Biol Cell**. **2003**. 14; (12): 5060-5068. Rap1 affects the length and heterogeneity of human telomeres.

Li, X. and W. D. Heyer **Cell Res**. **2008**. 18; (1): 99-113. Homologous recombination in DNA repair and DNA damage tolerance.

Li, Z., D. I. Dordai, J. Lee and S. Desiderio **Immunity**. **1996**. 5; (6): 575-589. A conserved degradation signal regulates RAG-2 accumulation during cell division and links V(D)J recombination to the cell cycle.

Liang, H. E., L. Y. Hsu, D. Cado, L. G. Cowell, G. Kelsoe and M. S. Schlissel **Immunity**. **2002**. 17; (5): 639-651. The "dispensable" portion of RAG2 is necessary for efficient V-to-DJ rearrangement during B and T cell development.

Lieber, M. R. **Annu Rev Biochem**. **2010**. 79; 181-211. The mechanism of double-strand DNA break repair by the nonhomologous DNA end-joining pathway.

Lin, W. C. and S. Desiderio **Science**. **1993**. 260; (5110): 953-959. Regulation of V(D)J recombination activator protein RAG-2 by phosphorylation.

Lin, Y. C. and C. Murre **Curr Opin Genet Dev**. **2013**. 23; (2): 104-108. Nuclear location and the control of developmental progression.

Liu, H., M. Schmidt-Supprian, Y. Shi, E. Hobeika, N. Barteneva, H. Jumaa, R. Pelanda, M. Reth, J. Skok, K. Rajewsky and Y. Shi **Genes Dev**. **2007**. 21; (10): 1179-1189. Yin Yang 1 is a critical regulator of B-cell development.

Liu, Y., R. Subrahmanyam, T. Chakraborty, R. Sen and S. Desiderio **Immunity**. **2007**. 27; (4): 561-571. A plant homeodomain in RAG-2 that binds hypermethylated lysine 4 of histone H3 is necessary for efficient antigen-receptor-gene rearrangement.

Liu, Z. M., J. B. George-Raizen, S. Li, K. C. Meyers, M. Y. Chang and W. T. Garrard **J Biol Chem**. **2002**. 277; (36): 32640-32649. Chromatin structural analyses of the mouse Igκ gene locus reveal new hypersensitive sites specifying a transcriptional silencer and enhancer.

Livak, F., M. Tourigny, D. G. Schatz and H. T. Petrie **J Immunol**. **1999**. 162; (5): 2575-2580. Characterization of TCR gene rearrangements during adult murine T cell development.

Lo, W. L. and P. M. Allen **Mol Immunol**. **2013**. 55; (2): 186-189. Self-awareness: how self-peptide/MHC complexes are essential in the development of T cells.

Lombardi, M. L., D. E. Jaalouk, C. M. Shanahan, B. Burke, K. J. Roux and J. Lammerding **J Biol Chem**. **2011**. 286; (30): 26743-26753. The interaction between nesprins and sun proteins at the nuclear envelope is critical for force transmission between the nucleus and cytoskeleton.

Lomberk, G., L. Wallrath and R. Urrutia **Genome Biol**. **2006**. 7; (7): 228. The Heterochromatin Protein 1 family.

Lukas, J., C. Lukas and J. Bartek **Nat Cell Biol**. **2011**. 13; (10): 1161-1169. More than just a focus: The chromatin response to DNA damage and its role in genome integrity maintenance.

Malissen, M., J. Trucy, E. Jouvin-Marche, P. A. Cazenave, R. Scollay and B. Malissen **Immunol Today**. **1992**. 13; (8): 315-322. Regulation of TCR α and β gene allelic exclusion during T-cell development.

Malissen, M., J. Trucy, F. Letourneur, N. Rebai, D. E. Dunn, F. W. Fitch, L. Hood and B. Malissen **Cell**. **1988**. 55; (1): 49-59. A T cell clone expresses two T cell receptor α genes but uses one $\alpha\beta$ heterodimer for allorecognition and self MHC-restricted antigen recognition.

Malu, S., V. Malshetty, D. Francis and P. Cortes **Immunol Res**. **2012**. 54; (1-3): 233-246. Role of non-homologous end joining in V(D)J recombination.

Martins, V. C., E. Ruggiero, S. M. Schlenner, V. Madan, M. Schmidt, P. J. Fink, C. von Kalle and H. R. Rodewald **J Exp Med**. **2012**. 209; (8): 1409-1417. Thymus-autonomous T cell development in the absence of progenitor import.

Mathieu, N., S. Spicuglia, S. Gorbatch, O. Cabaud, C. Fernex, C. Verthuy, W. M. Hempel, A. O. Hueber and P. Ferrier **J Biol Chem**. **2003**. 278; (20): 18101-18109. Assessing the role of the T cell receptor β gene enhancer in regulating coding joint formation during V(D)J recombination.

Matthews, A. G., A. J. Kuo, S. Ramon-Maiques, S. Han, K. S. Champagne, D. Ivanov, M. Gallardo, D. Carney, P. Cheung, D. N. Ciccone, K. L. Walter, P. J. Utz, Y. Shi, T. G. Kutateladze, W. Yang, O. Gozani and M. A. Oettinger **Nature**. **2007**. 450; (7172): 1106-1110. RAG2 PHD finger couples histone H3 lysine 4 trimethylation with V(D)J recombination.

Maul, R. W. and P. J. Gearhart **Adv Immunol**. **2010**. 105; 159-191. AID and somatic hypermutation.

McBlane, J. F., D. C. van Gent, D. A. Ramsden, C. Romeo, C. A. Cuomo, M. Gellert and M. A. Oettinger **Cell**. **1995**. 83; (3): 387-395. Cleavage at a V(D)J recombination signal requires only RAG1 and RAG2 proteins and occurs in two steps.

McMillan, R. E. and M. L. Sikes **J Immunol**. **2008**. 180; (5): 3218-3228. Differential activation of dual promoters alters Dβ2 germline transcription during thymocyte development.

Medvedovic, J., A. Ebert, H. Tagoh and M. Busslinger **Adv Immunol**. **2011**. 111; 179-206. Pax5: a master regulator of B cell development and leukemogenesis.

Medvedovic, J., A. Ebert, H. Tagoh, I. M. Tamir, T. A. Schwickert, M. Novatchkova, Q. Sun, P. J. Huis In 't Veld, C. Guo, H. S. Yoon, Y. Denizot, S. J. Holwerda, W. de Laat, M. Cogne, Y. Shi, F. W. Alt and M. Busslinger **Immunity**. **2013**. 39; (2): 229-244. Flexible long-range loops in the V_H gene region of the *Igh* locus facilitate the generation of a diverse antibody repertoire.

Meinke, P., T. D. Nguyen and M. S. Wehnert **Biochem Soc Trans**. **2011**. 39; (6): 1693-1697. The LINC complex and human disease.

Merkenschlager, M., S. Amoils, E. Roldan, A. Rahemtulla, E. O'Connor, A. G. Fisher and K. E. Brown **J Exp Med**. **2004**. 200; (11): 1437-1444. Centromeric repositioning of coreceptor loci predicts their stable silencing and the CD4/CD8 lineage choice.

Merkenschlager, M. and D. T. Odom **Cell**. **2013**. 152; (6): 1285-1297. CTCF and cohesin: linking gene regulatory elements with their targets.

Meuleman, W., D. Peric-Hupkes, J. Kind, J. B. Beaudry, L. Pagie, M. Kellis, M. Reinders, L. Wessels and B. van Steensel **Genome Res**. **2013**. 23; (2): 270-280. Constitutive nuclear lamina-genome interactions are highly conserved and associated with A/T-rich sequence.

Michie, A. M. and J. C. Zuniga-Pflucker **Semin Immunol**. **2002**. 14; (5): 311-323. Regulation of thymocyte differentiation: pre-TCR signals and β-selection.

Misteli, T. **Cell**. **2004**. 119; (2): 153-156. Spatial positioning; a new dimension in genome function.

Mitchell, J. A. and P. Fraser **Genes Dev**. **2008**. 22; (1): 20-25. Transcription factories are nuclear subcompartments that remain in the absence of transcription.

Mochan, T. A., M. Venere, R. A. DiTullio, Jr. and T. D. Halazonetis **DNA Repair (Amst)**. **2004**. 3; (8-9): 945-952. 53BP1, an activator of ATM in response to DNA damage.

Mombaerts, P., J. Iacomini, R. S. Johnson, K. Herrup, S. Tonegawa and V. E. Papaioannou **Cell**. **1992**. 68; (5): 869-877. RAG-1-deficient mice have no mature B and T lymphocytes.

Monroe, J. G., G. Bannish, E. M. Fuentes-Panana, L. B. King, P. C. Sandel, J. Chung and R. Sater **Immunol Res**. **2003**. 27; (2-3): 427-442. Positive and negative selection during B lymphocyte development.

Monroe, R. J., B. P. Sleckman, B. C. Monroe, B. Khor, S. Claypool, R. Ferrini, L. Davidson and F. W. Alt **Immunity**. **1999**. 10; (5): 503-513. Developmental regulation of TCR δ locus accessibility and expression by the TCR δ enhancer.

Morey, C., C. Kress and W. A. Bickmore **Genome Res**. **2009**. 19; (7): 1184-1194. Lack of bystander activation shows that localization exterior to chromosome territories is not sufficient to up-regulate gene expression.

Morris, G. P. and P. M. Allen **J Immunol**. **2009**. 182; (11): 6639-6643. Cutting edge: Highly alloreactive dual TCR T cells play a dominant role in graft-versus-host disease.

Mosammaparast, N. and L. F. Pemberton **Trends Cell Biol**. **2004**. 14; (10): 547-556. Karyopherins: from nuclear-transport mediators to nuclear-function regulators.

Mostoslavsky, R., F. W. Alt and K. Rajewsky **Cell**. **2004**. 118; (5): 539-544. The lingering enigma of the allelic exclusion mechanism.

Mostoslavsky, R., N. Singh, A. Kirillov, R. Pelanda, H. Cedar, A. Chess and Y. Bergman **Genes Dev**. **1998**. 12; (12): 1801-1811. κ chain monoallelic demethylation and the establishment of allelic exclusion.

Mostoslavsky, R., N. Singh, T. Tenzen, M. Goldmit, C. Gabay, S. Elizur, P. Qi, B. E. Reubinoff, A. Chess, H. Cedar and Y. Bergman **Nature**. **2001**. 414; (6860): 221-225. Asynchronous replication and allelic exclusion in the immune system.

Muck, J. S., K. Kandasamy, A. Englmann, M. Gunther and D. Zink **J Cell Biochem**. **2012**. 113; (8): 2607-2621. Perinuclear positioning of the inactive human cystic fibrosis gene depends on CTCF, A-type lamins and an active histone deacetylase.

Muljo, S. A. and M. S. Schlissel **Immunol Rev**. **2000**. 175; 80-93. Pre-B and pre-T-cell receptors: conservation of strategies in regulating early lymphocyte development.

Muljo, S. A. and M. S. Schlissel **Nat Immunol**. **2003**. 4; (1): 31-37. A small molecule Abl kinase inhibitor induces differentiation of Abelson virus-transformed pre-B cell lines.

Muramatsu, M., K. Kinoshita, S. Fagarasan, S. Yamada, Y. Shinkai and T. Honjo **Cell**. **2000**. 102; (5): 553-563. Class switch recombination and hypermutation require activation-induced cytidine deaminase (AID), a potential RNA editing enzyme.

Murre, C. **Nat Immunol**. **2005**. 6; (11): 1079-1086. Helix-loop-helix proteins and lymphocyte development.

Murre, C. **Nat Immunol**. **2008**. 9; (7): 718-720. Nuclear geography and allelic exclusion.

Neuberger, M. S., H. M. Caskey, S. Pettersson, G. T. Williams and M. A. Surani **Nature**. **1989**. 338; (6213): 350-352. Isotype exclusion and transgene down-regulation in immunoglobulin-λ transgenic mice.

Nishana, M. and S. C. Raghavan **Immunology**. **2012**. 137; (4): 271-281. Role of recombination activating genes in the generation of antigen receptor diversity and beyond.

Nodland, S. E., M. A. Berkowska, A. A. Bajer, N. Shah, D. de Ridder, J. J. van Dongen, T. W. LeBien and M. C. van Zelm **Blood**. **2011**. 118; (8): 2116-2127. IL-7R expression and IL-7 signaling confer a distinct phenotype on developing human B-lineage cells.

Oestreich, K. J., R. M. Cobb, S. Pierce, J. Chen, P. Ferrier and E. M. Oltz **Immunity**. **2006**. 24; (4): 381-391. Regulation of TCRβ gene assembly by a promoter/enhancer holocomplex.

Oettinger, M. A., D. G. Schatz, C. Gorka and D. Baltimore **Science**. **1990**. 248; (4962): 1517-1523. RAG-1 and RAG-2, adjacent genes that synergistically activate V(D)J recombination.

Oikawa, T. and T. Yamada **Gene**. **2003**. 303; 11-34. Molecular biology of the Ets family of transcription factors.

Osborne, C. S., L. Chakalova, K. E. Brown, D. Carter, A. Horton, E. Debrand, B. Goyenechea, J. A. Mitchell, S. Lopes, W. Reik and P. Fraser **Nat Genet**. **2004**. 36; (10): 1065-1071. Active genes dynamically colocalize to shared sites of ongoing transcription.

Osborne, C. S., L. Chakalova, J. A. Mitchell, A. Horton, A. L. Wood, D. J. Bolland, A. E. Corcoran and P. Fraser **PLoS Biol**. **2007**. 5; (8): e192. Myc dynamically and preferentially relocates to a transcription factory occupied by *Igh*.

Ottaviani, A., C. Schluth-Bolard, S. Rival-Gervier, A. Boussouar, D. Rondier, A. M. Foerster, J. Morere, S. Bauwens, S. Gazzo, E. Callet-Bauchu, E. Gilson and F. Magdinier **EMBO J**. **2009**. 28; (16): 2428-2436. Identification of a perinuclear positioning element in human subtelomeres that requires A-type lamins and CTCF.

Padovan, E., G. Casorati, P. Dellabona, S. Meyer, M. Brockhaus and A. Lanzavecchia **Science**. **1993**. 262; (5132): 422-424. Expression of two T cell receptor α chains: dual receptor T cells.

Palstra, R. J., M. Simonis, P. Klous, E. Brasset, B. Eijkelkamp and W. de Laat **PLoS One**. **2008**. 3; (2): e1661. Maintenance of long-range DNA interactions after inhibition of ongoing RNA polymerase II transcription.

Peaudecerf, L., S. Lemos, A. Galgano, G. Krenn, F. Vasseur, J. P. Di Santo, S. Ezine and B. Rocha **J Exp Med**. **2012**. 209; (8): 1401-1408. Thymocytes may persist and differentiate without any input from bone marrow progenitors.

Peric-Hupkes, D. and B. van Steensel **Cold Spring Harb Symp Quant Biol**. **2010**. 75; 517-524. Role of the nuclear lamina in genome organization and gene expression.

Perlot, T., F. W. Alt, C. H. Bassing, H. Suh and E. Pinaud **Proc Natl Acad Sci U S A**. **2005**. 102; (40): 14362-14367. Elucidation of *Igh* intronic enhancer functions via germ-line deletion.

Phillips, J. E. and V. G. Corces **Cell**. **2009**. 137; (7): 1194-1211. CTCF: master weaver of the genome.

Pickersgill, H., B. Kalverda, E. de Wit, W. Talhout, M. Fornerod and B. van Steensel **Nat Genet**. **2006**. 38; (9): 1005-1014. Characterization of the *Drosophila melanogaster* genome at the nuclear lamina.

Pieper, K., B. Grimbacher and H. Eibel **J Allergy Clin Immunol**. **2013**. 131; (4): 959-971. B-cell biology and development.

Pierce, A. J., P. Hu, M. Han, N. Ellis and M. Jasin **Genes Dev**. **2001**. 15; (24): 3237-3242. Ku DNA end-binding protein modulates homologous repair of double-strand breaks in mammalian cells.

Pinaud, E., M. Marquet, R. Fiancette, S. Peron, C. Vincent-Fabert, Y. Denizot and M. Cogne **Adv Immunol**. **2011**. 110; 27-70. The *Igh* locus 3' regulatory region: pulling the strings from behind.

Porritt, H. E., L. L. Rumfelt, S. Tabrizifard, T. M. Schmitt, J. C. Zuniga-Pflucker and H. T. Petrie **Immunity**. **2004**. 20; (6): 735-745. Heterogeneity among DN1 prothymocytes reveals multiple progenitors with different capacities to generate T cell and non-T cell lineages.

Probst, A. V. and G. Almouzni **Differentiation**. **2008**. 76; (1): 15-23. Pericentric heterochromatin: dynamic organization during early development in mammals.

Prosser, H. M., D. Wotton, A. Gegonne, J. Ghysdael, S. Wang, N. A. Speck and M. J. Owen **Proc Natl Acad Sci U S A**. **1992**. 89; (20): 9934-9938. A phorbol ester response element within the human T-cell receptor β-chain enhancer.

Queen, C. and D. Baltimore **Cell**. **1983**. 33; (3): 741-748. Immunoglobulin gene transcription is activated by downstream sequence elements.

Ragoczy, T., M. A. Bender, A. Telling, R. Byron and M. Groudine **Genes Dev**. **2006**. 20; (11): 1447-1457. The locus control region is required for association of the murine β-globin locus with engaged transcription factories during erythroid maturation.

Raices, M. and M. A. D'Angelo **Nat Rev Mol Cell Biol**. **2012**. 13; (11): 687-699. Nuclear pore complex composition: a new regulator of tissue-specific and developmental functions.

Ramirez, J., K. Lukin and J. Hagman **Curr Opin Immunol**. **2010**. 22; (2): 177-184. From hematopoietic progenitors to B cells: mechanisms of lineage restriction and commitment.

Ranganath, S., A. C. Carpenter, M. Gleason, A. C. Shaw, C. H. Bassing and F. W. Alt **J Immunol**. **2008**. 180; (4): 2339-2346. Productive coupling of accessible Vβ14 segments and DJβ complexes determines the frequency of Vβ14 rearrangement.

Reddy, K. L., J. M. Zullo, E. Bertolino and H. Singh **Nature**. **2008**. 452; (7184): 243-247. Transcriptional repression mediated by repositioning of genes to the nuclear lamina.

Reinhart, B. J. and D. P. Bartel **Science**. **2002**. 297; (5588): 1831. Small RNAs correspond to centromere heterochromatic repeats.

Reynaud, D., I. A. Demarco, K. L. Reddy, H. Schjerven, E. Bertolino, Z. Chen, S. T. Smale, S. Winandy and H. Singh **Nat Immunol**. **2008**. 9; (8): 927-936. Regulation of B cell fate commitment and immunoglobulin heavy-chain gene rearrangements by Ikaros.

Ribeiro de Almeida, C., R. Stadhouders, M. J. de Bruijn, I. M. Bergen, S. Thongjuea, B. Lenhard, W. van Ijcken, F. Grosveld, N. Galjart, E. Soler and R. W. Hendriks **Immunity**. **2011**. 35; (4): 501-513. The DNA-binding protein CTCF limits proximal Vκ recombination and restricts κ enhancer interactions to the immunoglobulin κ light chain locus.

Richmond, T. J. and C. A. Davey **Nature**. **2003**. 423; (6936): 145-150. The structure of DNA in the nucleosome core.

Ristic, D., M. Modesti, R. Kanaar and C. Wyman **Nucleic Acids Res**. **2003**. 31; (18): 5229-5237. Rad52 and Ku bind to different DNA structures produced early in double-strand break repair.

Rogakou, E. P., D. R. Pilch, A. H. Orr, V. S. Ivanova and W. M. Bonner **J Biol Chem**. **1998**. 273; (10): 5858-5868. DNA double-stranded breaks induce histone H2AX phosphorylation on serine 139.

Roldan, E., M. Fuxa, W. Chong, D. Martinez, M. Novatchkova, M. Busslinger and J. A. Skok **Nat Immunol**. **2005**. 6; (1): 31-41. Locus 'decontraction' and centromeric recruitment contribute to allelic exclusion of the immunoglobulin heavy-chain gene.

Rooney, S., J. Sekiguchi, C. Zhu, H. L. Cheng, J. Manis, S. Whitlow, J. DeVido, D. Foy, J. Chaudhuri, D. Lombard and F. W. Alt **Mol Cell**. **2002**. 10; (6): 1379-1390. Leaky Scid phenotype associated with defective V(D)J coding end processing in Artemis-deficient mice.

Roy, A. L., R. Sen and R. G. Roeder **Trends Immunol**. **2011**. 32; (11): 532-539. Enhancer-promoter communication and transcriptional regulation of *Igh*.

Rusinol, A. E. and M. S. Sinensky **J Cell Sci**. **2006**. 119; (Pt 16): 3265-3272. Farnesylated lamins, progeroid syndromes and farnesyl transferase inhibitors.

Sadaie, M., R. Kawaguchi, Y. Ohtani, F. Arisaka, K. Tanaka, K. Shirahige and J. Nakayama **Mol Cell Biol**. **2008**. 28; (23): 6973-6988. Balance between distinct HP1 family proteins controls heterochromatin assembly in fission yeast.

Sakaki, M., H. Koike, N. Takahashi, N. Sasagawa, S. Tomioka, K. Arahata and S. Ishiura **J Biochem**. **2001**. 129; (2): 321-327. Interaction between emerin and nuclear lamins.

Sarukhan, A., C. Garcia, A. Lanoue and H. von Boehmer **Immunity**. **1998**. 8; (5): 563-570. Allelic inclusion of T cell receptor α genes poses an autoimmune hazard due to low-level expression of autospecific receptors.

Sayegh, C. E., S. Jhunjhunwala, R. Riblet and C. Murre **Genes Dev**. **2005**. 19; (3): 322-327. Visualization of looping involving the immunoglobulin heavy-chain locus in developing B cells.

Schatz, D. G. and Y. Ji **Nat Rev Immunol**. **2011**. 11; (4): 251-263. Recombination centres and the orchestration of V(D)J recombination.

Schatz, D. G. and P. C. Swanson **Annu Rev Genet**. **2011**. 45; 167-202. V(D)J recombination: mechanisms of initiation.

Schlenner, S. M. and H. R. Rodewald **Trends Immunol**. **2010**. 31; (8): 303-310. Early T cell development and the pitfalls of potential.

Schlimgen, R. J., K. L. Reddy, H. Singh and M. S. Krangel **Nat Immunol**. **2008**. 9; (7): 802-809. Initiation of allelic exclusion by stochastic interaction of *Tcrb* alleles with repressive nuclear compartments.

Schlissel, M. **Semin Immunol**. **2002**. 14; (3): 207-212; discussion 225-206. Allelic exclusion of immunoglobulin gene rearrangement and expression: why and how?

Schlissel, M. S. **Nat Rev Immunol**. **2003**. 3; (11): 890-899. Regulating antigen-receptor gene assembly.

Schlissel, M. S. **Immunol Rev**. **2004**. 200; 215-223. Regulation of activation and recombination of the murine Igκ locus.

Schneider, R. and R. Grosschedl **Genes Dev**. **2007**. 21; (23): 3027-3043. Dynamics and interplay of nuclear architecture, genome organization, and gene expression.

Schoenfelder, S., T. Sexton, L. Chakalova, N. F. Cope, A. Horton, S. Andrews, S. Kurukuti, J. A. Mitchell, D. Umlauf, D. S. Dimitrova, C. H. Eskiw, Y. Luo, C. L. Wei, Y. Ruan, J. J. Bieker and P. Fraser **Nat Genet**. **2010**. 42; (1): 53-61. Preferential associations between co-regulated genes reveal a transcriptional interactome in erythroid cells.

Senoo, M., L. Wang, D. Suzuki, N. Takeda, Y. Shinkai and S. Habu **J Immunol**. **2003**. 171; (2): 829-835. Increase of TCR Vβ accessibility within Eβ regulatory region influences its recombination frequency but not allelic exclusion.

Shibata, A., D. Moiani, A. S. Arvai, J. Perry, S. M. Harding, M. M. Genois, R. Maity, S. van Rossum-Fikkert, A. Kertokalio, F. Romoli, A. Ismail, E. Ismalaj, E. Petricci, M. J. Neale, R. G. Bristow, J. Y. Masson, C. Wyman, P. A. Jeggo and J. A. Tainer **Mol Cell**. **2014**. 53; (1): 7-18. DNA Double-Strand Break Repair Pathway Choice Is Directed by Distinct MRE11 Nuclease Activities.

Shih, H. Y., B. Hao and M. S. Krangel **Immunol Res**. **2011**. 49; (1-3): 192-201. Orchestrating T-cell receptor α gene assembly through changes in chromatin structure and organization.

Shih, H. Y. and M. S. Krangel **J Exp Med**. **2010**. 207; (9): 1835-1841. Distinct contracted conformations of the *Tcra/Tcrd* locus during *Tcra* and *Tcrd* recombination.

Shih, H. Y. and M. S. Krangel **J Immunol**. **2013**. 190; (10): 4915-4921. Chromatin architecture, CCCTC-binding factor, and V(D)J recombination: managing long-distance relationships at antigen receptor loci.

Shih, H. Y., J. Verma-Gaur, A. Torkamani, A. J. Feeney, N. Galjart and M. S. Krangel **Proc Natl Acad Sci U S A**. **2012**. 109; (50): E3493-3502. Tcra gene recombination is supported by a *Tcra* enhancer- and CTCF-dependent chromatin hub.

Shiloh, Y. and Y. Ziv **Nat Rev Mol Cell Biol**. **2013**. 14; (4): 197-210. The ATM protein kinase: regulating the cellular response to genotoxic stress, and more.

Shinkai, Y., S. Koyasu, K. Nakayama, K. M. Murphy, D. Y. Loh, E. L. Reinherz and F. W. Alt **Science**. **1993**. 259; (5096): 822-825. Restoration of T cell development in RAG-2-deficient mice by functional TCR transgenes.

Shinkai, Y., G. Rathbun, K. P. Lam, E. M. Oltz, V. Stewart, M. Mendelsohn, J. Charron, M. Datta, F. Young, A. M. Stall and et al. **Cell**. **1992**. 68; (5): 855-867. RAG-2-deficient mice lack mature lymphocytes owing to inability to initiate V(D)J rearrangement.

Sikes, M. L., R. J. Gomez, J. Song and E. M. Oltz **J Immunol**. **1998**. 161; (3): 1399-1405. A developmental stage-specific promoter directs germline transcription of Dβ Jβ gene segments in precursor T lymphocytes.

Sikes, M. L., A. Meade, R. Tripathi, M. S. Krangel and E. M. Oltz **Proc Natl Acad Sci U S A**. **2002**. 99; (19): 12309-12314. Regulation of V(D)J recombination: a dominant role for promoter positioning in gene segment accessibility.

Sikes, M. L. and E. M. Oltz **Curr Top Microbiol Immunol**. **2012**. 356; 91-116. Genetic and epigenetic regulation of *Tcrb* gene assembly.

Singh, N., Y. Bergman, H. Cedar and A. Chess **J Exp Med**. **2003**. 197; (6): 743-750. Biallelic germline transcription at the κ immunoglobulin locus.

Skok, J. A., K. E. Brown, V. Azuara, M. L. Caparros, J. Baxter, K. Takacs, N. Dillon, D. Gray, R. P. Perry, M. Merkenschlager and A. G. Fisher **Nat Immunol**. **2001**. 2; (9): 848-854. Nonequivalent nuclear location of immunoglobulin alleles in B lymphocytes.

Skok, J. A., R. Gisler, M. Novatchkova, D. Farmer, W. de Laat and M. Busslinger **Nat Immunol**. **2007**. 8; (4): 378-387. Reversible contraction by looping of the *Tcra* and *Tcrb* loci in rearranging thymocytes.

Sleckman, B. P., C. G. Bardon, R. Ferrini, L. Davidson and F. W. Alt **Immunity**. **1997**. 7; (4): 505-515. Function of the TCRα enhancer in $\alpha\beta$ and $\gamma\delta$ T cells.

Sleckman, B. P., J. R. Gorman and F. W. Alt **Annu Rev Immunol**. **1996**. 14; 459-481. Accessibility control of antigen-receptor variable-region gene assembly: role of cis-acting elements.

Soille, P. (2003). Principles and Applications. Morphological Image Analysis. Springer, Springer-Verlag.

Somech, R., S. Shaklai, O. Geller, N. Amariglio, A. J. Simon, G. Rechavi and E. N. Gal-Yam **J Cell Sci**. **2005**. 118; (Pt 17): 4017-4025. The nuclear-envelope protein and transcriptional repressor LAP2β interacts with HDAC3 at the nuclear periphery, and induces histone H4 deacetylation.

Sonoda, E., Y. Pewzner-Jung, S. Schwers, S. Taki, S. Jung, D. Eilat and K. Rajewsky **Immunity**. **1997**. 6; (3): 225-233. B cell development under the condition of allelic inclusion.

Spencer, D. M., Y. H. Hsiang, J. P. Goldman and D. H. Raulet **Proc Natl Acad Sci U S A**. **1991**. 88; (3): 800-804. Identification of a T-cell-specific transcriptional enhancer located 3' of Cγ1 in the murine T-cell receptor γ locus.

Stanhope-Baker, P., K. M. Hudson, A. L. Shaffer, A. Constantinescu and M. S. Schlissel **Cell**. **1996**. 85; (6): 887-897. Cell type-specific chromatin structure determines the targeting of V(D)J recombinase activity *in vitro*.

Starr, T. K., S. C. Jameson and K. A. Hogquist **Annu Rev Immunol**. **2003**. 21; 139-176. Positive and negative selection of T cells.

Steinel, N. C., B. S. Lee, A. T. Tubbs, J. J. Bednarski, E. Schulte, K. S. Yang-Iott, D. G. Schatz, B. P. Sleckman and C. H. Bassing **J Exp Med**. **2013**. 210; (2): 233-239. The Ataxia Telangiectasia mutated kinase controls Igκ allelic exclusion by inhibiting secondary Vκ-to-Jκ rearrangements.

Stracker, T. H. and J. H. Petrini **Nat Rev Mol Cell Biol**. **2011**. 12; (2): 90-103. The MRE11 complex: starting from the ends.

Sutherland, H. and W. A. Bickmore **Nat Rev Genet**. **2009**. 10; (7): 457-466. Transcription factories: gene expression in unions?

Swanson, P. C., S. Kumar and P. Raval **V(D)J Recombination**. **2009**. 650; 1-15. Early Steps of V(D)J Rearrangement: Insights from Biochemical Studies of RAG-RSS Complexes.

Takata, M., M. S. Sasaki, E. Sonoda, C. Morrison, M. Hashimoto, H. Utsumi, Y. Yamaguchi-Iwai, A. Shinohara and S. Takeda **EMBO J**. **1998**. 17; (18): 5497-5508. Homologous recombination and non-homologous end-joining pathways of DNA double-strand break repair have overlapping roles in the maintenance of chromosomal integrity in vertebrate cells.

Taniura, H., C. Glass and L. Gerace **J Cell Biol**. **1995**. 131; (1): 33-44. A chromatin binding site in the tail domain of nuclear lamins that interacts with core histones.

ten Boekel, E., F. Melchers and A. G. Rolink **Immunity**. **1998**. 8; (2): 199-207. Precursor B cells showing H chain allelic inclusion display allelic exclusion at the level of pre-B cell receptor surface expression.

Tillman, R. E., A. L. Wooley, M. M. Hughes, B. Khor and B. P. Sleckman **Immunol Rev**. **2004**. 200; 36-43. Regulation of T-cell receptor γ-chain gene assembly by recombination signals: the beyond 12/23 restriction.

Towbin, B. D., A. Gonzalez-Sandoval and S. M. Gasser **Trends Biochem Sci**. **2013**. 38; (7): 356-363. Mechanisms of heterochromatin subnuclear localization.

Tripathi, R., A. Jackson and M. S. Krangel **J Immunol**. **2002**. 168; (5): 2316-2324. A change in the structure of Vbeta chromatin associated with TCRβ allelic exclusion.

Uematsu, Y., S. Ryser, Z. Dembic, P. Borgulya, P. Krimpenfort, A. Berns, H. von Boehmer and M. Steinmetz **Cell**. **1988**. 52; (6): 831-841. In transgenic mice the introduced functional T cell receptor β gene prevents expression of endogenous β genes.

Van Dyck, E., A. Z. Stasiak, A. Stasiak and S. C. West **Nature**. **1999**. 398; (6729): 728-731. Binding of double-strand breaks in DNA by human Rad52 protein.

van Gent, D. C. and M. van der Burg **Oncogene**. **2007**. 26; (56): 7731-7740. Non-homologous end-joining, a sticky affair.

Verma-Gaur, J., A. Torkamani, L. Schaffer, S. R. Head, N. J. Schork and A. J. Feeney **Proc Natl Acad Sci U S A**. **2012**. 109; (42): 17004-17009. Noncoding transcription within the *Igh* distal V(H) region at PAIR elements affects the 3D structure of the *Igh* locus in pro-B cells.

Vermeulen, M., H. C. Eberl, F. Matarese, H. Marks, S. Denissov, F. Butter, K. K. Lee, J. V. Olsen, A. A. Hyman, H. G. Stunnenberg and M. Mann **Cell**. **2010**. 142; (6): 967-980. Quantitative interaction proteomics and genome-wide profiling of epigenetic histone marks and their readers.

Vernooij, B. T., J. A. Lenstra, K. Wang and L. Hood **Genomics**. **1993**. 17; (3): 566-574. Organization of the murine T-cell receptor γ locus.

Vettermann, C., K. Herrmann and H. M. Jack **Semin Immunol**. **2006**. 18; (1): 44-55. Powered by pairing: the surrogate light chain amplifies immunoglobulin heavy chain signaling and pre-selects the antibody repertoire.

Vettermann, C. and M. S. Schlissel **Immunol Rev**. **2010**. 237; (1): 22-42. Allelic exclusion of immunoglobulin genes: models and mechanisms.

Villey, I., D. Caillol, F. Selz, P. Ferrier and J. P. de Villartay **Immunity**. **1996**. 5; (4): 331-342. Defect in rearrangement of the most 5' TCR-J alpha following targeted deletion of T early α (TEA): implications for TCR α locus accessibility.

Vincent-Fabert, C., R. Fiancette, E. Pinaud, V. Truffinet, N. Cogne, M. Cogne and Y. Denizot **Blood**. **2010**. 116; (11): 1895-1898. Genomic deletion of the whole *Igh* 3' regulatory region (hs3a, hs1,2, hs3b, and hs4) dramatically affects class switch recombination and *Ig* secretion to all isotypes.

Vlcek, S. and R. Foisner **Curr Opin Cell Biol**. **2007**. 19; (3): 298-304. Lamins and lamin-associated proteins in aging and disease.

Volpe, T. A., C. Kidner, I. M. Hall, G. Teng, S. I. Grewal and R. A. Martienssen **Science**. **2002**. 297; (5588): 1833-1837. Regulation of heterochromatic silencing and histone H3 lysine-9 methylation by RNAi.

Volpi, S. A., J. Verma-Gaur, R. Hassan, Z. Ju, S. Roa, S. Chatterjee, U. Werling, H. Hou, Jr., B. Will, U. Steidl, M. Scharff, W. Edelman, A. J. Feeney and B. K. Birshtein **J Immunol**. **2012**. 188; (6): 2556-2566. Germline deletion of *Igh* 3' regulatory region elements hs 5, 6, 7 (hs5-7) affects B cell-specific regulation, rearrangement, and insulation of the *Igh* locus.

von Boehmer, H., H. Kishi, Y. Uematsu, H. S. Teh, B. Scott and P. Kisielow **Princess Takamatsu Symp**. **1988**. 19; 107-113. T cell repertoire selection in T cell receptor transgenic mice.

Wang, X., G. Xiao, Y. Zhang, X. Wen, X. Gao, S. Okada and X. Liu **Nat Immunol**. **2008**. 9; (7): 794-801. Regulation of *Tcrb* recombination ordering by c-Fos-dependent RAG deposition.

Weissman, I. L., D. J. Anderson and F. Gage **Annu Rev Cell Dev Biol**. **2001**. 17; 387-403. Stem and progenitor cells: origins, phenotypes, lineage commitments, and transdifferentiations.

Westhorpe, F. G. and A. F. Straight **Curr Opin Cell Biol**. **2013**. 25; (3): 334-340. Functions of the centromere and kinetochore in chromosome segregation.

Weterings, E. and D. J. Chen **Cell Res**. **2008**. 18; (1): 114-124. The endless tale of non-homologous end-joining.

Weterings, E. and D. C. van Gent **DNA Repair (Amst)**. **2004**. 3; (11): 1425-1435. The mechanism of non-homologous end-joining: a synopsis of synapsis.

Whitehurst, C. E., S. Chattopadhyay and J. Chen **Immunity**. **1999**. 10; (3): 313-322. Control of V(D)J recombinational accessibility of the Dβ1 gene segment at the TCRβ locus by a germline promoter.

Will, C. L. and R. Luhrmann **Cold Spring Harb Perspect Biol**. **2011**. 3; (7): Spliceosome structure and function.

Williams, R. R., V. Azuara, P. Perry, S. Sauer, M. Dvorkina, H. Jorgensen, J. Roix, P. McQueen, T. Misteli, M. Merkenschlager and A. G. Fisher **J Cell Sci**. **2006**. 119; (Pt 1): 132-140. Neural induction promotes large-scale chromatin reorganisation of the Mash1 locus.

Wilson, K. L. and R. Foisner **Cold Spring Harb Perspect Biol**. **2010**. 2; (4): a000554. Lamin-binding Proteins.

Wu, C., C. H. Bassing, D. Jung, B. B. Woodman, D. Foy and F. W. Alt **Immunity**. **2003**. 18; (1): 75-85. Dramatically increased rearrangement and peripheral representation of Vβ14 driven by the 3'Dβ1 recombination signal sequence.

Xiang, Y. and W. T. Garrard **J Immunol**. **2008**. 180; (10): 6725-6732. The Downstream Transcriptional Enhancer, Ed, positively regulates mouse Igκ gene expression and somatic hypermutation.

Xiang, Y., X. Zhou, S. L. Hewitt, J. A. Skok and W. T. Garrard **J Immunol**. **2011**. 186; (9): 5356-5366. A multifunctional element in the mouse Igκ locus that specifies repertoire and Ig loci subnuclear location.

Xiong, N., J. E. Baker, C. Kang and D. H. Raulet **Proc Natl Acad Sci U S A**. **2004**. 101; (1): 260-265. The genomic arrangement of T cell receptor variable genes is a determinant of the developmental rearrangement pattern.

Xiong, N., C. Kang and D. H. Raulet **Immunity**. **2002**. 16; (3): 453-463. Redundant and unique roles of two enhancer elements in the TCRγ locus in gene regulation and γδ T cell development.

Xiong, N., L. Zhang, C. Kang and D. H. Raulet **J Exp Med**. **2008**. 205; (4): 929-938. Gene placement and competition control T cell receptor γ variable region gene rearrangement.

Xu, Y., L. Davidson, F. W. Alt and D. Baltimore **Immunity**. **1996**. 4; (4): 377-385. Deletion of the Igκ light chain intronic enhancer/matrix attachment region impairs but does not abolish Vκ Jκ rearrangement.

Xu, Z., H. Zan, E. J. Pone, T. Mai and P. Casali **Nat Rev Immunol**. **2012**. 12; (7): 517-531. Immunoglobulin class-switch DNA recombination: induction, targeting and beyond.

Yancopoulos, G. D. and F. W. Alt **Cell**. **1985**. 40; (2): 271-281. Developmentally controlled and tissue-specific expression of unrearranged V_H gene segments.

Yang-Iott, K. S., A. C. Carpenter, M. A. Rowh, N. Steinel, B. L. Brady, K. Hochedlinger, R. Jaenisch and C. H. Bassing **J Immunol**. **2010**. 184; (3): 1369-1378. TCRβ feedback signals inhibit the coupling of recombinationally accessible Vβ14 segments with DJβ complexes.

Yao, J., R. D. Fetter, P. Hu, E. Betzig and R. Tjian **Genes Dev**. **2011**. 25; (6): 569-580. Subnuclear segregation of genes and core promoter factors in myogenesis.

Yun, M. H. and K. Hiom **Nature**. **2009**. 459; (7245): 460-463. CtIP-BRCA1 modulates the choice of DNA double-strand-break repair pathway throughout the cell cycle.

Zal, T., S. Weiss, A. Mellor and B. Stockinger **Proc Natl Acad Sci U S A**. **1996**. 93; (17): 9102-9107. Expression of a second receptor rescues self-specific T cells from thymic deletion and allows activation of autoreactive effector function.

Zhang, W., J. Sloan-Lancaster, J. Kitchen, R. P. Trible and L. E. Samelson **Cell**. **1998**. 92; (1): 83-92. LAT: the ZAP-70 tyrosine kinase substrate that links T cell receptor to cellular activation.

Zhou, X., Y. Xiang, X. Ding and W. T. Garrard **J Immunol**. **2012**. 188; (6): 2722-2732. A new hypersensitive site, HS10, and the enhancers, E3' and Ed, differentially regulate Igκ gene expression.

Zink, D., M. D. Amaral, A. Englmann, S. Lang, L. A. Clarke, C. Rudolph, F. Alt, K. Luther, C. Braz, N. Sadoni, J. Rosenecker and D. Schindelhauer **J Cell Biol**. **2004**. 166; (6): 815-825. Transcription-dependent spatial arrangements of CFTR and adjacent genes in human cell nuclei.

Zullo, J. M., I. A. Demarco, R. Pique-Regi, D. J. Gaffney, C. B. Epstein, C. J. Spooner, T. R. Luperchio, B. E. Bernstein, J. K. Pritchard, K. L. Reddy and H. Singh **Cell**. **2012**. 149; (7): 1474-1487. DNA sequence-dependent compartmentalization and silencing of chromatin at the nuclear lamina.

Biography

I was born in Gainesville, FL on January 4th, 1985 to Chester and Lynn Wilcox. When 4, my family moved to Cocoa, FL, where my parents still reside. I graduated from West Shore Jr/Sr High School in 2003, and went on to study Microbiology & Immunology at the University of Miami. While in college, I spent a year abroad in the UK, where I met my now husband. After graduating college in 2007 I moved to Durham, NC to begin my Ph. D. training in the Duke University Immunology Department.